GAMMA IRRADIATION OF ANIONIC POLYSTYRENE

by

Janos Gyorgy Spiro, P. Eng.

A thesis submitted to the Faculty of Graduate Studies and Research in partial fulfilment of the requirements for the degree of Doctor of Philosophy

Department of Chemistry,
McGill University,
Montreal.

March 1960

ACKNOWLEDGEMENTS

The author wishes to express his sincere gratitude and appreciation for the constant advice and encouragement rendered him by his research directors, Drs. C.A. Winkler and D.A.I. Goring.

Acknowledgement is also extended

to the

National Research Council of Canada for financial assistance in the form of a studentship during the academic session 1962-63,

to the

Staff of the McGill University Computing Centre for compiling and running many of the computer programs,

to

Dr. H.W. McCormick of the Dow Chemical Company for donating the anionic polystyrene samples,

to the

Atomic Energy of Canada Limited for carrying out free of charge a number of irradiations, and

to

Messrs. N.B. Glick and D.S.C. Lee for performing many of the viscometric determinations.

TABLE OF CONTENTS

TABLE OF CONTENTS (continued) Page

TABLE OF CONTENTS (continued) Page

GENERAL INTRODUCTION

The discovery of radioactivity in 1896 was almost immediately followed by studies of the effects of high-energy radiation on materials. As early as 1899, the Curies reported the discoloring effect of radiation on glass, which was probably the first 'experimental result' in the radiation chemistry of high molecular substances. However, it was only within the last decade that the important changes produced by irradiation in organic polymers became apparent. Interest in the radiation chemistry of polymers was greatly stimulated when it became known that these changes could be beneficial.

On the basis of their behavior when exposed to high-energy radiation, polymers can be classified into two groups (1). To the first group belong, for example, polyethylene, nylon, natural rubber, and GR-S rubber. In these polymers irradiation leads to an increase in molecular weight, with the eventual formation of insoluble networks. The second group consists of polymers such as polymethyl methacrylate, polyvinyl chloride, cellulose, and teflon, in which the predominant reaction during irradiation is degradation of the molecular chains.

It is the first group that is of particular interest from a theoretical as well as a practical point of view. Much of the previous work has been done on polyethylene and natural rubber, polymers that offer perhaps the widest scope for the commercial applications of irradiation. From the point of view of basic research, however, polystyrene appears to be a more suitable substrate for irradiation. The

inconvenience of high dose requirements (2) is largely offset by well developed techniques for the characterization of samples of polystyrene. Moreover, as discussed later, this polymer offers unusual possibilities in studying the effects of molecular weight distribution. Most of the present work deals with radiation effects in polystyrene. However, the conclusions drawn from statistical calculations are of a general nature, and could be used to design and evaluate experiments with a variety of other polymers.

The original purpose of the work to be reported here was to test whether statistical theories are applicable to polystyrene and to develop reliable methods for distinguishing between different basic mechanisms of network formation. At the same time, it was attempted to determine some radiation chemical parameters, in particular the extent of degradation for this polymer, regarding which data in the literature (2-4) had been contradictory.

In many previously published experiments (5-12) the presence of solvents, oxygen, or both has made it difficult to draw conclusions concerning the important processes occurring in polystyrene under irradiation. In the present work irradiations were carried out in vacuo, and thus interferences with the primary radiation chemical reactions were avoided. Techniques of polymer characterization used were light-scattering, viscometry, osmotic measurements, and determinations of solubility.

Preliminary investigations indicated that a statistical approach was justified, and accordingly planning of experiments was based on

statistical theories (2,3,13-21). Formerly, studies of this type were considerably restricted by the unknown molecular weight distributions of the unirradiated polymers. In the work to be reported here uncertainties due to distribution effects were largely eliminated, by use of narrow range polymers and their mixtures for substrates.

As a consequence, it was possible to obtain irradiated samples of known characteristics, and it was decided to use these samples to study the effects of branching on solution properties, in particular the intrinsic viscosity, of polymers. This project, in turn, led to an extension of certain statistical theories (19,21) and a survey of existing methods (3,19,21-33) for estimating the intrinsic viscosities of branched polymers.

The theoretical and experimental work was limited to the effects of radiation doses not exceeding the dose required for incipient gel formation. After the gel point, statistical treatment becomes extremely difficult in most cases and, in particular, the consequences of ring formation (cyclization) are all but impossible to evaluate. Moreover the available irradiation facilities would have been inadequate for producing pronounced gel formation in polystyrene samples of intermediate molecular weight.

The scope of the investigation covers two distinct areas. Much of the theoretical and experimental work deals with the properties of irradiated polystyrene. However, the effect of branching on the viscosity is considered separately. Here irradiation is simply a means of producing branched macromolecules under controlled conditions.

PART I

RADIATION-INDUCED CROSSLINKING, ENDLINKING, AND DEGRADATION PROCESSES

This duality of purpose is reflected in the arrangement of the contents of the thesis. Part I contains information of interest primarily to the radiation chemist. The main points covered are the role of the molecular weight distribution and the relative importance of crosslinking and endlinking. Part II deals with the viscosity of branched molecules, with an emphasis on general considerations, rather than on the properties of irradiated polystyrene.

Both Part I and Part II contain a section on pertinent historical background, a theoretical section, and description and discussion of the results. This arrangement is consistent with the differences in the purpose and the mathematical development of the two parts. On the other hand, several experimental techniques were common to both parts, and are accordingly described in a single experimental section following Part II. Some details of the statistical calculations are given in appendices.

One aspect of the investigations, namely the extremely heavy volume of computations involved, may deserve special mention. Without the extensive use of digital computers of the McGill University Computing Centre this work would not have been possible.

HISTORICAL INTRODUCTION

I. Interaction of High-Energy Radiations with Matter

Recently growing interest in radiation chemistry has resulted in a considerable volume of information on the chemical effects of ionizing radiations. Nevertheless, the chemistry of radiation processes is not well understood, because the overall changes produced in irradiated compounds are difficult to evaluate in terms of the primary reactions. The transient species formed in primary processes undergo various transfer reactions, in such a way that the permanently destroyed or displaced chemical bonds are not necessarily the ones that were initially affected by the radiation.

Some of the more frequently encountered changes are dimerization or crosslinking, degradation, gas formation, and radiation-induced oxidation. To understand the mechanisms of these reactions it is necessary to consider the basic steps of the interaction of high-energy radiation with matter.

In the case of X rays and gamma rays energy transfer may take place by pair production, Compton scattering, or photoelectric absorption. For the 1.17 and 1.33 MeV gamma rays of the commonly used Co^{60} source the loss of energy is attributed almost exclusively to Compton scattering (34). In this process the change in the wavelength of a photon scattered by an electron through the angle θ is given by

$$\delta\lambda = \frac{h}{mc}(1 - \cos\theta), \qquad \text{I-1}$$

where m is the rest mass of the electron, h is Planck's constant, and c is the speed of light. The electrons ejected from the atoms have a broad, continuous spectrum of energies, given by

$$E = h\nu \frac{\delta\lambda}{\lambda+\delta\lambda} \quad , \qquad \text{I-2}$$

where ν and λ are the frequency and wavelength of the incident photon. The total energy transferred by Compton absorption is directly proportional to the number of electrons in unit volume, and hence to the density of the irradiated substance. Therefore when Compton absorption is predominant, the total energy transfer will be approximately proportional to the density.

The fast electrons ejected by Compton scattering have appreciable energy. A single fast electron is capable of producing chemical change in a large number of molecules. These electron-induced changes are therefore more important than those effected in the molecule actually 'hit' by the photon. Irradiation by charged particles, such as electrons, protons, and alpha particles, has similar effects to gamma radiation, because in all cases the reactions are produced mainly by secondary (and tertiary, etc.) electrons. Intermediate reactions are somewhat more complicated in the case of irradiation by neutrons. Here elastic collisions with nuclei as well as nuclear reactions are involved, but the consequence is still the liberation of high-energy charged particles inside the substrate.

Thus there is much in common between the chemical effects of different ionizing radiations. Nevertheless, different types of radiation

may produce different results, because of the importance of the linear density of events. In the case of bombardment with alpha particles, for example, reactive entities form sufficiently close to react with each other, due to the high linear density of ionization and excitation. When gamma rays are used the reactive entities are further apart (35), and the probability of their reaction with unaffected molecules is higher.

The reactions of the ionized and excited species are in general not well understood. There are several indications (36,37), however, that the chemical effects are produced by free radicals formed from the primary products. Direct proof for the existence of these radicals has been obtained by the electron spin resonance technique (38).

An alternate explanation for radiation chemical changes has been suggested by Weiss and collaborators (39,40). Their mechanism is ionic in nature and is based on the quantum mechanical theory of solids. They surmise that the important role of oxygen and other impurities lies in providing suitable electronic levels for the trapping and release of electrons. The ionic theory of radiation-induced crosslinking in solid polymers also explains the mobility of active sites below the glass temperature (39,40).

While the importance of ions in radiation chemical processes cannot be doubted, it has been proved that ions can account for but a part of the products formed. Essex and collaborators (41) measured the rates of radiation chemical reactions in gases, and found that the rapid removal of all the ions by a strong electric field reduced the rates by only about 50%, or even less. This indicated that radicals or excited

molecules contributed substantially to the chemical changes occurring.

Any effort to explain radiation chemical processes is necessarily hindered by factors such as special effects of the charged particle tracks, spatial inhomogeneity, and problems concerning the diffusion and recombination of ions and other active species. A particularly striking illustration of the complexity of the reactions is given by the work of Caffrey and Allen (42). According to these authors, the products obtainable from the radiolysis of pentane adsorbed on mineral solids are strongly dependent on the type of adsorbent used. Moreover, marked differences were observed when two different kinds of silica were used, showing that the chemical constitution of the solid was not the only factor involved. These results clearly demonstrate the need for further work on systems chosen for their simplicity.

II. The Radiation Chemistry of Polystyrene

Early experiments (2) established that high-energy radiation produces linking in polystyrene. It was also apparent that very large doses are required to effect changes in this polymer. The marked radiation stability of polystyrene has been attributed to the protective action of benzene rings, although recently it has been pointed out (43) that a detailed study of the reaction mechanisms is necessary to explain this effect.

A considerable part of the radiation chemical research on polystyrene was done by irradiation in solution (5-12). These experiments, however, were dependent on the radiation chemistry of the solvents as well as on that of the polymer. It has been shown that, depending on the choice of solvent, the viscosity either increases (crosslinking) or decreases (degradation), with the presence of oxygen strongly promoting degradation. It is difficult to draw any conclusions from these results concerning the mechanism of linking in the solid state.

One of the earliest attempts to obtain information on the mechanism of radiation chemical processes in solid polystyrene was made by Wall and Brown (44). By use of polystyrenes deuterated at specific positions, these researchers were able to show that the crosslinking reactions are not highly specific, i.e. that any of the hydrogen atoms may take part in the reactions. The authors have suggested that high local temperatures are responsible for the lack of specificity. The number of crosslinks was found to exceed the number of hydrogen molecules

produced, which suggested a hydrogenation of the benzene ring. While the results of Wall and Brown were not conclusive, they have indicated that radical formation by the loss of the alpha hydrogen atom plays an important role. Radicals formed in this way have also been detected by electron spin resonance study of irradiated polystyrene (45), although the evidence for their presence is incomplete. Such macroradicals may be long-lived (46) due to resonance stabilization.

The radiation susceptibility of specific sites in deuterated polystyrene has also been investigated by Burlant and Neerman (47). In general, their results were in accord with those of Wall and Brown, but they concluded that hydrogen evolution must be attributed solely to hydrogen abstraction. In a second paper (4) Burlant, Neerman, and Serment reported the effect of substituents in the p-position of the benzene ring. Irradiations were performed at different temperatures. The role of the p-substituents was interpreted on the basis of their contribution to the resonance stability of alpha-radicals formed under irradiation. The strong temperature dependence found for many substituted polystyrenes indicated that polystyryl radicals are responsible both for the crosslinking and the degradation processes. It would appear that crosslinking takes place when these radicals attack neighboring molecules, while chain scission may occur when the radicals undergo stabilization.

At the present time most of the evidence supports the hypothesis that the main reaction of the excited molecules is the breakage of the α-CH bond:

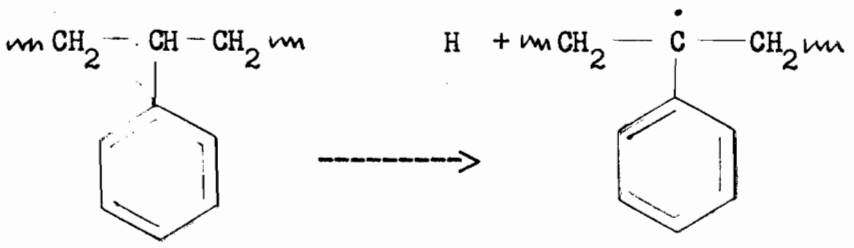

C-1

The role of the hydrogen atom split off is not clear, but many of the experimental data can be explained on the basis of the following scheme, due to Pravednikov and In Shen-Kan (43). The hydrogen atom is capable of reacting with neighboring monomer units either by abstracting hydrogen (C-2), or by adding to the double bond of a benzene ring, with the formation of a free radical of the cyclohexadienyl type (C-3).

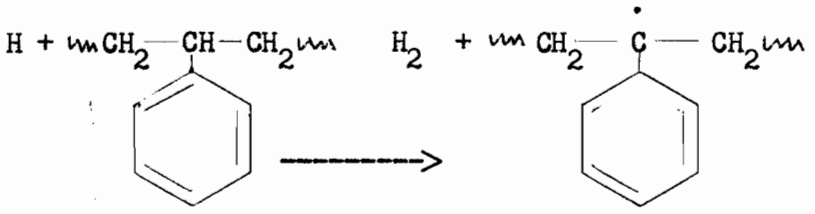

C-2

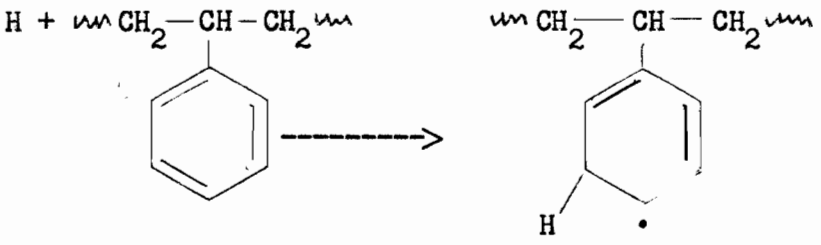

C-3

Owing to the low diffusion rate in glassy polymers, the radicals resulting from the above processes will be located near the primary radical formed in reaction C-1, so that the primary and secondary radicals may interact. The radicals of reactions C-1 and C-2 will form crosslinks (C-4), while

the reaction of primary radicals with cyclohexadienyl radicals may take two directions. One possibility is the formation of a crosslink (C-5); this reaction would account for the experimental result that the number of crosslinks is higher than the number of hydrogen molecules evolved. Alternatively, disproportionation may take place (C-6). It is the high probability of reaction C-6 that may serve as an explanation for the low crosslink yield in irradiated polystyrene.

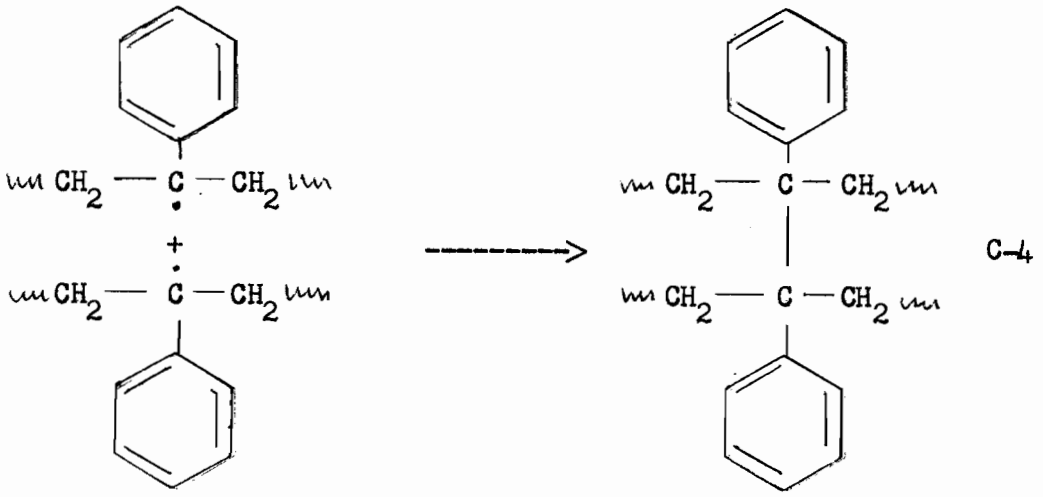

C-4

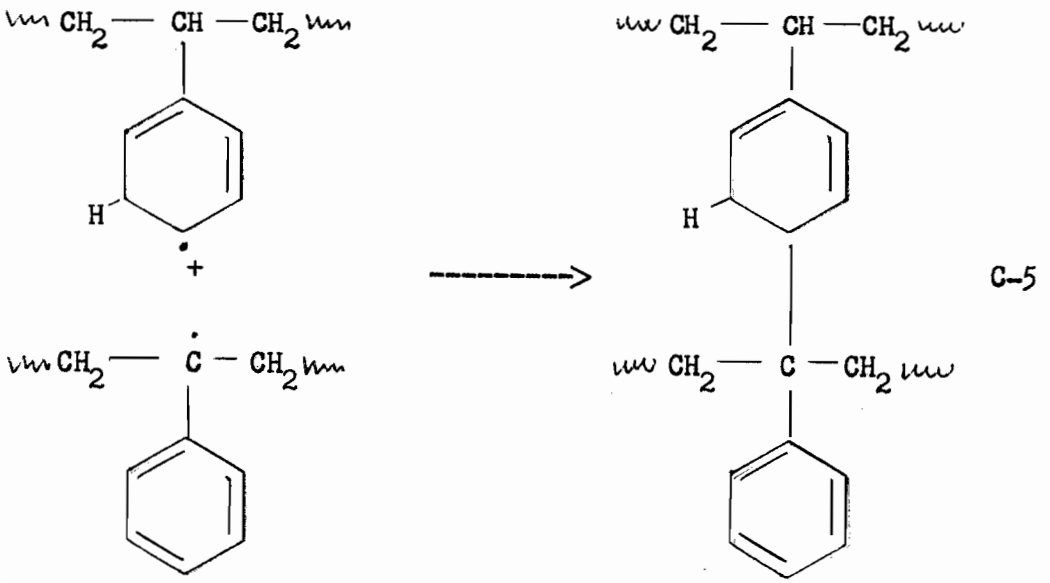

C-5

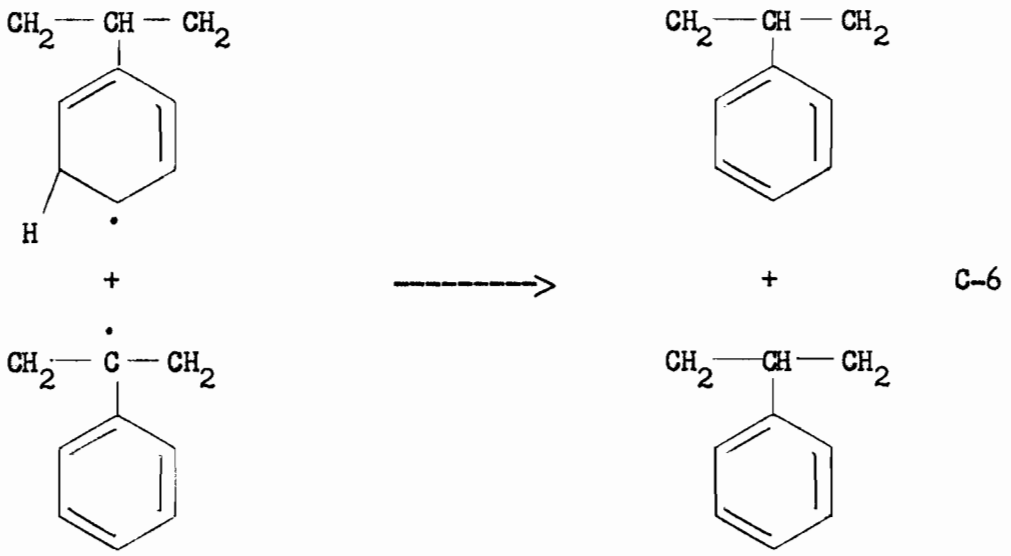

C-6

The supposition that reaction C-6 is responsible for the high energy requirement of crosslink formation has been confirmed by the irradiation of deuterated toluene in the frozen state (43). Upon irradiation of $C_6H_5CD_3$, radicals are formed according to reactions C-7 and C-8, and these radicals can then interact in a reaction (C-9) similar to C-6. Due to isotope effect, in general a hydrogen atom rather than deuterium is removed from the methylcyclohexadienyl radical.

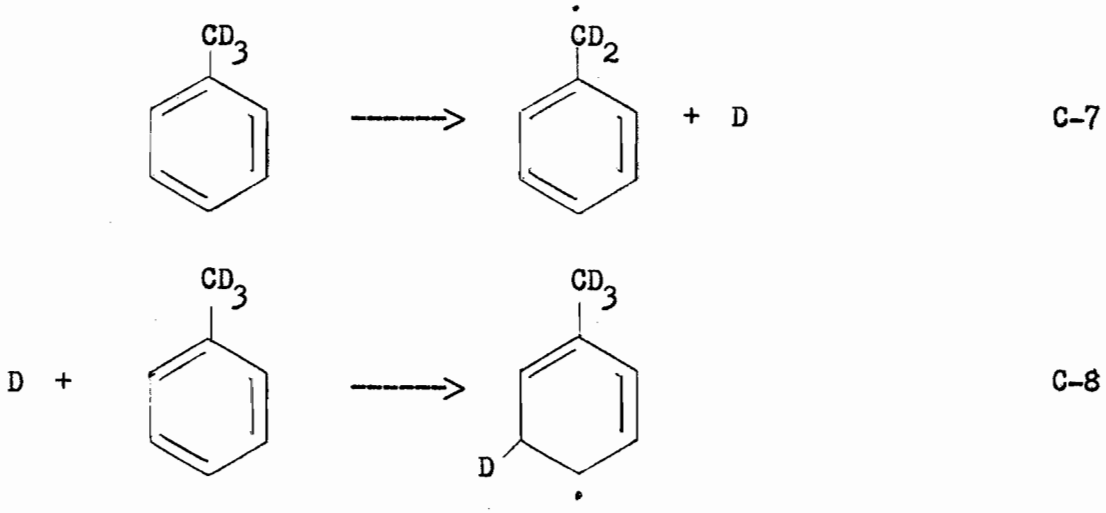

C-7

C-8

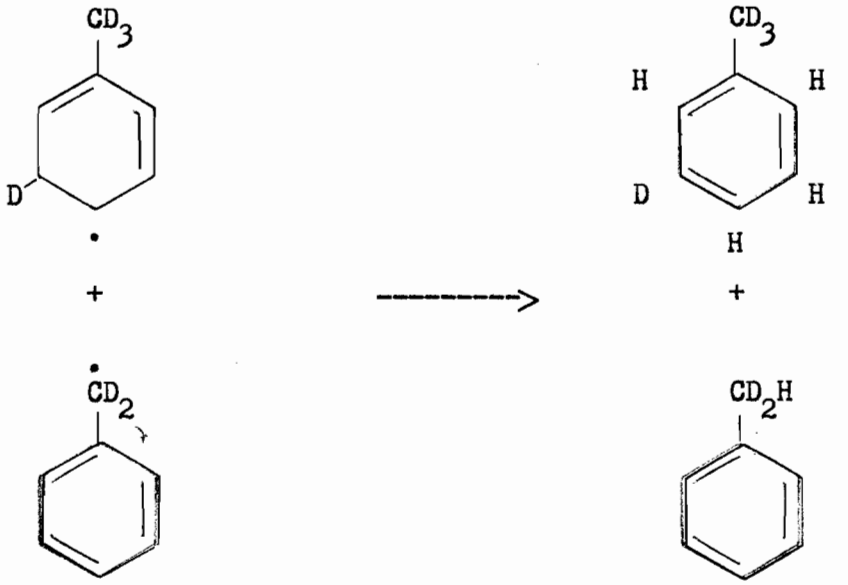

C-9

The resulting deuterated benzene ringscan be easily detected by semi-classical techniques. Infrared spectra (48) of electron-irradiated polystyrene are also in agreement with the proposed mechanism.

It may be concluded that, in spite of the complexity of the chemical reactions, considerable progress has been made in the elucidation of linking processes in irradiated polystyrene. Nevertheless, more experimental work will be required to obtain a clear and unambiguous understanding of the reactions involved.

III. Physical and Physico-Chemical Properties of Crosslinked Polymers

When polymers are exposed to high-energy radiation, usually their physical properties are altered considerably. One conspicuous change is the marked discoloration, due to the formation of polyunsaturated segments and other chromophores. Often strong surface fluorescence can be observed. It has also been found that crystalline polymers, when irradiated, tend to lose their crystallinity.

In the case of network forming polymers, important and often desirable changes may be observed in the mechanical properties and in behavior on heating. Polyethylene, for example, normally softens at comparatively low temperatures (110-115°C). Irradiated polyethylene becomes infusible, and tends to become rubbery rather than plastic at high temperatures. Unvulcanized rubbery polymers on irradiation acquire the increased toughness and elasticity characteristic of vulcanized rubbers.

None of these effects are very pronounced in polystyrene. Bopp and Sisman (49) have observed that both discoloration and changes in the mechanical properties are small in irradiated polystyrene, even at extreme doses. However, irradiation strongly increases the electrical conductivity of polystyrene (22,50), and this increased conductivity persists for several days after irradiation.

While the properties mentioned above may have considerable practical significance, their quantitative study and interpretation are difficult. A

more satisfactory way of studying radiation effects is by investigating the solubility and solution properties of irradiated polymers. When a crosslinking polymer is irradiated, the average molecular weight increases due to the formation of links, with the eventual formation of insoluble networks. The point of incipient gel formation is usually called the gel point, and the corresponding dose is the critical or gelling dose. The gel point, as will be discussed later, has important theoretical significance, and it also provides a dividing line between two stages in radiation effects.

Changes below the gel point

Up to the critical dose the irradiated polymer remains completely soluble, but the average molecular weight increases, with the formation of large, branched molecules. Linking is usually accompanied by scission, which may result in the decrease of the number average molecular weight, even while the weight average increases. The quantitative aspects of these processes will be discussed later.

For polystyrene irradiated in the solid state Shultz, Roth, and Rathmann (3) determined the increase in the weight average molecular weight by light-scattering. Assuming that the original distribution was random they found good agreement with weight average molecular weights predicted by statistical theory. Burlant, Neerman, and Serment (4) measured changes in the number average molecular weight for irradiated polystyrene and substituted polystyrenes, and used these values to estimate the gelling dose.

The easiest, and most common way of detecting radiation effects below the gel point, however, is viscometry. This technique has been particularly advantageous for studying the effects of irradiation on polymer solutions (5-12). However, while viscometry is an easy experimental technique, the interpretation of its results is difficult, because of the influence of distribution and branching on the intrinsic viscosity. Experimental results obtained by this technique, and the underlying theory, will be discussed in the second part of this thesis.

Changes after the gel point

As the radiation dose approaches its critical value, the weight average molecular weight increases steeply, and the gelling dose corresponds to the formation of 'infinitely' large molecules. The three-dimensional networks produced in this process are no longer soluble, and as irradiation is continued beyond the gel point the soluble fraction decreases rapidly.

Much of the experimental work done on the effects of high-energy radiations in polymers deals with solubility as a function of dose. The theoretical aspects of gel formation have been discussed by several authors (2,3,14-16,18) and a number of mathematical equations were developed for calculating radiation chemical parameters from solubility data. Quantitative information on the properties of polystyrene irradiated in vacuo has been obtained mainly in this way (2-4). The validity of this method, however, is affected by several factors, such as molecular weight distribution and cyclization. Moreover, gel content determinations are

not suitable for distinguishing between different mechanisms.

An alternative approach has been studying the swelling properties of the gel fraction produced by irradiation. The three-dimensional networks formed are no longer capable of dissolving even in good solvents, however there still is a tendency for solvent molecules to enter the polymer and produce swelling. The presence of crosslinks inhibits the stretching of the polymer molecules, and therefore the number of crosslinks can be estimated from the extent of swelling. Charlesby (51) has studied the properties of polystyrene exposed to atomic pile radiation, and has found a quantitative relationship between the degree of crosslinking and the extent of swelling, in accordance with his modification of the Flory-Rehner theory (52). However, this technique has not been well developed yet.

IV. Statistical Treatment of Linking and Scission Occurring in Polymers under Ionizing Radiation

One of the simple processes amenable to statistical treatment is degradation of a polymer due to main chain fractures. Much of the early work was associated with the degradation of cellulose and its derivatives by chemical methods. In the first mathematical analyses of degradation (53-56) it was assumed that all molecules in the original sample were equal in size. Later (57) the treatment was extended to polymers of random molecular weight distribution, and in 1954 Charlesby (13) developed equations valid for any initial distribution.

In the case of polymers where exposure to high-energy radiation increases the molecular weight, it is usually assumed that this increase is due to the formation of tetrafunctional links, called crosslinks (Fig. I-1). Radiation-induced crosslinking is mathematically similar to the formation of condensation polymers containing tetrafunctional units. For molecules of initially uniform distribution Flory's analysis (14) is therefore applicable. Charlesby (2) has extended the treatment to initially random distribution, and later (15) to an arbitrary distribution.

The calculations and evaluation of experimental results are made more complicated by the simultaneous occurrence of crosslinking and degradation. Formally, however, the two processes can be considered as occurring consecutively, rather than simultaneously. Therefore statistical treatments of crosslinking are often readily extended into theories of crosslinking with degradation. This approach, of course, depends on the

assumption that radiation-induced processes take place at random. While this assumption is in general reasonable, due to the large size of polymer molecules, the presence of 'weak links' (58) may partially invalidate the statistical conclusions.

In 1955 Charlesby (16) suggested an alternate mechanism for network formation. If it is assumed that on main chain fracture a polymer molecule gives rise to two smaller molecules with active ends at the point of fracture, and these active ends attack neighboring molecules, a linking process (endlinking) becomes possible. If some molecules are fractured more than once network formation may take place. Endlinking, as opposed to crosslinking, gives rise to trifunctional junction points (Fig. I-1). Thus endlinking and degradation are basically similar processes, distinguished merely by the reactivity of the fractured molecules. Charlesby has developed a mathematical analysis of endlinking for the random initial distribution.

Recently Saito (17-19) has introduced the powerful transform methods of modern operational mathematics into the analysis of linking and scission processes. Saito's theories deal with the most general cases, and give solutions for arbitrary initial distributions. Moreover, his method can be extended to include the effect of cyclization. Unfortunately, the equations obtained by Saito are generally inconvenient for detailed calculations. Kotliar and Anderson (20) have pointed out the advantages of using the Schulz function (59) for molecular weight distributions in connection with Saito's treatment. More recently, using the Monte Carlo sampling technique, Kotliar and Podger (33) have developed

FIG. I-1

Network formation by crosslinking and endlinking (16).

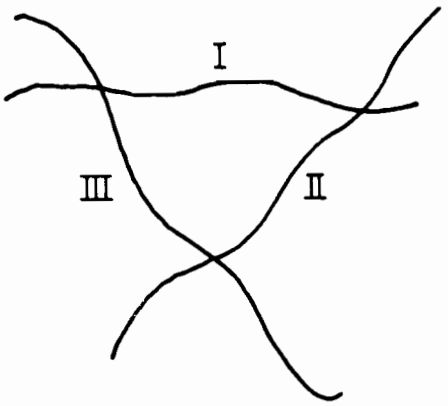

Initial conditions.
(Three separate molecules.)

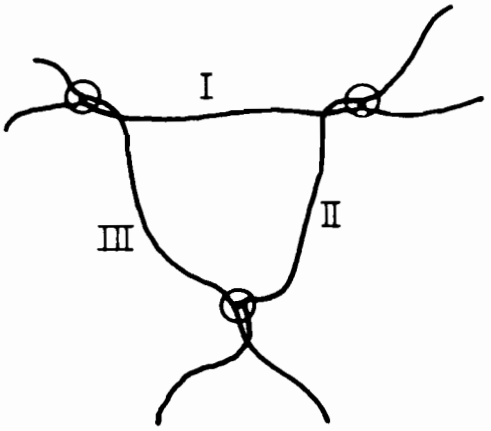

Network formation by crosslinking at three points.
(Each link is tetrafunctional.)

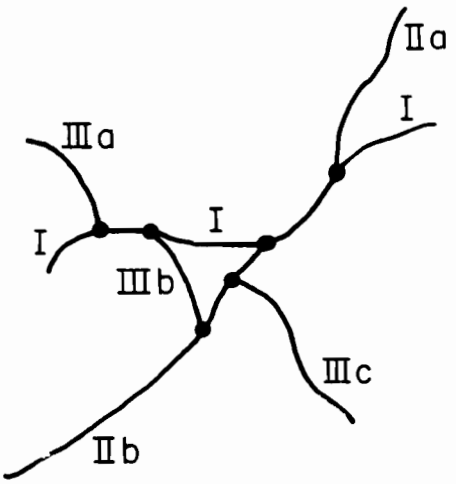

Network formation by endlinking.
(Molecule III fractured twice, Molecule II once. The active ends have linked to neighboring molecules. Each link is tri-functional.)

a quasi-experimental method of computing molecular weight distributions for crosslinked polymers. This method has not yet been adapted to endlinking.

The rapid progress in the mathematical theories of radiation chemistry has extended the scope of statistical investigations very considerably. Often, the problems facing researchers are now due to the large volume of calculations, rather than conceptual difficulties. In the present work high speed computers were used to deal with the extensive mathematical analyses required.

It is proper to mention at this point an inherent weakness of statistical treatments, namely that their application is limited to the overall effects of radiation. In order to obtain a thorough understanding of basic processes, it would be necessary to consider the elementary mechanisms and their kinetic consequences. Most of the work along these lines has been done in connection with the irradiation of polyethylene. Owing to the simple chemical structure of this polymer, the number of reactions involved is not very large, and the kinetic theory is comparatively simple. Okamoto and Isihara (60), and later Simha and Wall (61) have studied this problem. Perhaps the most important result of their work is that factors such as the radiation intensity, gradual saturation of irradiation effects, and specific surface may have an important role. Accordingly, in the present work evidence was sought concerning anisotropy and lack of dependence on intensity before undertaking the statistical analysis.

THEORETICAL

I. Distribution Functions

The central problem in the present part of the thesis concerns the effect of initial molecular weight distribution on the properties of irradiated polymers. The fact that molecular weight distribution has an important role is widely recognized but, in the past, no serious effort has been made to study this effect. Most researchers have not even attempted to determine the distribution of molecular weights in samples to be irradiated, because of the considerable effort required. Even if the necessary experimental data are available, the construction of distribution curves is a somewhat ambiguous procedure. Moreover, the mathematical treatment of radiation processes is highly complex, except for the more simple initial distributions. In the present work advantage was taken of two recent developments, in order to avoid certain mathematical difficulties and laborious fractionation procedures.

On the theoretical side, the ingenious mathematical techniques of Saito (17-19) have opened up new methods for calculating the characteristics of irradiated polymers. Kotliar and Anderson (20) have shown how Saito's treatment can be applied to initial distributions that were heretofore difficult to study.

At about the same time, the subject of molecular weight distributions was also greatly advanced, by the discovery of anionic polymerization techniques (62). It is now possible to synthetize polymers of very narrow

and consequently well defined distributions, and such samples have been used successfully in studies where molecular weight distribution was of importance (63,64).

The present work gained particular impetus when it was found that these two apparently unrelated advances could be exploited together by using the Schulz function (59), or generalized exponential distribution function, for describing anionic polystyrene samples. The advantages of using this function in connection with Saito's treatment have been shown by Kotliar and Anderson (20). It appears, however, that some of the expressions derived by these authors are unduly complicated. Moreover, they have not treated endlinking. Therefore the calculations of Kotliar and Anderson were revised and extended in the present work, using a somewhat different form of the Schulz function (65).

A normalized form of this distribution function, that resembles the well known gamma distribution, is

$$n(u) = \frac{A_o}{\Gamma(\lambda)} \left(\frac{\lambda}{u_1}\right)^{\lambda} u^{\lambda-1} \exp\left(-\lambda u/u_1\right), \qquad \text{I-3}$$

where n(u) is the number of molecules of degree of polymerization u, A_o is the total number of molecules, λ is a positive parameter, giving the sharpness of the distribution, and u_1 is the number average degree of polymerization.

It will be noted that the commonly employed exponential or random distribution function, given by

$$n(u) = \frac{A_o}{u_1} \exp\left(-u/u_1\right) , \qquad \text{I-4}$$

is merely a special case of the Schulz function, corresponding to $\lambda = 1$. In the radiation chemical literature the somewhat misleading term 'Poisson distribution' is often used to describe Eq. I-4.

It is easy to show (Cf. Eqs. I-8 and I-9) that the parameter λ is related to the number and weight average molecular weights by the formula

$$\lambda = \frac{M_n}{M_w - M_n} \quad . \qquad \text{I-5}$$

Therefore the parameters of the Schulz function for a given polymer sample can be readily computed from experimental data. In actual calculations it is often convenient to consider only integral values of λ. This is no serious restriction for mixtures of narrow distribution samples, because the possible error introduced by rounding off λ will be less than the experimental error associated with the determination of molecular weights.

McCormick (63) has experimentally determined the distributions of several samples of polystyrene. Fig. I-2 shows the distribution of a sample of narrow range polystyrene, comparable to the ones used in the present work, as determined by McCormick. The excellent agreement with the Schulz function which approximates the experimental curve is also shown in Fig. I-2. Based on the experimental results the parameters of the Schulz function were calculated to be $u_1 = 2480$ and $\lambda = 25$.

For mixtures of anionic polystyrene samples, Eq. I-3 can be immediately extended to

FIG. I-2

Approximation of molecular weight distribution of anionic polystyrene sample by the Schulz function. The full curve was obtained by McCormick experimentally (63), the dashed curve was plotted on the basis of Eq. I-3, with $u_1 = 2480$ and $\lambda = 25$.

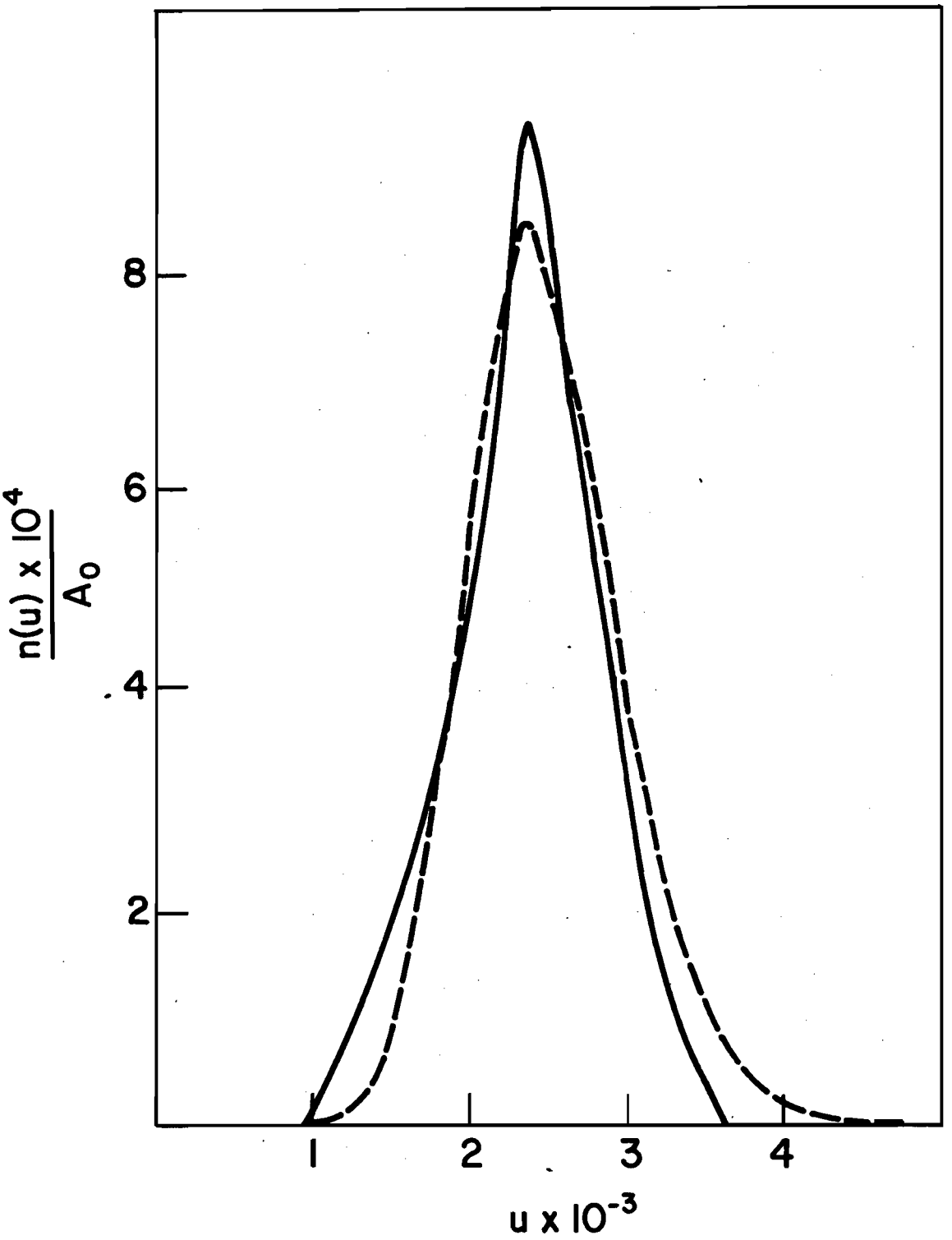
8
6
4
2
1
2
3
4
$\frac{n(u) \times 10^4}{A_0}$
u x 10^-3

$$n(u) = \sum_{\ell=1}^{s} \frac{A_{o\ell}}{\Gamma(\lambda_\ell)} \left(\frac{\lambda_\ell}{u_{1\ell}}\right)^{\lambda_\ell} u^{\lambda_\ell - 1} \exp\left(-\lambda_\ell u / u_{1\ell}\right) , \quad \text{I-6}$$

which represents a sum of generalized exponential distributions. The subscript ℓ refers to the ℓ-th component of a given mixture, and s is the number of components.

Then the total number of monomer units will be

$$N = \sum_{\ell=1}^{s} A_{o\ell} u_{1\ell} , \quad \text{I-7}$$

and the number and weight average degrees of polymerization are given by

$$u_1 = \frac{\int_o^\infty un(u)du}{\int_o^\infty n(u)du} = \frac{\sum_{\ell=1}^{s} A_{o\ell} u_{1\ell}}{\sum_{\ell=1}^{s} A_{o\ell}} \quad \text{I-8}$$

and

$$u_2 = \frac{\int_o^\infty u^2 n(u)du}{\int_o^\infty un(u)du} = \frac{\sum_{\ell=1}^{s} \frac{\lambda_\ell + 1}{\lambda_\ell} A_{o\ell} u_{1\ell}^2}{\sum_{\ell=1}^{s} A_{o\ell} u_{1\ell}} , \quad \text{I-9}$$

respectively.

II. Basic Assumptions

The derivation of statistical formulas used in the radiation chemistry of polymers always involves a number of assumptions. The assumptions made by Saito (17-19) automatically put a certain limitation on the validity of the equations developed in the present work. However, the experimental results to be described later clearly indicate the soundness of Saito's theoretical treatment, and its applications in the present investigations.

Perhaps the most important hypotheses in these calculations are that the number of linkages and scissions is small compared to the number of available monomer units, and is proportional to the radiation dose. Linking and scission are presumed to take place at random, all monomer units being equally likely to be affected by radiation. These assumptions are generally accepted as valid, at least for low doses where saturation effects cannot be important. In fact, they are a consequence of the nature of the interaction between radiation and matter, and have been justified by many experimental results (66).

The possibility of link formation between two monomers of the same molecule (cyclization) is usually neglected. While the influence of cyclization may be considerable at high crosslinking densities, it has been shown (17,18) that below the gel point its effects are small. Linking and degradation are considered independent of each other, and are consequently treated as if they occurred consecutively rather than simultaneously. It is obvious that in endlinking, for example, linking

must be preceded by main chain scissions, and the two processes are not physically independent. Nevertheless, as a mathematical approach, superposition of linking on degradation is justified (17,18). This procedure is also generally accepted (2).

Finally, it has been assumed throughout the calculations that the degree of polymerization can be considered as being continuous from zero to infinity.

It may be concluded that the statistical calculations are based on plausible hypotheses. However, the condition of low crosslinking (or endlinking) densities is important, and therefore the validity of detailed statistical calculations is doubtful beyond the critical dose. Accordingly the investigations of the present work were limited to doses below the gelling dose.

III. Crosslinking without Degradation

Charlesby (15) has shown that for any initial distribution the increase in number average, weight average, Z average, or higher average molecular weights can be expressed in terms of the crosslinking index and crosslinking coefficient. The crosslinking index is defined (67) as the number of crosslinked units per number average primary molecule, while the crosslinking coefficient equals the number of crosslinked units per weight average primary molecule. Saito (17) has obtained the various average molecular weights from one basic integro-differential equation. Saito's equation may be derived as shown in the following paragraphs.

Let the function $n(u,R)$ describe the number of molecules of degree of polymerization u in a sample exposed to radiation dose R. Let $\dot{c}$ represent the probability that a monomer unit, irradiated by unit dose, becomes an active center for crosslinking. Molecules containing an active center will attack neighboring molecules, forming a crosslink. One active center thus leads to two crosslinked units.

In view of the suggested mechanism for crosslink formation in polystyrene, as discussed in the Historical Introduction, this picture is an oversimplification. However, from the statistical point of view it matters but little how crosslinks are formed. The final results will depend merely on the number and distribution of crosslinks. Therefore Saito's mathematically convenient approach is acceptable.

The increase of the radiation dose from R to R + dR will result

in the formation of active centers in $un(u,R)\dot{c}dR$ molecules of degree of polymerization u. The number of molecules with two or more active centers is proportional to the square or higher powers of dR, and therefore can be neglected. Molecules containing an active center will link with other molecules, and if either of the reacting molecules is of degree of polymerization u, n(u,R) will tend to decrease. Here again, reaction between two molecules, each containing an active center, may be neglected if the interval between R and R + dR is small enough.

Thus the decrease in n(u,R), due to the above effects, will be

$$un(u,R)\dot{c}dR + \frac{un(u,R)}{\int_0^\infty un(u,R)du} \int_0^\infty un(u,R)\dot{c}dR\,du \qquad \text{I-10}$$

$$= 2un(u,R)\dot{c}dR.$$

The integral in the numerator represents the total number of molecules with an active center, while the integral in the denominator equals N, the total number of monomer units in the sample. The latter quantity is considered independent of the dose.

Some of the crosslinked molecules generated by the irradiation will contain u monomers, which will tend to increase n(u,R). If we denote the degree of polymerization of 'active' molecules by v, the number of u-mers forming in the dose interval between R and R + dR will be given by

$$\int_0^u \left\{ \frac{(u-v)\, n(u-v,R)}{\int_0^\infty un(u,R)du}\, vn(v,R)\dot{c}dR \right\} dv \qquad \text{I-11}$$

$$= \frac{\dot{c}}{N} \int_0^u v(u-v)\, n(v,R)\, n(u-v,R)dRdv.$$

The overall change in the number of u-mers will therefore be

$$dn(u,R) = -2un(u,R)\dot{c}dR + \frac{\dot{c}}{N}\int_0^u vn(v,R)(u-v)n(u-v,R)dRdv. \qquad \text{I-12}$$

Introducing the notation $\dot{c}R = t$, and $n(u,R)/N = m(u,t)$, Saito's fundamental integro-differential equation of crosslinking without degradation will be obtained as

$$\frac{\partial m(u,t)}{\partial t} + 2um(u,t) = \int_0^u vm(v,t)(u-v)m(u-v,t)dv. \qquad \text{I-13}$$

Explicit solution of equation I-13 does not seem to be possible, but moments of the distribution function $m(u,t)$ have been evaluated by Saito (17). Some of the more important results of Saito's treatment are expressions for the number and weight average molecular weights:

$$\frac{M_n''(t)}{M_n(0)} = \frac{1}{1 - u_1 t}, \qquad \text{I-14}$$

and

$$\frac{M_w''(t)}{M_w(0)} = \frac{1}{1 - 2tu_2}, \qquad \text{I-15}$$

where the double primes refer to the crosslinked polymer. For the distribution functions studied in the present investigations (given in Eqs. I-3 and I-6), the weight average molecular weight of irradiated polymers can be calculated by substituting Eq. I-9 into Eq. I-15. However, there exists a more convenient way of studying irradiation effects. Mathematically, the gel point is defined by the dose where the weight

average molecular weight increases beyond limit. Then from equation I-15 t_g, the number of crosslinks per monomer unit at the gel point, is given by

$$t_g = \frac{1}{2u_2} \quad . \qquad \text{I-16}$$

This is identical to the result obtained by Charlesby (15), who showed that for any initial distribution the crosslinking coefficient must equal one at the gel point. It is convenient to express the dose as a fraction of the critical dose R_g, and since $R/R_g = t/t_g$, it follows from Eq. I-15 that

$$\frac{M_w''(R)}{M_w(0)} = \frac{1}{1 - R/R_g} \quad . \qquad \text{I-17}$$

It is evident from Eq. I-17 that when $M_w''(R)/M_w(0)$ is plotted against R/R_g the curve obtained (Fig. I-3) will be independent of the initial distribution. This, as will be shown in the following sections, is not so in endlinking or crosslinking with degradation. Nevertheless, even in the latter cases the calculated $M_w''(R)/M_w(0)$ versus R/R_g curves are all very similar to the curve describing the variation of $M_w''(R)$ in crosslinking without degradation. The significance of this result will be discussed later.

By considerations similar to the ones used for deducing Eqs. I-14 and I-15, Saito (17) has developed expressions for the number and weight average branching indices as well. The number average branching index B_n is defined as

$$B_n = \frac{\sum_i q_i}{N} , \qquad \text{I-18}$$

FIG. I-3

The increase of the weight average molecular weight with R/R_g for crosslinking with no degradation.

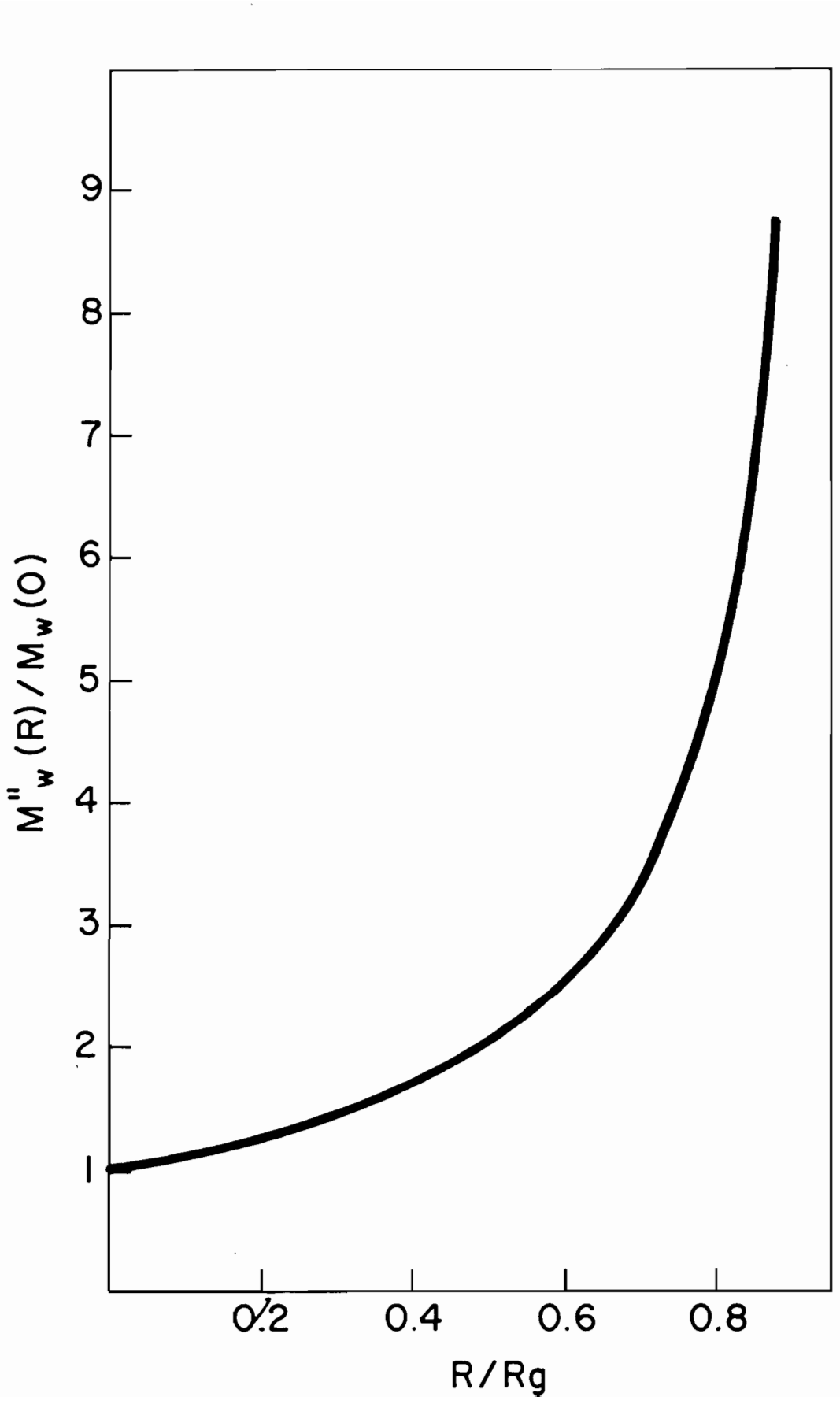
9
8
7
6
5
4
3
2
1
$M''_w(R) / M_w(O)$
0.2
0.4
0.6
0.8
R/Rg

where q_i is one half the number of ends of the i^{th} molecule. The weight average branching index B_w is defined as

$$B_w = \frac{\sum_i q_i w_i}{\sum_i w_i} , \qquad \text{I-19}$$

where w_i is the weight of the i^{th} molecule. In crosslinking without degradation the values of these indices will be given by

$$B_n = \frac{1}{1 - u_1 t} , \qquad \text{I-20}$$

and

$$B_w = \frac{1}{1 - 2u_2 t} . \qquad \text{I-21}$$

IV. Degradation

Even when the predominant reaction is the formation of links between molecules, there is always a simultaneous degradation of some molecules taking place. Statistical analysis of the latter process may be based on Saito's deduction (17), in the following manner.

Let $\dot{r}$ equal the probability of the event that a monomer, or a bond between two monomers, is ruptured by unit radiation dose. If the number of u-mers at dose R is given by n(u,R), the number of u-mers undergoing scission when the radiation dose increases from R to R + dR will be $un(u,R)\dot{r}dR$. The number of molecules of degree of polymerization u forming due to the breakdown of molecules of degree of polymerization higher than u will be $2\int_u^\infty n(v,R)\dot{r}dvdR$. The integro-differential equation describing degradation then becomes

$$\frac{\partial n(u,\tau)}{\partial \tau} + un(u,\tau) = 2\int_u^\infty n(v,\tau)dv, \qquad \text{I-22}$$

where $\tau = \dot{r}R$. Saito (17) has obtained the solution of equation I-22 in the form

$$n(u,\tau) = \left\{n(u) + 2\tau\int_u^\infty n(u)du + \tau^2\int_u^\infty dv\int_v^\infty n(u)du\right\}e^{-u\tau}, \qquad \text{I-23}$$

where $n(u) = n(u,0)$.

Let the original number of molecules in a sample be A_o. Then the total number of main chain fractures at any dose will be given by

$A_o u_1 \tau$, increasing the number of molecules from A_o to $A_o (1 + u_1 \tau)$. Therefore, for an arbitrary initial distribution, the number average molecular weight of the degraded polymer will be

$$M_n'(\tau) = \frac{M_n(0)}{1 + u_1 \tau} . \qquad \text{I-24}$$

Calculation of the weight average molecular weight of the degraded polymer is more difficult. By use of the Schulz function in Eq. I-23, Kotliar and Anderson (20) have obtained expressions for various molecular weight averages in degradation. However, these expressions are very complicated. In the present work it has been found possible to derive a comparatively simple formula for $u_2'(\tau)$, the weight average degree of polymerization after main chain scissions. The derivation is based on the distribution function given by Eq. I-6. As a consequence of using Eq. I-6 rather than the simple Schulz function, the results are immediately applicable to mixtures of anionic polystyrene samples.

By definition

$$u_2'(\tau) = \frac{\int_o^\infty u^2 n(u, \tau) du}{\int_o^\infty un(u, \tau) du} = \frac{\int_o^\infty u^2 n(u, \tau) du}{\sum_{\ell=1}^{s} A_{o\ell} u_{1\ell}} . \qquad \text{I-25}$$

Saito (17) has shown that the numerator in Eq. I-25 can be obtained from the expression

$$u_2'(\tau) = \frac{1}{N} \int_o^\infty u^2 n(u, \tau) du = \frac{2}{\tau} - \frac{2}{N\tau^2} \int_o^\infty n(u)(1 - e^{-u\tau}) du, \qquad \text{I-26}$$

where N, as before, is the total number of monomer units in the sample. Substituting from Eq. I-6 into Eq. I-26, $\int_0^\infty n(u)du$ is, of course, equal to $\sum_{\ell=1}^{s} A_{o\ell}$, the total number of primary molecules, while

$$\int_0^\infty n(u)e^{-u\tau}du$$

$$= \sum_{\ell=1}^{s} \frac{A_{o\ell}}{\Gamma(\lambda_\ell)} \left(\frac{\lambda_\ell}{u_{1\ell}}\right)^{\lambda_\ell} \int_0^\infty u^{\lambda_\ell - 1} \exp\left[-u(\lambda_\ell + u_{1\ell}\tau)/u_{1\ell}\right] du. \qquad \text{I-27}$$

The substitution

$$\frac{u(\lambda_\ell + u_{1\ell}\tau)}{u_{1\ell}} = x_\ell \qquad \text{I-28}$$

transforms the integral into a Γ-function, and thus Eq. I-27 simplifies to

$$\int_0^\infty n(u)e^{-u\tau}du = \sum_{\ell=1}^{s} A_{o\ell} \left(\frac{\lambda_\ell}{\lambda_\ell + u_{1\ell}\tau}\right)^{\lambda_\ell}. \qquad \text{I-29}$$

Hence

$$u_2'(\tau) = \frac{2}{\tau} - \frac{2}{\tau^2} \frac{\sum_{\ell=1}^{s} A_{o\ell}\left[1 - \left(\frac{\lambda_\ell}{\lambda_\ell + u_{1\ell}\tau}\right)^{\lambda_\ell}\right]}{\sum_{\ell=1}^{s} A_{o\ell}\, u_{1\ell}}. \qquad \text{I-30}$$

From the point of view of actual computations the quantity $u_2'(\tau)$ is of particular importance. Therefore Eq. I-30 will be used extensively in the derivations and calculations which follow.

V. Crosslinking with Degradation

Having obtained the first two moments of the distribution function for the 'degraded' polymer, parameters for crosslinking with degradation can now be determined. From equations I-14 and I-24 the number average molecular weight is given by

$$M_n''(R) = \frac{M_n'(\tau)}{1 - u_1'(\tau)t} = \frac{M_n(0)}{(1 + u_1\tau)(1 - u_1'(\tau)t)} \qquad \text{I-31}$$

$$= \frac{M_n(0)}{(1 + u_1\tau)(1 - \frac{u_1 t}{1 + u_1\tau})} = \frac{M_n(0)}{1 + u_1(\tau - t)} .$$

The weight average degree of polymerization can be computed from equation I-15 in the form

$$u_2''(R) = \frac{u_2'(\tau)}{1 - 2u_2'(\tau)t} . \qquad \text{I-32}$$

For samples used in the present investigations, the $u_2'(\tau)$ values to be used with equation I-32 were calculated from equation I-30 of the previous section.

The gelling dose is given by

$$1 - 2u_2'(\tau)t = 0 . \qquad \text{I-33}$$

Substituting from I-30, for mixtures of narrow range polystyrene samples

the writer has obtained the equation

$$\frac{1}{\sigma_c} - 4 + \frac{4}{\tau_g}\left\{\sum_{\ell=1}^{s} A_{o\ell}\left[1 - \left(\frac{\lambda_\ell}{\lambda_\ell + u_{1\ell}\tau_g}\right)^{\lambda_\ell}\right]\right\}\Bigg/\sum_{\ell=1}^{s} A_{o\ell}u_{1\ell} = 0, \qquad \text{I-34}$$

where τ_g is the value of τ at the gel point, and

$$\sigma_c = \frac{\dot{c}}{\dot{r}} = \frac{t}{\tau} = \frac{t_g}{\tau_g} . \qquad \text{I-35}$$

Equation I-34 was then used extensively to estimate critical doses for irradiated polystyrene samples.

At the time when these computations were first performed experimental results were not yet available. Moreover, data published by other researchers (2-4) were somewhat contradictory. Therefore in the calculations values of σ_c were assumed to range from 0.50 to 5.00.

It was found that the left hand side of Eq. I-34, as well as that of the corresponding equation obtained for endlinking (Eq. I-46), monotonically decreases with increasing values of the argument (τ_g). Accordingly, numerical solutions for these equations could be readily determined. In practice, the calculations were performed on digital computers, using the principle of inverse linear interpolation. The roots were roughly estimated from the molecular weights, and two initial estimates, differing by about 10%, were fed to the computer. Then the formula

$$x_3 = x_2 + \frac{(x_1 - x_2)F(x_2)}{F(x_2) - F(x_1)} \qquad \text{I-36}$$

was used iteratively. In Eq. I-36, x_1 and x_2 are the initial estimates, and the function F represents the left-hand side of Eq. I-34. Details of the computational technique are given in Fig. I-4, in terms of a flow diagram. The computations were speeded up considerably by arranging input data in such a way that the zero of one equation served as an estimate for the solution of the next one. In addition to the calculation of critical doses in crosslinking with degradation and endlinking, this technique was also used for obtaining certain intermediate values related to the viscosity of solutions of irradiated polymers.

The number and weight average branching indices were also computed for some samples, by extending equations I-20 and I-21. The resulting formulas are

$$B_n = \frac{1}{1 - u_1^{\dagger}(\tau)t} = \frac{1 + u_1\tau}{1 + u_1(\tau - t)} \qquad \text{I-37}$$

and

$$B_w = \frac{1}{1 - 2u_2^{\dagger}(\tau)t} \quad . \qquad \text{I-38}$$

FIG. I-4

Computer flow diagram for numerical solution of equations by the method of inverse linear interpolation.

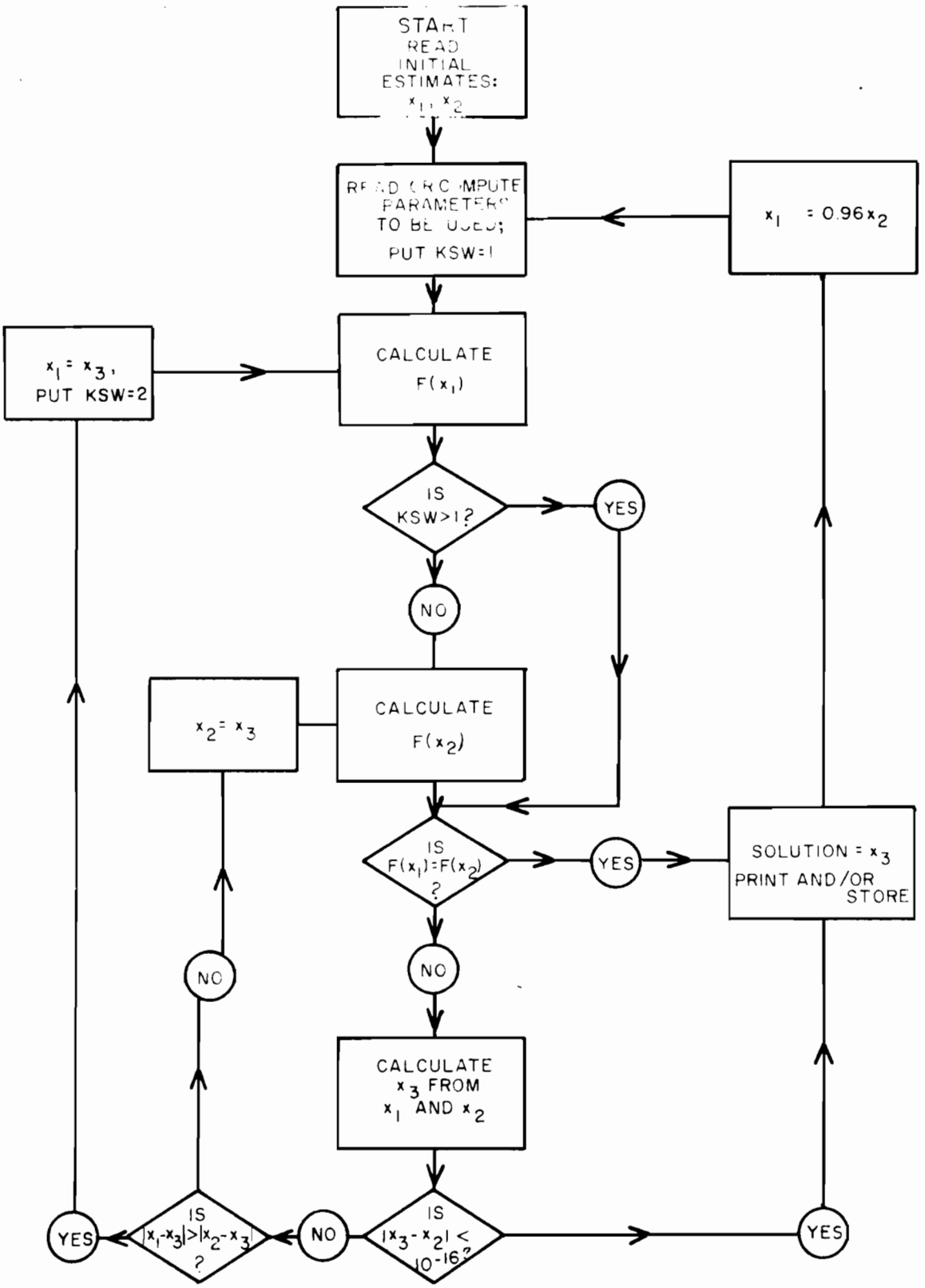
START
READ INITIAL ESTIMATES: x_1, x_2
READ (OR COMPUTE) PARAMETERS TO BE USED; PUT KSW=1
$x_1 = 0.96x_2$
CALCULATE $F(x_1)$
$x_1 = x_3$, PUT KSW=2
IS KSW>1?
YES
NO
CALCULATE $F(x_2)$
$x_2 = x_3$
IS $F(x_1)=F(x_2)$?
YES
SOLUTION = x_3 PRINT AND/OR STORE
NO
CALCULATE x_3 FROM x_1 AND x_2
IS $|x_3 - x_2| < 10^{-16}$?
YES
NO
IS $|x_1-x_3| > |x_2-x_3|$?
YES
NO

VI. Endlinking

For calculating the parameters of irradiated polymers on the basis of an endlinking mechanism, it is again mathematically convenient to consider chain scission separately. Corresponding to any dose, the distribution of the 'degraded' polymer will be given by Eq. I-23. Linking may be considered as a process superimposed on degradation. This can be most easily done by introducing a virtual radiation dose R', which varies from 0 to R, and which may be considered responsible for the changes produced by linking of the active ends to other molecules. The following derivation is due to Saito (18).

Let a polymer be exposed to dose R. Let $\dot{\varsigma}$ represent the probability that a given monomer, or bond between two monomers, will be ruptured by unit dose. If σ_e is the probability that an end newly produced by scission links with a monomer unit of another molecule, then the total number of linkages will be $2N\sigma_e\dot{\varsigma}R$, where N is the total number of monomer units. In the virtual dose interval between R' and $R' + dR'$ $2N\sigma_e\dot{\varsigma}dR'$ of the ends produced by scission will form endlinks. The number of active ends having already formed links at R' is $2N\sigma_e\dot{\varsigma}R'$. Therefore the total number of ends, active or otherwise, is given by $2N/u_1 + 2NR\dot{\varsigma} - 2N\sigma_e\dot{\varsigma}R'$. Thus the probability that an end chosen at random will join another molecule in the virtual dose interval between R' and $R' + dR'$ is

$$\omega(R')dR' = \frac{2N\sigma_e\dot{\varsigma}\,dR'}{2N/u_1 + 2N(R\dot{\varsigma} - \sigma_e\dot{\varsigma}R')} = \frac{\sigma_e\dot{\varsigma}\,dR'}{1/u_1 + R\dot{\varsigma} - \sigma_e\dot{\varsigma}R'}.$$

Let the functions $n_k(u,R')$ represent the number of u-mers with k ends at the virtual dose R'. The change in $n_k(u,R')$ as R' increases will be due to three factors:

1. $kn_k(u,R')\omega(R')dR'$ u-mers with k ends will form endlinks through their active ends. In principle no difference is made between active and inactive ends, for the differences are taken into account through the factor $\omega(R')$. In this respect Saito's treatment resembles that of Charlesby (16). Charlesby, for the sake of mathematical convenience, used the concept of 'virtual links' with inactive molecules.

2. $$\frac{un_k(u,R')}{N} \int_0^{\infty} \sum_{i=2}^{\infty} in_i(v,R')\omega(R')\, dv\, dR' \qquad \text{I-40}$$

u-mers with k ends will form higher molecules, as a result of endlinks formed with active molecules.

3. The number of u-mers of k ends newly produced in the interval $(R', R' + dR')$ is

$$\sum_{i=2}^{k-1} \int_0^{u} in_i(v,R')\omega(R') \frac{(u-v)n_{k-i+1}(u-v,R')}{N} dv\, dR' \,. \qquad \text{I-41}$$

Thus the integro-differential equation of endlinking is

$$\frac{\partial n_k(u,R')}{\partial R'} + kn_k(u,R')\omega(R') + \frac{un_k(u,R')}{N} \int_0^{\infty} \sum_{i=2}^{\infty} in_i(v,R')\omega(R')dv =$$

$$= \sum_{i=2}^{k-1} \int_{o}^{u} i n_i(v,R^*)\omega(R^*) \frac{(u-v)n_{k-i+1}(u-v,R^*)}{N} dv. \qquad I-42$$

Saito's solution of Eq. I-42 yields general formulas, describing the effects of irradiation for an arbitrary initial distribution. The number average molecular weight is given by

$$M_n''(\tau) = \frac{M_n(0)}{1 + (1 - 2\sigma_e)u_1\tau}, \qquad I-43$$

where $\tau = \dot{S}R$. The weight average degree of polymerization will be

$$u_2''(\tau) = \frac{u_2'(\tau)(1+\gamma)^2}{\left[1 + (1-2\sigma_e)\gamma\right]^2 - \frac{2\sigma_e^2\gamma^2(1+\gamma)u_2'(\tau)}{u_1}}, \qquad I-44$$

where

$$\gamma = u_1\tau, \qquad I-45$$

and $u_2'(\tau)$ may be obtained from equation I-26.

The gel point, as before, corresponds to $M_w''(R) \rightarrow \infty$, which from Eq. I-44 leads to

$$1 + \gamma_g - \left\{2 + \sqrt{\frac{2(1+\gamma_g)u_2'(\tau_g)}{u_1}}\right\}\sigma_e\gamma_g = 0. \qquad I-46$$

The solution corresponding to the negative value of the square root must be discarded.

For the distributions studied in this work $u_2'(\tau)$ is given by Eq. I-30. Thus the critical dose can be computed by substituting Eq. I-30

into Eq. I-46, and solving the resulting equation as described under crosslinking with degradation.

Similarly, the weight average molecular weight can be calculated by combining Eqs. I-30 and I-44. The resulting formulas simplify to

$$\tau_g = \frac{1}{u_1 (4\sigma_e - 1)} \qquad \text{I-47}$$

and

$$M_w''(\tau) = \frac{M_w(0)}{1 + (1 - 4\sigma_e)u_1\tau} \qquad \text{I-48}$$

for a random initial distribution.

Formulas for the branching indices have also been derived by Saito (18), who found

$$B_n = \frac{1 + (1 - \sigma_e)\gamma}{1 + (1 - 2\sigma_e)\gamma} \qquad \text{I-49}$$

and

$$B_w = \frac{1 + (1 - \sigma_e)\gamma}{2\sigma_e\gamma} \left\{ \frac{(1 + \gamma)\left[1 + (1 - 2\sigma_e)\gamma\right]}{\left[1 + (1 - 2\sigma_e)\gamma\right]^2 - (2/u_1)\sigma_e^2\gamma^2(1 + \gamma)u_2'(\tau)} - 1 \right\}. \qquad \text{I-50}$$

In order to use Eqs. I-43 to I-50 for actual computations, it is necessary to know the value of σ_e, i.e. the reactivity of the ends produced by scission. In principle, σ_e for endlinking could be estimated from solubility-dose curves, using the equation of Charlesby (16)

$$s' = \left\{ \frac{1/u_1 + \dot{\varsigma} R(1 - \sigma_e)}{3 \dot{\varsigma} R \sigma_e} \right\}^2 . \qquad \text{I-51}$$

Here s' is the soluble fraction at dose R. Eq. I-51 is analogous to the commonly used equation (2) for crosslinking with degradation

$$s' + \sqrt{s'} = \frac{1}{2\sigma_c} + \frac{1}{2u_1 \dot{c} R} . \qquad \text{I-52}$$

Both equations are valid for an initially random distribution.

Unfortunately, most of the solubility-dose curves have never been published for irradiated polystyrene, and the experimental results of Charlesby (2) are rather badly scattered. Therefore it was not possible to calculate σ_e from data in the literature with any precision. However, for large doses Eq. I-51 reduces to

$$s' = \left(\frac{1 - \sigma_e}{3 \sigma_e}\right)^2 . \qquad \text{I-53}$$

Therefore the usually observed low solubility of heavily irradiated polystyrene indicates that in a hypothetical endlinking mechanism σ_e will exceed 0.5. In the computations, the results of which are given in the next section, σ_e values ranging from 0.30 to 1.00 were used.

It will be seen that for testing statistical hypotheses and distinguishing between crosslinking and endlinking the exact value of σ_e need not be known.

VII. Computations

One of the most important purposes of the present investigation has been to develop a method for distinguishing between crosslinking and endlinking as mechanisms of network formation in irradiated polymers. As Charlesby pointed out (68): "...at least mathematically, there is little to choose between crosslinking and endlinking as an explanation of network formation, solubility, or elastic modulus. Such quantitative differences as occur may be readily obscured by minor differences in molecular weight distribution." This conclusion of Charlesby applies to effects produced in polymers of random distribution by doses equal to or higher than the gelling dose. To investigate whether differences between the two mechanisms could be detected below the gel point, the increase of the number and weight average molecular weights was calculated for various initial distributions, and several values of the parameters σ_c and σ_e.

It should be noted that in practice it is not easy to decide whether degradation, or a low value of, say, $\dot{c}$ is responsible for a high gelling dose. Therefore in statistical calculations doses are usually expressed in relation to the critical dose, rather than in absolute units. This method has been followed throughout the present investigations.

For the random distribution Eq. I-30 simplifies to

$$u_2^t(\tau) = \frac{u_2}{1 + u_1\tau} \quad . \qquad \text{I-54}$$

Then it is easy to show from Eqs. I-32 and I-44 that for any degree of degradation compatible with network formation the previously given equation

$$\frac{M''_w(R)}{M_w(0)} = \frac{1}{1 - R/R_g} \qquad \text{I-17}$$

applies to both endlinking and crosslinking. As shown later, the ratio $M''_n(R)/M_n(0)$ does depend on the mechanism and on the extent of degradation, but high accuracy is required for differentiation if the initial distribution is random.

Accordingly, it was decided to investigate the behavior of narrow range samples and their mixtures under irradiation. In particular, it was anticipated from preliminary calculations that a comparison of the properties of irradiated samples of different initial distributions would be useful in elucidating mechanisms of radiation-induced network formation.

To facilitate interpretation of subsequent experimental results, most of the computations were done for mixtures that could be made up from the available samples of narrow range polystyrene, listed in Table E-1 of the Experimental section. Gelling doses were calculated for several thousand possible mixtures. The results indicated that the extent of polydispersity had little influence on the critical dose for a crosslinking mechanism. In contrast, the gelling dose for endlinking was sensitive to the polydispersity. When two samples were compared, the higher the difference in the M_w/M_n ratios the easier it appeared to detect dissimilarities between crosslinking and endlinking.

As a result of these computations it was decided to use the following two samples for more detailed theoretical analysis and subsequent experimental investigations.

a. Pure S105, designated sample I. (M_n = 147,500, M_w = 153,500).

b. A mixture of S102 and S108 in the molar ratio 4:1, designated sample II. (M_n = 112,200, M_w = 164,000).

The initial distributions of these samples are shown in Fig. I-5.

Some of the theoretically expected values of t_g and τ_g, for different mechanisms and degrees of degradation, are given in Table I-1. More detailed results of the gelling dose calculations are tabulated in Appendix I. It will be noted that τ_g and t_g are proportional to the gelling dose. Therefore

$$\frac{t_g^{II}}{t_g^{I}} = \frac{\tau_g^{II}}{\tau_g^{I}} = \frac{R_g^{II}}{R_g^{I}} , \qquad \text{I-55}$$

where the superscripts I and II refer respectively to pure S105 and the mixture S102/S108. Included in Table I-1 are the ratios of gelling doses predicted for each mechanism and degree of degradation. It is evident that R_g^{II}/R_g^{I} predicted for endlinking exceeds the ratio anticipated for a crosslinking mechanism by nearly 30%. Thus the experimentally determined ratio R_g^{II}/R_g^{I} may be used as a criterion of crosslinking or endlinking, and it is apparent that no very great accuracy is required to choose between the two mechanisms.

It is expected that this technique will be particularly convenient to apply when differences in molecular weight distribution between two samples

FIG. I-5

Molecular weight distributions of samples S105 and S102/S108. The curves were plotted from Eqs. I-3 and I-6. The parameters u_1 and λ for each of the samples S102, S105, and S108 were calculated from the molecular weights, as listed in Table E-1 of the Experimental section.

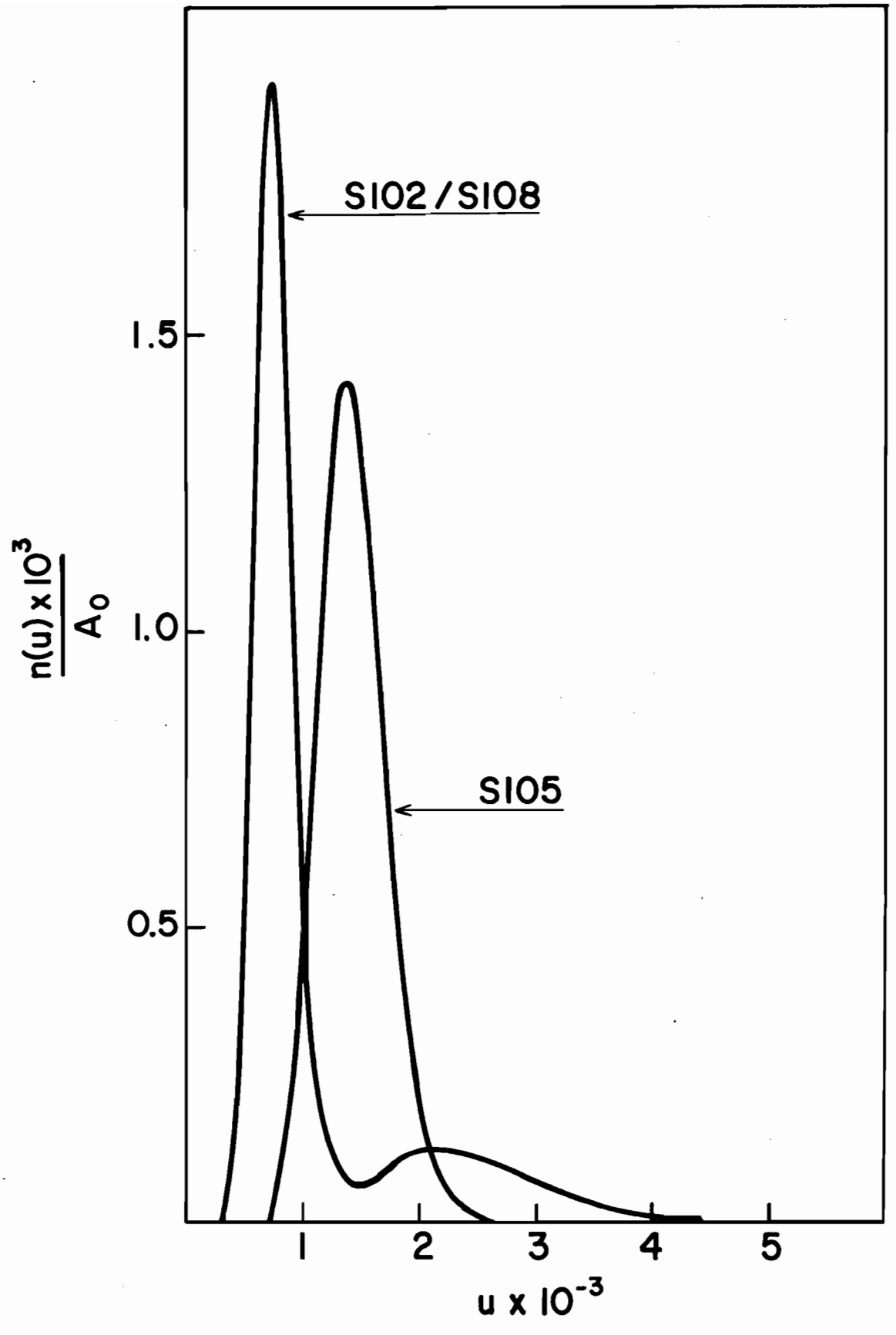
S102 / S108
S105
1.5
1.0
0.5
$\frac{n(u) \times 10^3}{A_0}$
1
2
3
4
5
u x 10^{-3}

TABLE I-1

Results of the gelling dose calculations for samples S105 and S102/S108

Sample	t_g for crosslinking x 10^4					τ_g for endlinking x 10^4					
	δ_c=1.5	δ_c=2.0	δ_c=2.5	δ_c=3.5	δ_c=∞	δ_e=0.5	δ_e=0.6	δ_e=0.7	δ_e=0.8	δ_e=0.9	δ_e=1.0
I	3.85	3.72	3.65	3.57	3.39	8.04	5.79	4.52	3.71	3.14	2.73
II	3.77	3.60	3.51	3.41	3.18	9.99	7.14	5.56	4.55	3.85	3.34
R_g^{II}/R_g^{I}	0.98	0.97	0.96	0.96	0.94	1.24	1.23	1.23	1.23	1.23	1.22

compared are large. It is, however, difficult to predict the gelling dose for substrates of high polydispersity. In such samples the probability of a second link formation between two long molecules may be of the same order of magnitude as the probability of link formation with short chains. This will interfere with the application of statistical treatments. Nevertheless, if a small amount of low molecular weight fraction were found to increase the gelling dose considerably for a pure high molecular weight polymer, this should prove that network formation in that substrate is due to endlinking.

From the results of Table I-1 it is clear that gelling dose ratios are insensitive to the value of δ_c or δ_e. However, it was found that the increase in the number average molecular weight up to the gel point could be used to determine the extent of degradation. The increase in the number average molecular weight is usually not pronounced during irradiation. Eq. I-14 can be written in the form

$$\frac{M_n''(R)}{M_n(0)} = \frac{1}{1 - \frac{u_1}{u_2} u_2 t_g \frac{t}{t_g}} = \frac{1}{1 - \frac{u_1}{2u_2} \frac{t}{t_g}} , \qquad \text{I-56}$$

which shows that for a crosslinking mechanism and an initially random distribution the number average molecular weight cannot exceed 1.33 times the initial value. However, as illustrated in Table I-2, calculations based on Eqs. I-14, I-31, and I-43 demonstrated that for the narrow distribution samples the maximum $M_n''(R_g)/M_n(0)$ value can be over 1.9, and comparatively small differences in the extent of degradation will result in a 10% change. Thus molecular weight measurements by osmometry appear

TABLE I-2

Calculated $M_n''(R_g)/M_n(0)$ values for S102 and random distribution samples

Sample	$M_n''(R_g)/M_n(0)$ for crosslinking					$M_n''(R_g)/M_n(0)$ for endlinking					
	$\sigma_c=1.5$	$\sigma_c=2.0$	$\sigma_c=2.5$	$\sigma_c=3.5$	$\sigma_c=\infty$	$\sigma_e=0.5$	$\sigma_e=0.6$	$\sigma_e=0.7$	$\sigma_e=0.8$	$\sigma_e=0.9$	$\sigma_e=1.0$
S102	1.22	1.35	1.44	1.56	1.91	1.00	1.20	1.34	1.46	1.55	1.63
Random	1.11	1.17	1.20	1.24	1.33	1.00	1.17	1.29	1.38	1.44	1.50

to be a good way of determining the values of σ_c and σ_e if narrow range polymers of known distribution are used. It can also be seen that if no degradation takes place osmotic measurements constitute a method of distinguishing between crosslinking and endlinking, provided sufficient accuracy may be achieved in the determination of M_n.

The number average branching indices at the gel point were computed from Eqs. I-20, I-37, and I-49, and are given in Table I-3. For crosslinking there is a strong dependence on molecular weight distribution and on the extent of degradation, while the results obtained for endlinking are comparatively insensitive to these factors. It is difficult to see, however, how B_n could be determined experimentally with any degree of accuracy.

Values of $M_w''(R)/M_w(0)$ were calculated from Eqs. I-17, I-32, and I-44, and are plotted against R/R_g in Fig. I-6. For small degrees of degradation, and in the case of crosslinking even for considerable degradation, the shapes of the curves are almost independent of the number of scissions. Also, the effect of molecular weight distribution is small, and in general there is little difference between curves obtained by assuming different mechanisms. Therefore it would be extremely difficult to establish the mechanism by light-scattering measurements. On the other hand, light-scattering may be a suitable technique for testing the validity of basic statistical assumptions, because of the lack of strong dependence of M_w on various interfering factors. This will be discussed in more detail in the Experimental Results and Discussion part.

The weight average branching index, as calculated from Eqs. I-21,

TABLE I-3

Calculated values of the number average branching index at the gel point for S102 and random distribution samples

Sample	B_n at $R = R_g$ for crosslinking					B_n at $R = R_g$ for endlinking					
	$\sigma_c=1.5$	$\sigma_c=2.0$	$\sigma_c=2.5$	$\sigma_c=3.5$	$\sigma_c=\infty$	$\sigma_e=0.5$	$\sigma_e=0.6$	$\sigma_e=0.7$	$\sigma_e=0.8$	$\sigma_e=0.9$	$\sigma_e=1.0$
S102	1.66	1.71	1.74	1.78	1.91	1.57	1.59	1.60	1.61	1.62	1.63
Random	1.33	1.33	1.33	1.33	1.33	1.50	1.50	1.50	1.50	1.50	1.50

FIG. I-6

The increase of the weight average molecular weight during irradiation. Within the accuracy of this graph, the curve for crosslinking is representative of the expected increase in molecular weight for both samples S102/S108 and S105, and for no degradation as well as for a significant extent of degradation ($\sigma_c = 0.50$). The other full curves refer to the sample S105, while the dashed curves represent the sample S102/S108.

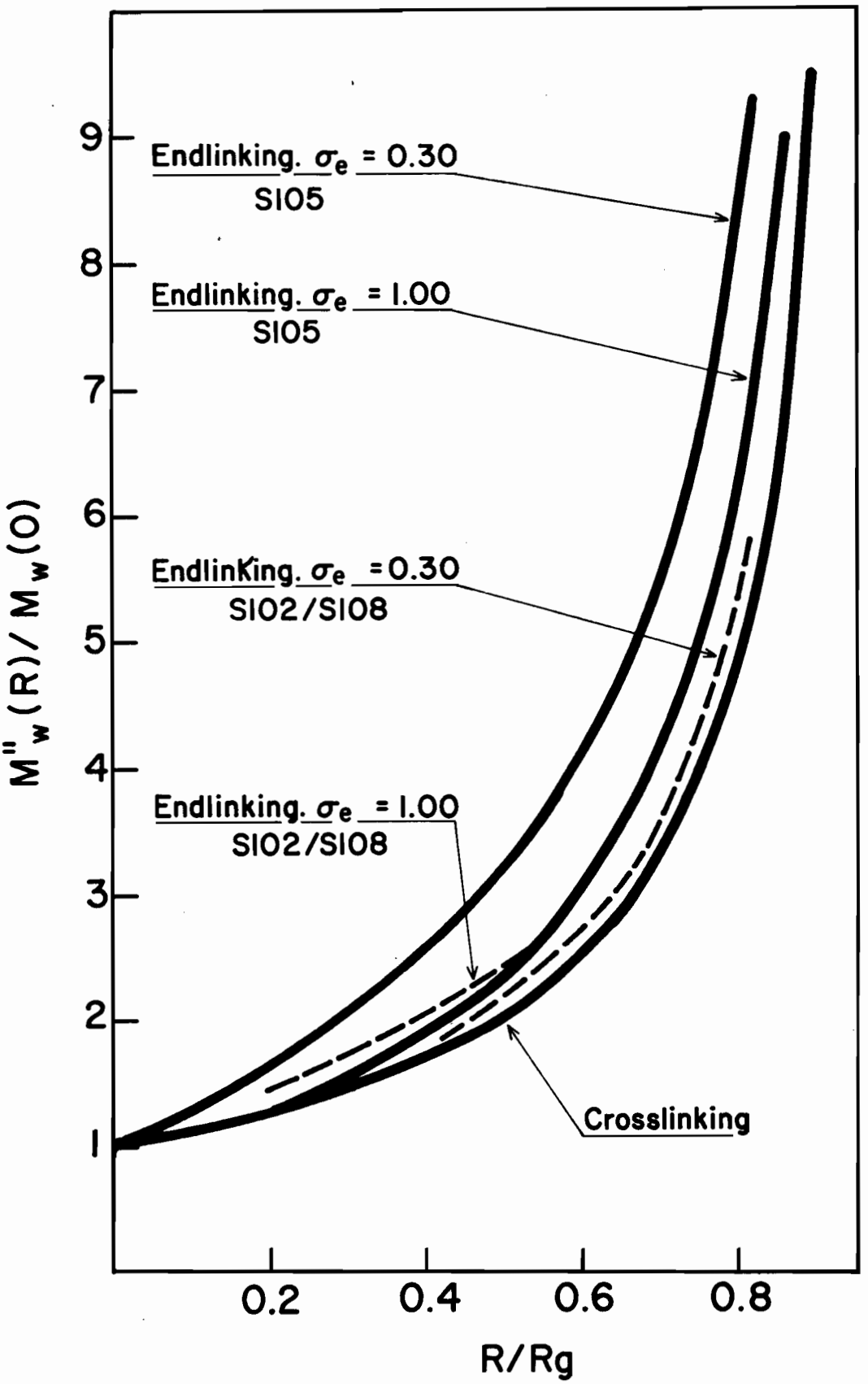
Endlinking. σ_e = 0.30
S105
Endlinking. σ_e = 1.00
S105
EndlinKing. σ_e = 0.30
S102/S108
Endlinking. σ_e = 1.00
S102/S108
Crosslinking
$M''_w(R)/M_w(0)$
R/Rg
1
2
3
4
5
6
7
8
9
0.2
0.4
0.6
0.8

I-38, and I-50, is also largely independent of the mechanism, at least if the extent of degradation is small. A high proportion of scissions leads to the formation of a significant number of heavily branched molecules before gel formation can take place. This is reflected in the curves of Fig. I-7.

It should be noted that the above conclusions regarding the importance of molecular weight distribution are of a perfectly general nature. In particular, there is every reason to expect that the effect of distribution could be used to establish the mechanism in polymers other than polystyrene.

Application of the statistical conclusions of the present section will be described in the Experimental Results and Discussion part.

FIG. I-7

Weight average branching index
as a function of radiation dose.
Calculated values for samples
S105 and S102/S108.

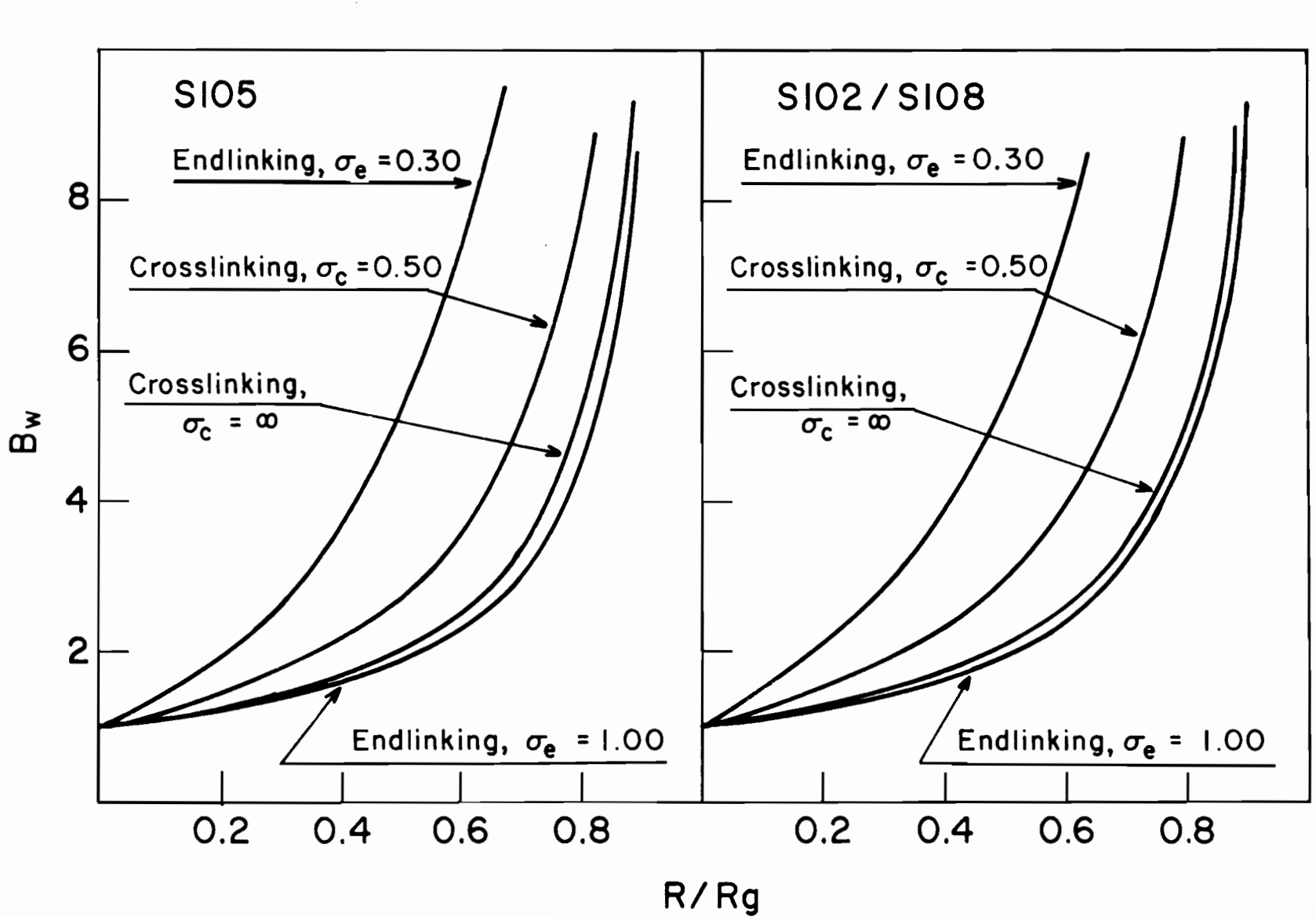
S105
Endlinking, σ_e = 0.30
Crosslinking, σ_c = 0.50
Crosslinking, σ_c = ∞
Endlinking, σ_e = 1.00
S102 / S108
Endlinking, σ_e = 0.30
Crosslinking, σ_c = 0.50
Crosslinking, σ_c = ∞
Endlinking, σ_e = 1.00
B_w
2
4
6
8
0.2
0.4
0.6
0.8
R / Rg

EXPERIMENTAL RESULTS AND DISCUSSION

Surface Effects

It is now generally accepted that the formation of polystyryl radicals and free hydrogen atoms is one of the fundamental processes in the irradiation of polystyrene. Hydrogen atoms may take a significant part in crosslinking processes, by producing new macroradicals through addition or hydrogen abstraction and by entering into recombination reactions with other free radicals (61). It is reasonable to expect that a number of hydrogen atoms will leave the substrate without participating in reactions. The probability of such 'escapes' will increase with the specific surface. Therefore the magnitude of the effect of ionizing radiations may be strongly dependent on the particle size (60). This, of course, would considerably limit the applicability of statistical calculations. Accordingly, prior to undertaking a detailed statistical analysis, it was thought advisable to investigate the possible role of specific surface in the radiation chemistry of polystyrene.

As a first step, the irradiation of polystyrene beads of two different sizes was performed. The samples were M1 and M2, with specific surfaces of 25 and 100 $cm.^{-1}$, respectively, as shown in Table E-2 of the Experimental part. The increase of intrinsic viscosity with dose is shown in Table I-4. From the trends in Table I-4 it appears that the differences in the behavior of M1 and M2 are negligible, although comparable variations in particle size have a significant effect when polyethylene is irradiated in air (69).

TABLE I-4

The effect of irradiation on the intrinsic viscosities of polystyrene beads

Dose	$[\eta]$		$[\eta]/[\eta]_o$	
	M1	M2	M1	M2
Mrad.	dl.g.$^{-1}$			
0	0.957	0.827	1.00	1.00
13.8	1.080	0.947	1.13	1.15
17.8	1.076	0.926	1.12	1.12
29.7	1.150	0.982	1.20	1.19

The results for samples M1 and M2 indicated that surface effects, if existing at all, would be small and perhaps could be masked by the action of impurities or differences in molecular weight distribution. Accordingly, further experiments were carried out, in which high purity polystyrene in the form of rods of low specific surface or highly porous freeze-dried material was used. Preparation of these samples is described in the Experimental part. As shown in Table I-5, no appreciable differences could be detected between the increase of the intrinsic viscosity produced in the rods and in the freeze-dried polystyrene, in spite of the extremely large difference in specific surface. The increase in $[\eta]$ for the freeze-dried material at higher doses is opposite to the trend expected if escape of reactive hydrogen atoms from the samples

TABLE I-5

The effect of irradiation on the intrinsic viscosities of polystyrene samples obtained by thermal polymerization

Dose	$[\eta]$	
	Rods	Freeze-dried P/S
Mrad.	$g.dl.^{-1}$	
0	1.45	1.45
6.6	1.63	1.66
11.7	1.65	1.54
13.3	1.65	1.73
19.8	1.83	1.94
26.2	Trace of gel	Trace of gel

were reducing the chemical effect of the irradiation. Although these results do not exclude altogether the possibility of surface effects, at least such effects must be small in the radiation chemistry of polystyrene. This conclusion is in agreement with previous measurements of Alexander and Toms (70).

The absence of surface effects would be expected if it is assumed that hydrogen atoms react with the monomer units so readily that atomic

hydrogen cannot escape from the irradiated polymer. This hypothesis is strongly supported by the mass spectrometric results of Burlant and Neerman (47). According to these authors hydrogen evolution in irradiated polystyrene is due to hydrogen abstraction, rather than a gas phase combination of free hydrogen atoms. Furthermore, there is some experimental evidence (71) that the addition of atomic hydrogen to double bonds (reaction C-3 of the Historical Introduction) takes place at a reaction rate high enough virtually to exclude diffusion processes.

In all subsequent experiments of the present work surface effects were assumed to be negligible, and no particular care was taken to measure or control the surfaces of samples to be irradiated. However, only freeze-dried material was used when two samples of different distributions were compared.

Effect of Intensity

Statistical calculations are always based on the supposition that the intensity of the radiation source does not affect the chemical yields, except through the total absorbed dose. Good agreement between experimental results obtained under different conditions has often justified this assumption.

Comparison of experimental data yielded by different irradiation techniques is facilitated by defining the so-called G values, which give the number of radiation chemical events per 100 eV energy absorbed. For polystyrene several researchers (2-4,44) have determined crosslink yields

and, as shown in Table I-9, their G values are in good agreement, in spite of the widely different radiation sources used. This seems to be at variance with the results of Feng and Kennedy (22), who found a strong dependence of the increase of intrinsic viscosity on dose-rates.

In the present work experiments were not specifically designed to test the possible role of intensity. It is significant, however, that within experimental error no differences could be detected between samples irradiated in Ottawa and those irradiated in Montreal, even though the ratio of the actual dose-rates of the two radiation sources was almost 15 to 1. The standard deviation of the G value for cross-link formation, as calculated from the data listed in Table I-7, is only about 3%, which compares very favorably with previously reported measurements (4,44). The data of Table I-7 include results obtained both for samples irradiated in Montreal and samples irradiated in the more powerful Gammacell unit in Ottawa. Therefore these results indicate that over a wide range of intensities crosslink yields are proportional to the total absorbed dose.

Tests of the Statistical Theory by M_w Determinations

Direct evidence for the applicability of statistical results was given by the variation of weight average molecular weight, as determined by the light-scattering technique.

It was shown in the Theoretical section that one of the conseq-

uences of the random nature of linking and scission processes is that when $M''_w(R)/M_w(0)$ is calculated as a function of R/R_g, the results are largely independent of the initial distribution (Fig. I-6). Moreover the curves of Fig. I-6 are remarkably similar for crosslinking and endlinking, at least if degradation is not pronounced. The results of weight average molecular weight determinations can therefore be predicted with considerable accuracy even if the linking mechanism and the proportion of scissions and linkages are not precisely known. Thus light-scattering measurements on irradiated polymers appear to be a useful technique for investigating the validity of basic statistical assumptions when no details of the radiation chemical processes are known.

Accordingly, it was decided to test the statistical theory by light-scattering measurements on S105 and S102/S108 samples irradiated to various extents. The molecular weight distributions of these samples were given in the Theoretical section (Fig. I-5). Preparation, evacuation, and irradiation of the samples is discussed in the Experimental part. The gelling doses for S105 and S102/S108, as given in Table I-7, were calculated from viscometric data. In Fig. I-8 $M''_w(R)/M_w(0)$ is plotted against R/R_g. The curve in Fig. I-8 is the theoretical curve for crosslinking without degradation. As discussed in the Theoretical section, this curve would be essentially unchanged for all but very large extents of degradation and would also represent endlinking reasonably well both for S105 and S102/S108.

As shown in Fig. I-8, the experimental values of $M''_w(R)/M_w(0)$

FIG. I-8

Increase of the weight average molecular weight of samples S105 and S102/S108 plotted against R/R_g. The full curve is the theoretical increase in crosslinking.

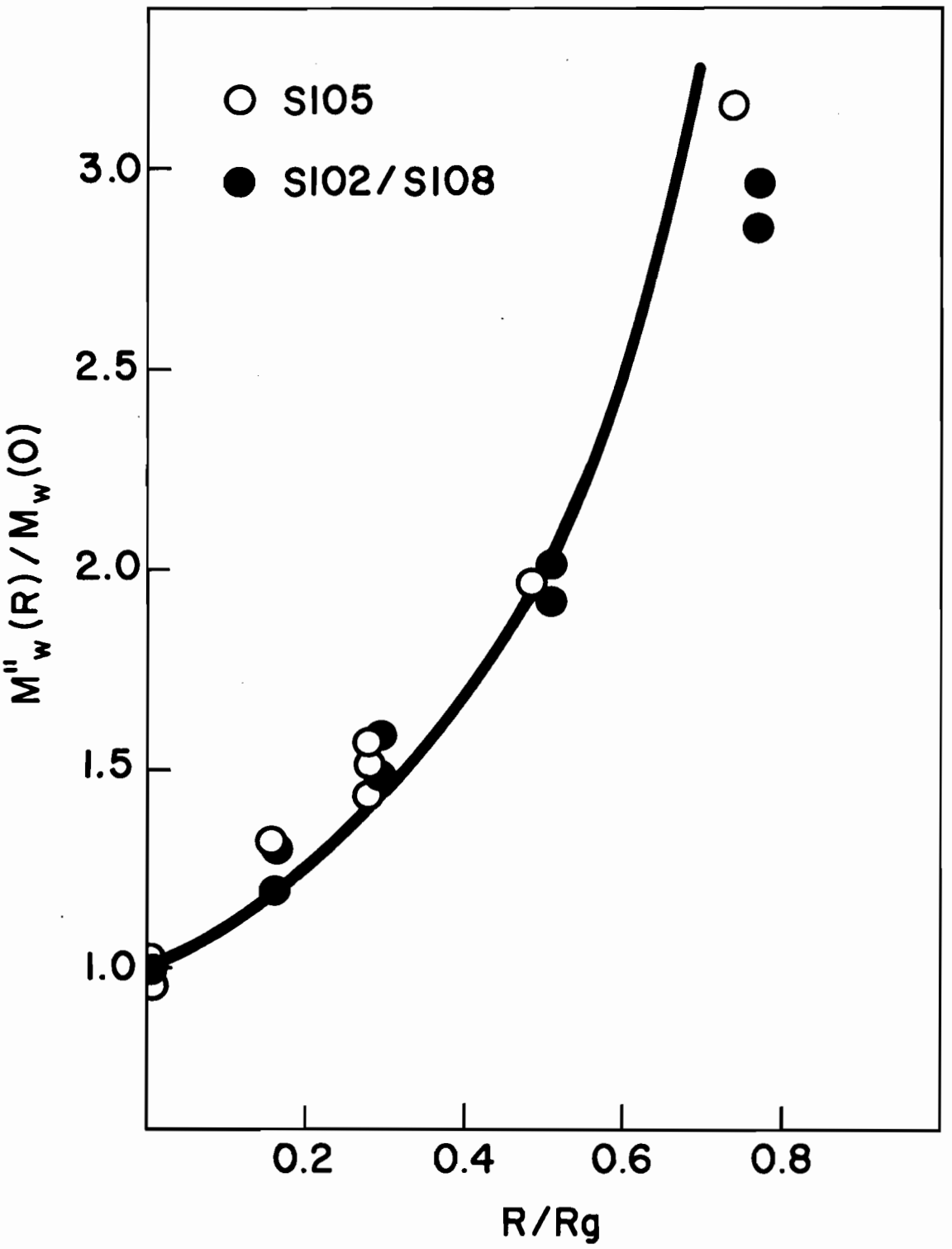
S105
S102/S108
3.0
2.5
2.0
1.5
1.0
$M''_w(R)/M_w(0)$
0.2
0.4
0.6
0.8
R/Rg

were in agreement with the statistical theory. The increase in the molecular weight was in accordance with the predicted trend, although molecular weights at high doses fell somewhat below the theoretical curve. However, the latter result could have been due to the loss of some highly crosslinked polymer during centrifugation. Also, no appreciable differences could be observed between S105 and S102/S108, in spite of the widely different initial distributions (Fig. I-5 of the Theoretical section). Thus, light-scattering data confirmed the validity of assumptions implicit in the statistical derivations. In view of the lack of interfering surface and intensity effects, it therefore seemed justified to interpret further experimental data in the light of previously described theoretical results.

Relative Importance of Crosslinking and Endlinking

It was shown in the Theoretical part that the relative importance of crosslinking versus endlinking may be determined by comparing samples of different initial distributions. The samples specifically considered were S105 (sample I) and S102/S108 (sample II), i.e. the same substrates that were used in the light-scattering measurements discussed in the previous paragraphs. From the statistical analysis it was predicted (Table I-1 of the Theoretical section) that the ratio R_g^{II}/R_g^{I} would be approximately 0.96 for crosslinking and 1.23 for endlinking, with the exact value depending on the degree of simultaneous degradation.

Accordingly, S105 and S102/S108 samples were irradiated, and the

relative viscosities of their solutions in toluene were measured at 25°C, at a concentration of 0.6 $g.dl.^{-1}$ The critical doses were determined by extrapolating the viscosity-dose curves to 'infinite' viscosity, as shown in Fig. I-9. The obtained critical dose values were in good agreement with other viscometric data (Table I-7).

R_g^{II}/R_g^I was found to be 0.95, in excellent agreement with the theoretical value for crosslinking. This result confirms conclusively that crosslinking is the predominant mechanism in the irradiation of polystyrene, and thereby supports the previous hypotheses of Wall and Brown (44), Burlant, Neerman, and Serment (4,47), and Pravednikov and In Shen-Kan (43), as reviewed in the Historical Introduction.

It should be pointed out that the theoretical basis of the above method of distinguishing between crosslinking and endlinking is perfectly general. Moreover any systematic errors in the gelling dose determinations are likely to cancel out when the ratio is calculated. Therefore application of the above technique should lead to reliable conclusions for a variety of polymers. In particular, it could be a powerful tool of detecting endlinking in polymers such as irradiated polyvinyl alcohol, where this mechanism has been suggested to occur in aqueous solution (72).

Critical Dose Determinations

Apart from the results mentioned in the previous paragraphs, experimental values of the gelling doses were obtained by extrapolating

FIG. I-9

Determination of the gelling dose for samples S105 and S102/S108. The empty circles represent experimental points for S105, full circles represent S102/S108.

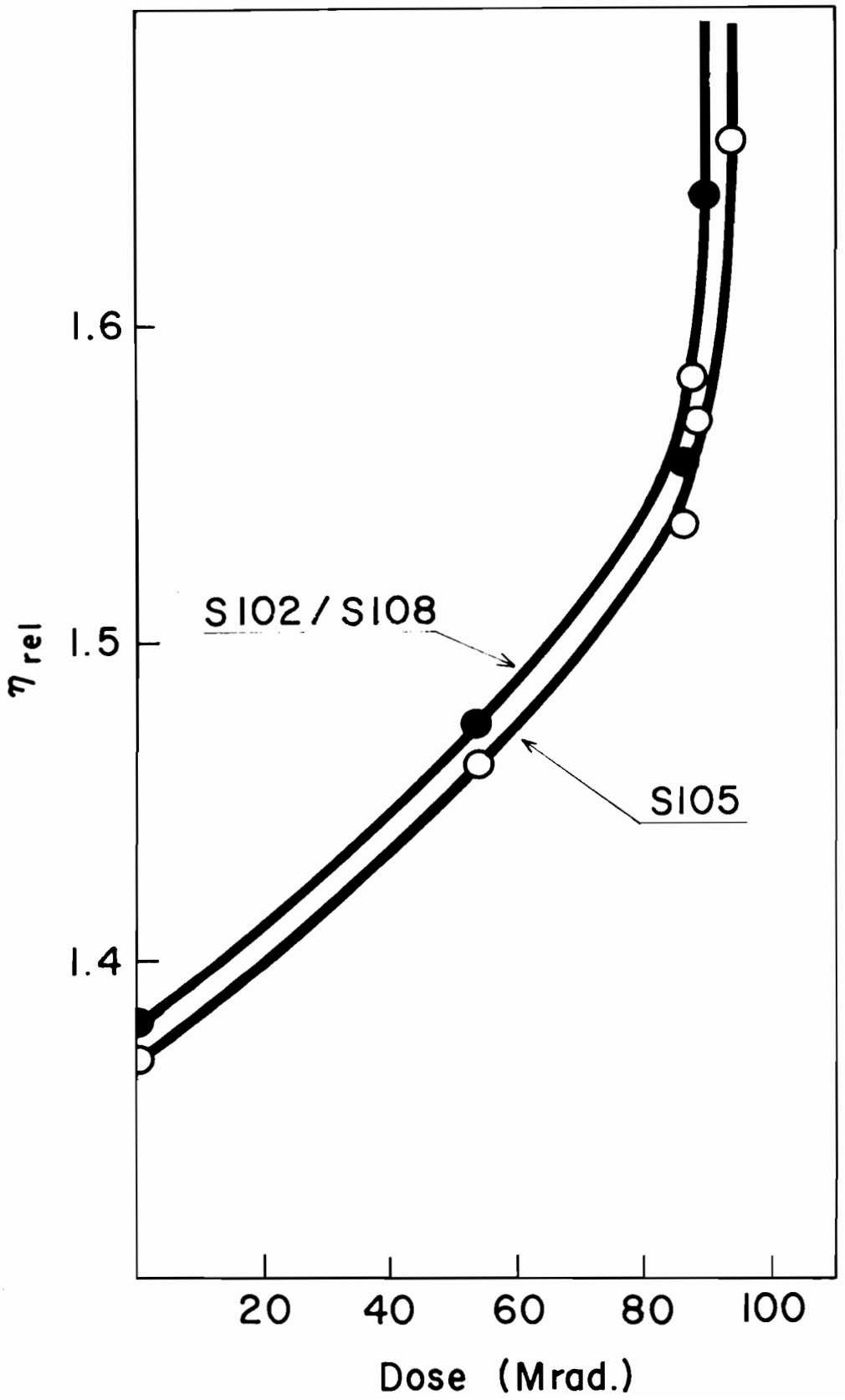
1.6
1.5
1.4
η_{rel}
S102 / S108
S105
20
40
60
80
100
Dose (Mrad.)

TABLE I-6

Calculated values of the product $t_g x u_2(0)$ for anionic polystyrene samples

Sample	$t_g x u_2(0)$			
	σ_c=1.0	σ_c=2.0	σ_c=3.5	σ_c=5.0
S102	0.611	0.549	0.526	0.518
S105	0.611	0.549	0.526	0.518
S108	0.615	0.550	0.527	0.519
S109	0.612	0.549	0.527	0.518
S102/S108	0.657	0.567	0.536	0.525

intrinsic viscosity-dose curves (Fig. I-10).

As shown in Table I-6, it was anticipated from gelling dose calculations that the product $u_2 x R_g$ would be essentially the same for all samples studied. The $u_2 x R_g$ values calculated from experimentally obtained critical doses are in agreement with the theory* (Table I-7). The average value of $u_2 x R_g$ was found to be 1.33×10^5 Mrad., with a standard deviation of 0.04×10^5 Mrad. The good agreement obtained for different samples constitutes an added proof of the applicability of statistical calculations.

---

* For the S102/S108 sample a small correction was applied for polydispersity, based on the data of Table I-6.

FIG. I-10

Determination of the critical dose by extrapolation of intrinsic viscosity-dose curves. The full circles represent the mean of two or three almost coincident experimental points.

TABLE I-7

Experimental values of the critical dose for anionic polystyrene samples of various degrees of polymerization

Sample	u_2	R_g from viscometry	$u_2 R_g \times 10^{-5}$	Smoothed out values of R_g
		Mrad.	Mrad.	Mrad.
S105	1470	94.1	1.383	90.2
S108	2570	47.5	1.221	51.7
S109	1850	71.4	1.321	71.8
S102/S108	1570	89.8	1.385[a]	85.9

[a] Corrected for polydispersity.

From the average value of $u_2 \times R_g$ the gelling doses were recalculated, leading to the 'smoothed out' results of Table I-7. In subsequent calculations these corrected R_g values were used for expressing doses in the form R/R_g.

Degradation

As shown by Eqs. I-14, I-31, and I-43 of the Theoretical section, irradiation usually increases the number average molecular weight of network-forming polymers, although this effect is often small. The validity

of Eqs. I-14, I-31, and I-43 is limited to doses not exceeding the critical dose. After the gel point M_n of the soluble fraction decreases rapidly (15). Therefore osmotic measurements on solutions of irradiated polymers are best to perform near the point of incipient gel formation.

Table I-2 of the Theoretical section illustrates the influence of initial molecular weight distribution on the maximum value of M_n, and the advantage of using narrow range samples. It is evident from Table I-2 that for such samples the value of $M_n''(R_g)/M_n(0)$ is highly sensitive to the extent of degradation, in particular when degradation is not pronounced, as in the case of polystyrene irradiated in vacuo.

Accordingly, the extent of degradation was estimated from osmotic measurements. In Table I-8 the osmotic results are compared to values obtained by McCormick. The agreement is as reasonable as can be expected for measurements carried out by different techniques, in different laboratories. The number average molecular weight of unirradiated SiO2 was taken to be the average of the value obtained in the present study and the one calculated by McCormick.

From the results of gelling dose determinations R_g for SiO2 was calculated to be 167.8 Mrad. The actual dose given the irradiated SiO2 sample used in osmotic measurements was slightly higher (169.2 Mrad.). After the gel point the number average molecular weight of the soluble fraction begins to decrease at roughly the same rate as it increases when approaching the gel point (15), and therefore in the computation of $\sigma_c R/R_g = 0.992$ was assumed. Then from equation I-31 and the computed

TABLE I-8

Results of the number average molecular weight determinations

Sample	M_n	
	Present osmotic measurements	McCormick
unirradiated S105	139,400	147,500
unirradiated S102	62,800	78,500
169 Mrad. S102	108,900	-

values of τ_g given in Appendix I σ_c could be determined. The result obtained was $\sigma_c = 3.5$, which corresponded to a rather low degree of degradation.

It is of interest to compare this value with results reported by other researchers. The majority of published data show the extent of degradation to be very small (2,4), however Shultz and collaborators (3) reported a comparatively high degradation. It has been suggested (73) that their results might have been due to the presence of oxygen. In contrast, certain data derived from solubility studies have indicated the total absence of degradation (4). The determination of σ_c from solubility measurements is usually based on the previously given equation

$$s' + \sqrt{s'} = \frac{1}{2\delta_c} + \frac{1}{2u_1'R}, \qquad \text{I-52}$$

where s' is the soluble fraction at dose R. It will be noted that if δ_c = 3.5 then the soluble fraction at high doses will be less than 2%. Accordingly small degrees of degradation can easily remain undetected by the solubility technique. Therefore the osmotic technique, as used in the present work, is superior to solubility measurements for determining the number of main chain scissions in irradiated polystyrene.

Calculation of G Values

Once the critical doses and the extent of degradation were known the G values for crosslinks and scissions could be computed. At the gel point

$$1 - 2u_2'(\tau)t = 0, \qquad \text{I-33}$$

which means that the number of crosslinks per gram of polymer equals $\underline{N}/(2M_w'(R_g))$, where $\underline{N}$ is Avogadro's number. If R_g is measured in megarads, the formation of the above number of crosslinks corresponds to the absorption of $R_g \times 10^8$ ergs, or $R_g \times 0.624 \times 10^{20}$ eV, because 1 rad corresponds to the absorption of 100 ergs of energy per gram of exposed sample. Therefore the number G of crosslinks formed per 100 eV absorbed energy is given by

$$G = \frac{1}{R_g \times M_w'(R_g)} \times \frac{6.02 \times 10^{23}}{2 \times 0.624 \times 10^{18}} = \frac{0.48 \times 10^6}{R_g \times M_w'(R_g)}. \qquad \text{I-57}$$

If the 'smoothed out' values of R_g are used in the calculations, the product $R_g x M'_w(R_g)$, and hence the G value, will be constant. Calculation of this radiation chemical parameter may be illustrated as follows.

For S105, R_g = 90.2 Mrad. (Table I-7), and ζ_g, the zero of Eq. I-34 for u_1 = 1417, λ= 25, and σ_c = 3.50, equals 1.02 x 10^{-4}. Then from Eq. I-30 $u'_2(\zeta_g)$ = 1400, i.e. $M'_w(R_g)$ = 145,800. Substituting this result into Eq. I-57, the G value for crosslink formation was found to be 0.0365, from which the energy absorption per crosslink equals 100/ 0.0365 = 2740 eV per crosslink. According to the results discussed in the previous paragraphs, only one main chain scission occurs per 3.5 crosslinks formed. Therefore the energy absorption per main chain scission is 3.5 x 2740 = 9600 eV. The main results are compared with the data of other researchers in Table I-9.

It is interesting to note that the crosslink yields of the present work are lower than those previously reported in the literature. It is difficult to say whether the difference is meaningful, since the G values quoted in the literature are usually considered accurate only to $\pm$ 20% (73). It may be, however, that crosslink formation is indeed less pronounced for the anionic polystyrenesused in the present investigations.

To the best of the writer's knowledge there have been no indications that the bulk properties of polystyrene prepared by the method of Szwarc (62) are different from those of ordinary polystyrene, in a manner that could influence radiation chemical yields. Also it seems

TABLE I-9

G values for crosslinking and scission in irradiated polystyrene, as obtained by various experimental techniques

Reference	G (cross-link)	G (scission)	σ_c	Radiation source	Techniques of polymer characterization
Charlesby (2)	0.048[a]	0-0.02	2.5-∞	Atomic pile	Solubility and swelling measurements
Shultz et al. (3)	0.058	0.041	1.43	Electron beam generator	Solubility measurements
Wall and Brown (44) (three different samples)	0.054 0.049 0.045	- - -	- - -	Co^{60} gamma rays	Viscometric gelling dose determinations
Burlant et al. (4)	0.048[b] 0.051[c]	0[d]	∞	Co^{60} gamma rays	Viscometric gelling dose determinations, M_n, solubility measurements
Present work	0.036	0.01	3.50	Co^{60} gamma rays	As described in text

[a] The initial molecular weight of the polymer used in this work was not known accurately. Two estimates given in (2) are $M_w(0)$ = 310,000 and 430,000. G values were calculated by the writer on the basis of $M_w(0)$ = 370,000.

[b] From viscometric data.

[c] From the number average molecular weight of irradiated samples.

[d] From solubility measurements.

unlikely that the nature of end groups could have a significant effect. Therefore one would tend to ascribe differences in G values to the unusual molecular weight distribution produced by the anionic process. Commercially available polystyrenes usually contain a significant portion of material with molecular weight well below 50,000. In contrast, none of the anionic samples used in the present work contained an appreciable fraction of low molecular weight material. Thus, although the results indicated the lack of distribution effects, the influence of very low molecular weight material was not considered.

It has been shown (64) that the high shear melt viscosity of anionic polystyrene is greater than that of broad distribution samples of the same molecular weight. It was suggested (64) that this difference could arise as a consequence of the plasticizing effect of shorter molecules in the more polydisperse samples. According to this hypothesis the presence of molecules of low degree of polymerization would decrease the melt viscosity by facilitating the disentanglement of the long molecules. In an analogous manner, it seems possible that the presence of short chains in solid polymers might facilitate microbrownian motion, which, in turn, could contribute to the probability that a crosslink will form at a given site. This hypothesis is somewhat contradicted by the results of Burlant, Neerman, and Serment (4), who found that between -196 and 65°C crosslink yields in polystyrene are largely independent of the temperature - and hence of the microbrownian motion. However, these findings are difficult to reconcile with the pronounced effect of temperature on hydrogen yields, as reported in the same paper.

It must be concluded that more, and highly accurate experimental work will be required to obtain a definitive answer concerning the role of molecular weight distribution and other second order effects in the radiation chemistry of polystyrene.

Virial Coefficients

The experiments discussed so far were all related to the testing and application of the statistical theories of linking and degradation. The quantities determined depended on the number and distribution of radiation-induced linkages and scissions. No experiments were specifically designed to study intermolecular interaction in solution, as measured by the osmotic and light-scattering second virial coefficients (A_2). Nevertheless, values of A_2 were calculated, and may be compared with certain theoretically predicted and experimentally observed trends described in the literature.

The osmotic coefficients (A_2^{π}) were computed from the slopes of the linear h/c vs. c plots (Fig. E-7 of the Experimental section) by means of Eq. E-9, and are given in Table I-10. Coefficients were determined for only three different samples, and therefore it is difficult to draw conclusions from their values. The results for the unirradiated samples, however, are in excellent agreement with data reported in the literature (74-76).

The light-scattering second virial coefficients (A_2^{τ}), as calculated from the slopes of the turbidity plots by means of Eq. E-5 of the Experimental section, are given in Fig. I-11. As expected (77), these

TABLE I-10

Experimental values of the osmotic second virial coefficient

Sample	$A_2^{\pi} \times 10^4$
	mole $g.^{-2}$ $cm.^3$
Unirradiated S105	4.75
Unirradiated S102	5.73
169 Mrad. S102	3.90

values are somewhat lower than those obtained by osmotic measurements. The most conspicuous feature of Fig. I-11 is the lack of difference between the S105 and S102/S108 samples. At first sight this appears to contradict previous results, since it has been established both theoretically (78-80) and experimentally (81) that polydispersity decreases A_2^{τ}. Closer examination of the literature reveals, however, that the theory predicts and experiments show a significant reduction in the values of virial coefficients only when the components of the polymer mixtures are of widely different (by a factor of ten or more) molecular weights. In particular, Cooper, Evans, and Vaughan (81) attributed experimentally found decreases in A_2^{τ} mainly to the presence of microgel. Moreover, it has been shown theoretically (78,82) that in two-component systems A_2^{τ} may actually assume a maximum at a certain

FIG. I-11

The effect of irradiation on the light-scattering second virial coefficient of samples S105 and S102/S108.

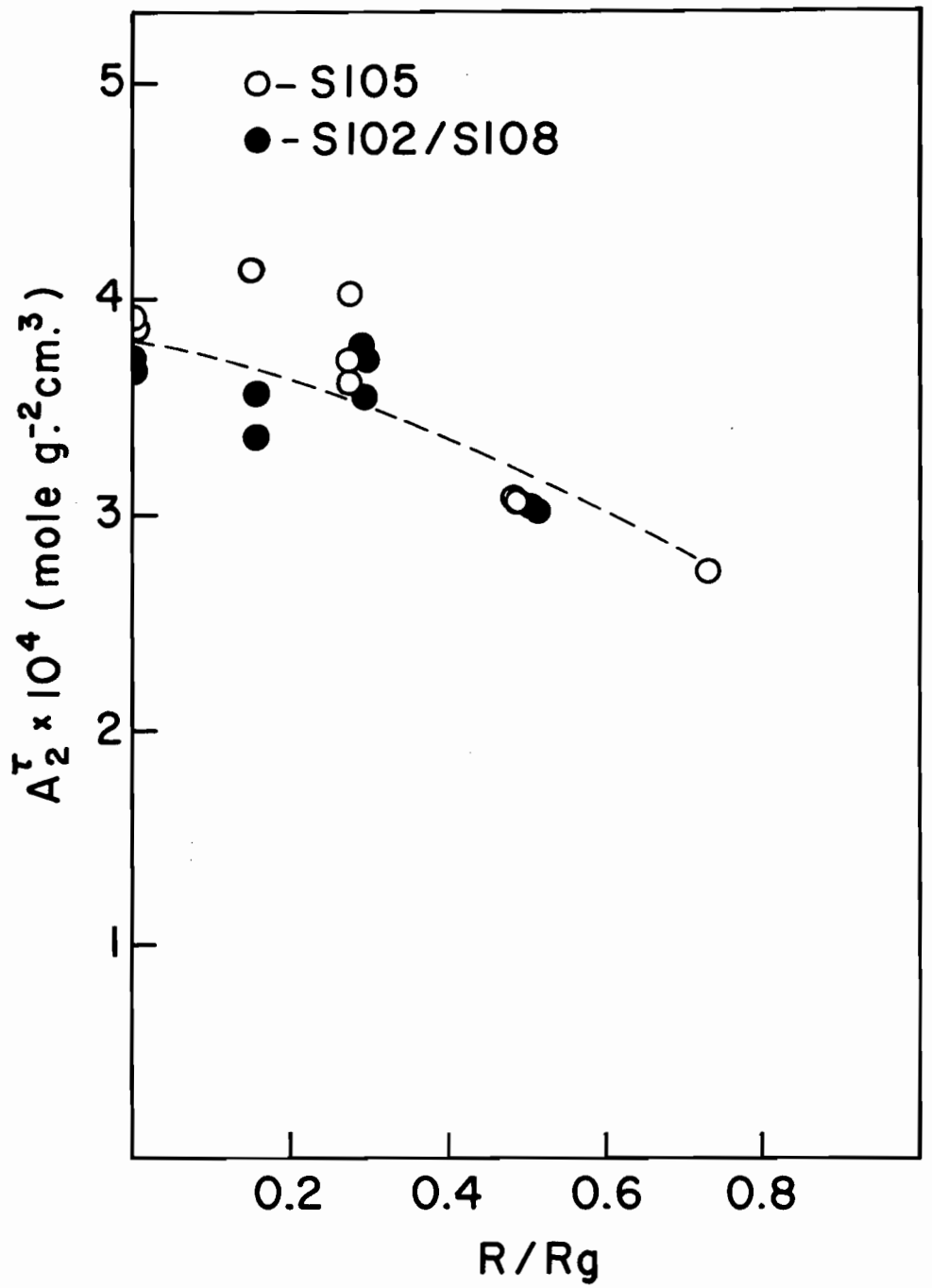
O- S105
● - S102/S108
$A_2^{\tau} \times 10^4$ (mole g.$^{-2}$cm.^{3})
5
4
3
2
1
0.2
0.4
0.6
0.8
R/Rg

proportion of the high and low molecular weight components. In view of the relatively low polydispersity of the mixed sample it is therefore not surprising that no appreciable differences in A_2^{τ} were found between the S105 and S102/S108 samples.

As shown in Fig. I-11, there was a small but definite decrease in A_2^{τ} with increasing dose, which was probably caused by branching. The effect of branching on second virial coefficients has been studied by several authors (26,77,81,83-87), and almost invariably a lowering of A_2^{π} and A_2^{τ} was found. Morton and collaborators (87) succeeded in synthetising virtually monodisperse samples of branched polystyrene, by reacting 'living' polystyrene with silicon tetrachloride. These authors found that branching reduced A_2^{τ} by about 40% in benzene solution, but the influence of branching was difficult to detect in a poor solvent (butanone). However, in many investigations polydisperse samples were used, and the changes observed in A_2 may have been due to changes in molecular weight distribution, rather than branching. To separate the effects of branching from those of polydispersity, Cooper and collaborators (81) carried out a rigorous experimental analysis of the properties of polybutadiene and trans-polyisoprene. They concluded that the significant decrease of A_2^{τ} accompanying branching was mostly due to polydispersity. Also, Peterlin's data for branched polyvinyl chloride (86) show that A_2 may be actually higher for branched molecules than for the corresponding linear polymer.

It is then difficult to evaluate the influence of branching on second virial coefficients from the existing experimental data. The results

of theoretical treatments are also somewhat inconclusive. Some of the better known formulas for calculating virial coefficients are due to Zimm, Stockmayer, and Fixman (27,88). Their results for tetrafunctional cruciform molecules indicate that branching should decrease A_2, but, as Stockmayer and Fixman (27) pointed out, the formulas are quantitatively of little value. Flory and Krigbaum (78) have also developed an expression for A_2, which should be valid for branched molecules too (27). The quantitative validity of this formula is again doubtful (75), but it also indicates that branching decreases the second virial coefficients.

In conclusion it would thus appear that many experimental and theoretical results can be accounted for by assuming that branching does lower A_2, but the effect is not pronounced. The data of the present work, as shown in Fig. I-11, are in agreement with this hypothesis. There is a slight decrease in A_2^{τ} with dose but, in view of the changes expected due to increased molecular weight and polydispersity, the influence of branching must be small.

SUMMARY

In an effort to develop new techniques for studying the effects of irradiation on high polymers, and in particular on polystyrene, the influence of molecular weight distribution was investigated. From general mathematical expressions obtained by Saito, equations were developed to be used specifically for narrow distribution polymers and their mixtures. Subsequent computations indicated that by comparing gelling doses for samples of different initial distributions, it would be possible to distinguish between crosslinking and endlinking as alternative mechanisms of network formation.

The applicability of the statistical theory to the radiation chemistry of polystyrene was tested in several ways. It was found that interfering surface and intensity effects were absent, and from light-scattering and gelling dose measurements direct evidence was obtained concerning the correctness of the basic assumptions.

From the effect of molecular weight distribution on the critical dose it was established that network formation in polystyrene takes place through crosslinking, in agreement with mechanisms suggested by several authors.

From osmotic measurements and viscometric gelling dose determinations, the extent of radiation-induced degradation was found to be one main chain scission per seven crosslinked units. The energy absorption per crosslink was determined to be 2740 eV. This value is higher than results obtainable from the literature, which suggests that the plastic-

izing effect of low molecular weight species in polydisperse polymers increases the probability of crosslink formation.

It is believed that the simple technique developed to distinguish between crosslinking and endlinking should be valuable for studying radiation processes in a variety of network forming polymers.

PART II

THE INTRINSIC VISCOSITY OF BRANCHED POLYMERS

HISTORICAL INTRODUCTION

The theory of solutions of branched polymers is, as may be expected, closely connected to the theoretical and experimental results obtained for solutions of linear polymers. Many of the difficulties which arise when it is attempted to predict the intrinsic viscosities of branched polymers are, in fact, a consequence of our incomplete knowledge of the behavior of linear chains. New data on the effects of branching can provide important information on the properties of polymer solutions in general. Therefore it seems in order to review briefly the viscosity theory of solutions of linear polymers before discussing the particular problems posed by branching.

The exact hydrodynamic calculation of the viscosity increment produced by a particle in a flowing liquid is possible only for very simple systems (89). Thus, considerable simplifications must be introduced in order to develop a mathematical treatment of the viscosity of polymer solutions. One of the most useful approaches has been to consider polymer molecules as statistical chains, consisting of beads connected by rigid links without lateral extension (the 'pearl-necklace' model). The configurations of such chains in solution are closely related to random flight sequences, and can therefore be analyzed mathematically. Many of the fundamental results of such analyses have been given by Chandrasekhar (90). With certain modifications (91,92) random flight calculations can also allow for the effect of fixed bond angles and hindered rotation. The influence of the finite volume of monomer units (excluded volume effect) and polymer-solvent interactions are more difficult to treat in

an analogous manner, but considerable advances are being made along these lines (93).

An important result of the statistical calculations has been the conclusion that the average linear dimensions of polymer molecules, such as the root-mean-square (rms) end-to-end distance $< L^2 >^{1/2}$, or the rms radius of gyration $< S^2 >^{1/2}$, are proportional to the square root of the molecular weight.

When the motion of polymer coils through liquids is considered, it is justifiable to assume that the center of mass of the polymer molecule is at rest, and liquid is flowing through and around the coil. Then we can think of two extreme cases (94):

1. The polymer chain can be considered as a loose net which offers little resistance to liquid flow, except in the immediate vicinity of the 'beads'. This case is referred to as the free-draining coil. The hydrodynamic behavior of such chains was considered by Debye (95), who found that their intrinsic viscosity would be proportional to $< S^2 >$, i.e. to the molecular weight.

2. Alternatively, a polymer molecule may immobilize the liquid enclosed by it to such a large extent that the chain and the enclosed liquid will form a single hydrodynamic entity. This model is known as the impermeable coil. An impermeable coil may be considered as a solid sphere of radius R_e, R_e being the equivalent hydrodynamic radius. From Einstein's equation for suspensions of solid spheres, the intrinsic viscosity will be proportional to R_e^3/M, where M is the molecular weight (94).

Assuming that R_e is proportional to $< S^2 >^{1/2}$, and neglecting the excluded volume and polymer-solvent interaction effects, $[\eta]$ would thus become proportional to $M^{0.5}$.

It is well known that for many polymers the dependence of $[\eta]$ on the molecular weight can be expressed with considerable accuracy by equations of the type

$$[\eta] = KM^a \quad , \qquad \text{II-1}$$

where K and a are constants. The value of a is usually between 0.5 and 0.8, which suggests that the properties of polymer molecules in solution are intermediary between those of the free-draining and the impermeable coil. Thus it has been necessary to introduce modifications to the limiting cases quoted above. Kirkwood and Riseman (96), and Debye and Bueche (97) have assumed that the flow around the outermost segments is essentially unhindered by the presence of other segments, and as the center of the molecule is approached the 'beads' become more shielded, due to the interaction of the flow patterns of individual segments. For a sufficiently large coil the liquid near the center will be completely immobilized. This implies that in the limit very large molecules will behave as dense spheres, with $[\eta] = KM^{0.5}$. For molecules of intermediate size the depth of solvent penetration into the coil can be expressed in terms of a shielding length. In effect, consideration of the shielding length (or permeation factor) results in a hydrodynamic radius which increases with M more rapidly than does the rms end-to-end distance. This is in accordance with experimentally observed values of a in the Mark-Houwink (98) equation (Eq. II-1). Never-

theless, the quantitative application of the Kirkwood-Riseman and Debye-Bueche theories has been only moderately successful in relating the hydrodynamic behavior of a monomer unit to the intrinsic viscosity of the macromolecule (99).

A somewhat different approach has been taken by Flory and Fox (100-102), who introduced a theory based on three major postulates,

(a) that for flexible polymer chains the permeation factors of the Kirkwood-Riseman and Debye-Bueche treatments are at their asymptotic limits over the entire molecular weight range of interest,

(b) that the effective hydrodynamic radius is approximately proportional to the average linear dimensions, and

(c) that due to the excluded volume and polymer-solvent interactions these dimensions are expanded by a factor α, which increases with the size of the coil, i.e. with the molecular weight.

The mathematical analysis carried out by Flory and Fox is derived from thermodynamic considerations. The expansion factor α is given by the equation

$$\alpha^5 - \alpha^3 = C_M (1 - 2\chi)M^{1/2} = 2C_M \psi_1 (1 - \theta/T)M^{1/2}, \quad \text{II-2}$$

where C_M is a constant depending on the dimensions and properties of the coil, χ and ψ_1 are interrelated thermodynamic parameters, characterizing a given polymer-solvent pair, M is the molecular weight of the polymer, and θ is the temperature of total miscibility for a polymer homolog of infinitely high molecular weight. It can be seen that at $T = \theta$, the so-called Flory θ temperature, $\alpha = 1$ and the polymer molecules

may be represented by an equivalent random chain, obeying random flight statistics.

Flory and collaborators have collected a wealth of experimental data to justify the excluded volume theory, and the correctness of postulates (a) and (c) has been adequately demonstrated (103). There remains the question of how closely the proportionality of R_e and $< L^2 >^{1/2}$ or $< S^2 >^{1/2}$ is obeyed. For linear molecules postulate (b) has been stated as

$$[\eta] = \Phi' < S^2 >^{3/2}/M = \Phi < L^2 >^{3/2}/M , \qquad \text{II-3}$$

where Φ and Φ' are supposedly universal constants. In the Flory-Fox treatment

$$< L^2 >^{1/2} = \alpha < L^2 >_o^{1/2} , \qquad \text{II-4}$$

where $< L^2 >_o^{1/2}$ is the unperturbed rms end-to-end distance, i.e. the size of the coil in the absence of excluded volume effect and polymer-solvent interaction. Thus it would be a consequence of the complicated dependence of α on M that the exponent in the Mark-Houwink equation can take various values. From Eq. II-3, Φ can be calculated if the intrinsic viscosity, molecular weight, and the dimensions of polymer molecules are determined experimentally. Krigbaum and Carpenter (103) have carried out a thorough analysis of the properties of cyclohexane solutions of polystyrene, and also reviewed data in the literature. They have come to the conclusion that the universal constant Φ is not strictly independent of the temperature, and have established that Φ decreases somewhat with

increasing light-scattering second virial coefficients. Even in this critical study, however, the observed changes in Φ were small. Thus it can be concluded that for most dilute solutions of linear polymers the Flory-Fox theory explains the frictional phenomena remarkably well. However, as demonstrated later, this theory appears to be unsuitable for quantitative interpretation of the intrinsic viscosity of branched macromolecules.

It has been clearly established experimentally (26,87,104,105) that the intrinsic and bulk viscosities of branched polymers are lower than those of the corresponding linear polymers of equal molecular weight. The size of branched molecules is usually expressed in terms of the parameter g, which is defined as the ratio of $< S^2 >$ of the branched chain to $< S^2 >$ of the corresponding linear molecule of equal molecular weight. For free-draining coils $[\eta]$ is proportional to the mean-square radius of gyration, and thus

$$[\eta]_{br}/[\eta]_{lin} = < S^2 >_{br}/< S^2 >_{lin} = g \quad \text{II-5}$$

The theory underlying Eq. II-5 was abandoned when the free-draining model proved unsatisfactory for linear polymers, and it was attempted (26) to apply the Flory-Fox theory to branched molecules. Eq. II-3, if adopted for branched polymers, leads to

$$[\eta]_{br}/[\eta]_{lin} = < S^2 >^{3/2}_{br}/< S^2 >^{3/2}_{lin} = g^{3/2} . \quad \text{II-6}$$

In view of the successes of the Flory-Fox theory, Eq. II-6 was at first expected to be reliable but, as Zimm (106), and Stockmayer and Fixman (27) pointed out, early experiments (26) conclusively showed that the

$g^{3/2}$ factor considerably overestimates the effect of branching.

Following this realization, it was attempted to introduce improvements into the calculation of intrinsic viscosities of branched polymers. Basically, all the theoretical treatments have been designed to correlate the intrinsic viscosity and certain linear dimensions of branched molecules. Several analyses (27,28,30) have been based on the assumption that the radius of gyration is comparatively simply related to the hydrodynamic radius, at least empirically. However, Stockmayer and Fixman (27), and F. Bueche (31) have pointed out that the radius of gyration is not a good measure of the hydrodynamic radius, for increased segment density will increase R_e even if $< S^2 >$ remains constant. This makes it questionable whether any of the proposed formulas (25-28) of the type

$$[\eta]_{br}/[\eta]_{lin} = \varphi(g) \qquad \text{II-7}$$

can describe the influence of branching on $[\eta]$ with sufficient generality. As shown in the Results and Discussion section, it was possible to obtain information regarding this problem by considering solutions in 'good' and 'poor' solvents.

The experimental investigation of the effects of branching is beset with difficulties. In order to test the theories, it would be desirable to measure the viscosities of essentially monodisperse samples of known degrees of branching. Such samples, however, are extremely difficult to prepare, unless in minute quantities. Recently, Morton and collaborators (87) succeeded in synthetizing polymers with three or four

uniform branches emanating from a single point. Their experimental results lend considerable support to the theoretical work of Zimm and Kilb (28). It is still doubtful, however, whether this theory is applicable to randomly branched polymers.

One of the more convenient ways of obtaining branched polymers under controlled conditions is by irradiation of linear polymers of known distribution. Although the resulting polymers are highly polydisperse, the number and distribution of branches obey statistical laws. Therefore the study of irradiated polymers offers an experimentally simple, and yet effective technique for investigating the influence of branching on the intrinsic viscosity.

The change of intrinsic viscosity on irradiation of a polymer has been studied by several workers. In general the mathematical difficulties encountered have been considerable, because calculation of the viscosity average molecular weight of irradiated polymers requires more complicated techniques (17,19,33) than the estimation of M_n and M_w. Branching introduces further special problems (21,30,33). Therefore in many of the computations reported only samples of initially random distribution were considered (19,21,30).

In the present work it was found possible to extend some of the existing statistical treatments (19,21), so that any theory in which the effects of branching on $[\eta]$ can be expressed as a function of the number of branch units, may be tested by studying irradiated polymers. For reasons mentioned above the calculations have been limited to the initially random distribution. However, it will be shown that the effect

of initial molecular weight distribution is probably small and that the results obtained are applicable to polymers of various initial distributions, including narrow range polymers.

THEORETICAL

Basic Mathematical Approach

The calculations to be discussed in the present section are based essentially on Saito's calculation of the viscosity average molecular weight of irradiated polymers (19). Saito's treatment has been expanded subsequently by other authors (23,24), but the most important improvement is due to Katsuura (21), who succeeded in introducing the effect of branching into Saito's formulas. The computations of Katsuura (21) were based on the assumption that the effect of branching can be expressed by the equation

$$[\eta]_{br}/[\eta]_{lin} = g^{2-a} , \qquad \text{II-8}$$

where a is the exponent of the Mark-Houwink equation (Eq. II-1) for the linear molecule, and $g = \langle S^2 \rangle_{br} / \langle S^2 \rangle_{lin}$. Eq. II-8 follows from the theoretical treatment of Debye and Bueche (97), and it implies that branching causes the hydrodynamic shielding to be greater than in the case of a linear random coil. On the other hand, the influence of branching as predicted by Eq. II-8 is smaller than that expected from the direct application of the Flory-Fox theory (Eq. II-6 of the Historical Introduction).

As will be shown in the Results and Discussion section, experimental data indicate that Eq. II-8 still overestimates the effect of branching. Nevertheless, Katsuura's treatment has opened the way towards a general approach for the interpretation of the intrinsic

viscosity of irradiated polymers. In the following paragraphs this concept is explained and applied to several recent theories of the influence of branching on the solution properties of polymers.

First it is necessary to consider the assumptions and mathematical methods involved in the derivations. The Katsuura expression for the intrinsic viscosity is given by

$$[\eta] = K w_o^a \int_0^\infty dq \int_0^\infty g^{2-a} u^{a+1} \frac{n(u,q,R)}{N} du , \qquad \text{II-9}$$

where K = coefficient of the Mark-Houwink equation for the original linear polymer

w_o = monomer molecular weight

q = half of the number of chain ends of a given molecule

u = degree of polymerization

$n(u,q,R)$ = number of u-mers with 2q ends at dose R

N = total number of monomer units.

Eq. II-9 is based on the hypothesis that intrinsic viscosity is a weight average quantity. This proposal was first clearly stated by Flory (107), and has been amply justified by experimental work (108). For a mixture of polymers belonging to the same homologous series we have

$$[\eta] = \frac{\sum_i [\eta]_i w_i}{\sum_i w_i} , \qquad \text{II-10}$$

where $[\eta]_i$ and w_i are the intrinsic viscosity and weight fraction of the i^{th} component. For polydisperse samples it is customary to rewrite

Eq. II-10 by substituting for $[\eta]_i$ from the Mark-Houwink equation and replacing the summation by an integral. This leads to

$$[\eta] = K \frac{\int_0^\infty M^a \, Mn(M)dM}{\int_0^\infty Mn(M)dM} \quad , \qquad \text{II-11}$$

where M is the molecular weight of a given species, and n(M) is the number of molecules of molecular weight M. From Eq. II-11 the viscosity average molecular weight is defined as

$$M_v = \left\{ \frac{\int_0^\infty M^{a+1} \, n(M)dM}{\int_0^\infty Mn(M)dM} \right\}^{1/a} . \qquad \text{II-12}$$

When the intrinsic viscosity of mixtures containing branched molecules is calculated, the $[\eta]_i$ values of Eq. II-10 cannot be obtained directly from the Mark-Houwink equation. Statistically, however, the ratio of the viscosities of linear and randomly branched molecules of equal molecular weight depend only on the number of branches. Thus

$$[\eta]_{i,br} / [\eta]_{i,lin} = f(q) . \qquad \text{II-13}$$

Moreover, if a relation can be found between the number of branch units and the radius of gyration as expressed by the g value, Eq. II-13 can be written as

$$[\eta]_{i,br} = [\eta]_{i,lin} \cdot \varphi(g) \quad , \qquad \text{II-14}$$

where

$$\varphi(g) = \varphi[g(q)] = f(q) \quad . \qquad \text{II-15}$$

$[\eta]_{i,lin}$ can be calculated from the Mark-Houwink equation, and substitut- into Eq. II-10 the generalized expression

$$[\eta] = Kw_o^a \int_o^\infty dq \int_o^\infty \varphi(g) u^{a+1} \frac{n(u,q)}{N} du \qquad \text{II-16}$$

may be obtained, analogously to Eq. II-11. It can be seen that Katsuura's Eq. II-9 is simply a special case of Eq. II-16.

Thus, in the calculations to be discussed no major assumptions are involved beyond those inherent in the statistical determination of the number and distribution of crosslinks and scissions. Accordingly, it may be concluded that Eq. II-16 will give the intrinsic viscosity of irradiated polymers accurately, provided the correction factor $\varphi(g) = f(q)$ describes the dependence of $[\eta]$ on branching correctly.

As mentioned before, several expressions for $\varphi(g)$ have been proposed in the literature (25-28). Katsuura's computations (21) were limited to use of the g^{2-a} factor, but it is interesting to note that the form in which Katsuura used this correction for branching was a number of expansions

$$[g(q)]^{2-a} = B_1 e^{-c_1 q} + B_2 e^{-c_2 q} + B_3 \quad .$$

This suggests that Katsuura's mathematical technique will be applicable whenever the dependence of $[\eta]_{br}/[\eta]_{lin}$ on the number of branch units

can be expressed as a sum of exponential functions.

In the present work various $[\eta]_{br}/[\eta]_{lin} = \psi(g)$ relationships were considered:

1. $$[\eta]_{br}/[\eta]_{lin} = g^{3/2} \qquad \text{(II-6)}$$

2. $$[\eta]_{br}/[\eta]_{lin} = g^{2-a} \qquad \text{(II-8)}$$

3. $$[\eta]_{br}/[\eta]_{lin} = g^{1/2} \text{ , and} \qquad \text{II-17}$$

4. $$[\eta]_{br}/[\eta]_{lin} = h^{3} \text{ ,} \qquad \text{II-18A}$$

where $$h = \sqrt{f}\left[2 - f + \sqrt{2}\,(f-1)\right]^{-1} \text{ , and} \qquad \text{II-18B}$$

$$f = \frac{3 + \sqrt{9 - 8g}}{2g} \text{ .} \qquad \text{II-18C}$$

In Eqs. II-18, h is the ratio of the effective hydrodynamic radius of the branched molecule to that of the linear molecule of equal molecular weight, and f is the number of branches of a given cruciform molecule. As mentioned before, Eqs. II-6 and II-8 follow from the Flory-Fox and Debye-Bueche theories, respectively. Zimm and Kilb (28) calculated the intrinsic viscosities of several star-shaped molecules, and found that Eq. II-17 would describe the hydrodynamic properties of such molecules satisfactorily. The use of Eqs. II-18 was first suggested by Stockmayer and Fixman (27), based on their calculation of the friction constant for cruciform molecules. The mathematical approach used by these authors was an extension of the Kirkwood-Riseman treatment (96).

It should be noted that none of the above equations was developed for randomly branched polymers. The properties of heavily

branched species, which are formed in significant quantities near the gel point, may be quite different from those of the star-shaped molecules for which Eqs. II-17 and II-18 were derived. At the present time, however, it appears that a direct calculation of $[\eta]$ is possible for only the simplest branched molecules. Therefore it was assumed that differences between the segment densities of cruciform and randomly crosslinked molecules of the same number of branches could be neglected.

Expansion of the $\varphi(g)$ Factors into Finite Dirichlet Series

As mentioned previously, in the treatment of Katsuura (21) dependence of the intrinsic viscosity on branching was expressed in terms of exponential functions of q. In order to expand the correction factors used in the present work into finite Dirichlet series, it was first necessary to calculate $\varphi(g)$ corresponding to a number of q values. Even these simple computations, however, posed a difficulty, due to the considerable differences between relevant equations developed by Kataoka (109) on one hand and Zimm and Stockmayer (25) on the other hand. To avoid possibly erroneous conclusions due to using the wrong expression for calculating g, and also to evaluate the importance of differences between the two treatments, in the computations of the present work both methods were used.

For tetrafunctionally branched molecules of random branch lengths Zimm and Stockmayer obtain*

* The authors have been able to simplify somewhat Eq. II-19, however, the alternative formula is not advantageous when digital computers are used.

$$g(q) = \frac{3(q-1)!(2q)!}{(3q)!} \sum_{\nu=0}^{q-1} \binom{2q+\nu}{\nu}, \qquad \text{II-19}$$

the asymptotic form of which for large q is

$$g(q) \simeq \frac{1}{2}\sqrt{\frac{3\pi}{q-1}} - \frac{2}{3(q-1)} . \qquad \text{II-20}$$

The formula of Kataoka corresponding to Eqs. I-19 and I-20 is

$$g(q) = \frac{3q^3 + 9q^2 - 18q + 8}{q(3q-1)(3q-2)} . \qquad \text{II-21}$$

The results shown in Table II-1 illustrate that the two methods give similar or even identical results for low degrees of branching. As q increases, an increasing discrepancy is found between the two treatments. In the limit of an infinite number of branches Eq. II-21 leads to g = 1/3, while the asymptotic equation of Zimm and Stockmayer (Eq. II-20) indicates that $\lim_{q\to\infty} g(q) = 0$. Katsuura (21) has shown that for highly branched molecules Eq. II-21 underestimates the effect of branching, however, according to his calculations, after the necessary corrections have been applied $\lim_{q\to\infty} g(q)$ would still equal 0.297. The effects of the uncertainty introduced by the differences between the two methods will be considered in the Results and Discussion section.

Values of the functions $\varphi(g) = f(q)$ were calculated for 40 different values of q, ranging from 1 to 116. The alternative methods of Kataoka and Zimm and Stockmayer were both used for computing $\varphi(g)$ factors, excepting that given by the Stockmayer-Fixman theory (27), the latter being explicitly connected to the statistical treatments of Zimm

TABLE II-1

Values of the parameter g calculated from the equations of Zimm and Stockmayer (25) and Kataoka (109)

q	g		q	g	
	Zimm and Stockmayer	Kataoka		Zimm and Stockmayer	Kataoka
1	1.0000	1.0000	21	0.3099	0.3951
2	0.8000	0.8000	26	0.2803	0.3835
3	0.6905	0.6905	31	0.2580	0.3756
4	0.6182	0.6182	36	0.2404	0.3698
5	0.5656	0.5692	41	0.2260	0.3654
6	0.5251	0.5343	46	0.2140	0.3620
7	0.4925	0.5083	51	0.2037	0.3592
8	0.4656	0.4881	56	0.1949	0.3569
9	0.4428	0.4721	61	0.1871	0.3550
10	0.4232	0.4591	66	0.1801	0.3534
11	0.4061	0.4483	71	0.1739	0.3520
12	0.3910	0.4392	76	0.1684	0.3507
13	0.3775	0.4314	81	0.1633	0.3497
14	0.3654	0.4247	86	0.1586	0.3487
15	0.3544	0.4189	91	0.1544	0.3479
16	0.3443	0.4137	96	0.1505	0.3471
17	0.3351	0.4092	101	0.1468	0.3465
18	0.3266	0.4051	106	0.1435	0.3458
19	0.3188	0.4014	111	0.1403	0.3453
20	0.3115	0.3981	116	0.1373	0.3448

and Stockmayer. In computations based on Zimm and Stockmayer's equations the asymptotic formula (Eq. II-20) was used for $q > 20$. Some of the results of these calculations are given in Table II-2. A complete listing may be found in Appendix II.

Having computed the correction factors $\gamma(g)$ as a function of q in several ways, it was now necessary to express them in terms of exponential functions. This problem is similar to that encountered by radiochemists in the least-squares analysis of counting data. The mathematical procedure for such analyses is not quite straightforward, for the equations used to fit a calculated curve to the data are non-linear in the parameters to be determined. Shortly before the calculations of the present work were carried out, a computer program (110) was published by the Nuclear Chemistry Group of the Massachusetts Institute of Technology for the analysis of exponential growth and decay processes. The mathematical approach used in this program was based on expanding the exponential functions in a Taylor series about the point defined by the previous estimates of the parameters. By neglecting all terms of the series beyond first order, a set of simultaneous equations linear in the differences between the current estimates of the parameters and the correct values is obtained. From these equations the difference terms are evaluated, the previous estimates are corrected, and to eliminate errors due to the neglected higher order terms the process is repeated a number of times to meet convergence criteria.

The above computer program (FRANTIC) was adapted to the IBM 1410 computer of the McGill University Computing Centre. Considerable simplifications could be introduced, for the corrections normally used for the raw

TABLE II-2

Values of the correction factor f(q) for randomly branched molecules, as calculated from several theories concerning the effects of branching

q	f(q)						
	$\varphi(g) = g^{3/2}$		$\varphi(g) = g^{1.26}$		$\varphi(g) = g^{1/2}$		$\varphi(g) = h^3$
	Zimm and Stockmayer	Kataoka	Zimm and Stockmayer	Kataoka	Zimm and Stockmayer	Kataoka	(Zimm and Stockmayer)
2	0.7155	0.7155	0.7549	0.7549	0.8944	0.8944	0.8680
3	0.5737	0.5737	0.6270	0.6270	0.8309	0.8309	0.7731
4	0.4860	0.4860	0.5455	0.5455	0.7862	0.7862	0.7023
5	0.4254	0.4294	0.4877	0.4916	0.7520	0.7544	0.6468
7	0.3456	0.3623	0.4097	0.4262	0.7018	0.7129	0.5645
10	0.2753	0.3110	0.3384	0.3749	0.6505	0.6775	0.4815
15	0.2109	0.2711	0.2705	0.3340	0.5952	0.6472	0.3951
20	0.1738	0.2512	0.2300	0.3133	0.5581	0.6309	0.3400
31	0.1310	0.2301	0.1814	0.2911	0.5079	0.6128	0.2706
41	0.1074	0.2208	0.1535	0.2812	0.4754	0.6044	0.2293
61	0.0809	0.2115	0.1209	0.2711	0.4324	0.5958	0.1797
81	0.0660	0.2067	0.1019	0.2660	0.4040	0.5913	0.1502
101	0.0563	0.2039	0.0892	0.2630	0.3831	0.5886	0.1303
116	0.0509	0.2024	0.0820	0.2613	0.3705	0.5871	0.1190

counting data were omitted, together with parts of the original program which were not essential for iterative least-squares analysis.

Using this modified FRANTIC program, the $\varphi(g) = f(q)$ correction factors for branching were expanded into sums of exponential functions of the type $\sum_i B_i e^{-c_i q}$. As shown in Appendix II, three exponential terms, plus an appropriate constant for values based on Eq. II-21 of Kataoka, were always sufficient to obtain a good approximation to f(q). The parameters B_i and c_i for each expansion are also given in Appendix II.

Derivation of the Equation Used to Compute $[\eta]/[\eta]_o$ as a Function of R/R_g in Crosslinking with Degradation

Having obtained $\varphi(g)$ in terms of exponential functions of q, Eq. II-16 can be expressed as

$$[\eta] = K w_o^a \sum_i B_i \, \mathcal{J}(c_i) \quad , \qquad \text{II-22}$$

where

$$\mathcal{J}(c_i) = \int_o^\infty dq \int_o^\infty u^{a+1} e^{-c_i q} \frac{n(u,q,R)}{N} du \quad (i = 1,2,3,\ldots) \, .$$

II-23

Katsuura (21) has shown that for a random initial distribution Eqs. II-23 can be transformed into integrals from which the increase of the intrinsic viscosity in crosslinking may be evaluated. The resulting expression in

the absence of degradation is*

$$\mathrm{J}(c_i) = \frac{2u_1^a\, e^{-c_i}}{\Gamma(1-a)} \int_0^{y_{oi}} \frac{y^{a+1}\,dy}{\left\{1 - y - 2u_1 yt(1 - y^2\, e^{-c_i})\right\}^a} \quad (i = 1,2,3,\ldots) \quad ,$$

II-24

where u_1 is the initial number average degree of polymerization, a is the exponent in the Mark-Houwink equation for the linear polymer, t is the average number of crosslinks per monomer unit in the irradiated polymer, and y_{oi} is a root of the equation

$$1 - y - 2u_1 yt\,(1 - y^2\, e^{-c_i}) = 0 \quad , \qquad \text{II-25}$$

such that $0 < y_{oi} \leq 1$.

As Katsuura pointed out (21), due to the invariance of the form of the random distribution function under degradation, Eq. II-24 can be applied to crosslinking with degradation if $u_1/(1 + u_1\tau)$ is substituted for u_1. As before, $\tau = t/\sigma_c$ can be computed if the extent of degradation is known.

In actual calculations it is convenient to express the dose as a fraction of the gelling dose R_g. For samples of initially random distribution, Eq. I-33 of the Theoretical section of Part I leads to

$$t_g = \frac{\sigma_c}{u_1(4\sigma_c - 1)} \quad . \qquad \text{II-26}$$

---

* As shown in Appendix III, there is a misprint in the corresponding equation given by Katsuura (21).

Therefore if R/R_g is denoted by p we obtain

$$t = pt_g = \frac{p\sigma_c}{u_1(4\sigma_c - 1)} \qquad \text{II-27}$$

and

$$\tau = \frac{p}{u_1(4\sigma_c - 1)} \quad . \qquad \text{II-28}$$

The change in the intrinsic viscosity on irradiation is usually expressed by the ratio $[\eta]/[\eta]_o$, where $[\eta]_o$ refers to the unirradiated polymer. It is easy to show that for a sample of random distribution

$$[\eta]_o = Kw_o^a u_1^a \Gamma(a + 2) \quad . \qquad \text{II-29}$$

Then, if we combine Eqs. II-22, II-24, and II-27, and replace u_1 in Eq. II-24 by $u_1/(1 + u_1\tau)$ with the aid of Eq. II-28, the formula

$$\frac{(4\sigma_c + p - 1)^a \Gamma(1 - a)\, \Gamma(2 + a)}{2(4\sigma_c - 1)^a} \cdot \frac{[\eta]}{[\eta]_o} =$$

$$\sum_i B_i e^{-c_i} \int_o^{y_{oi}} \frac{y^{a+1} dy}{\left\{1 - y - \frac{2yp\sigma_c}{4\sigma_c + p - 1}(1 - y^2 e^{-c_i})\right\}^a} \qquad \text{II-30}$$

will be obtained. The y_{oi} values are now roots of the equations

$$1 - y - \frac{2yp\sigma_c}{4\sigma_c + p - 1}\left(1 - y^2 e^{-c_i}\right) = 0 \quad , \qquad \text{II-31}$$

such that for all i $0 < y_{oi} \leq 1$. It is evident from Eqs. II-30 and II-31 that the relative change in the intrinsic viscosity does not depend on the initial molecular weight.

Numerical Integration

The evaluation of Eq. II-30 involved two distinct numerical procedures. Eqs. II-31 were readily solved for y_{oi} values by successive approximation, as described in the Theoretical section of Part I. Evaluation of the integrals of Eq. II-30, however, posed considerable difficulties, because the integrands of Eq. II-30 become infinite at the upper limit.

The problems involved when numerical integration is attempted in the neighborhood of a singularity of the integrand have been discussed in some detail by Hartree (111). Basically, difficulties arise because in the derivation of integration formulas it is assumed that the integrand is expansible in Taylor series at every interval. This assumption does not hold if there is a singularity at any point, including the end-points. Therefore, in an effort to apply Gaussian quadrature, Eq. II-30 was transformed, using integration by parts. This procedure eliminated the singularity for many values of the parameters involved. However, the difference between results obtained by 15- and 16-point Gaussian quadrature was, at least in one case, over 5%, which made the applicability of this approach questionable.

Accordingly, it was decided to evaluate Eq. II-30 by direct numerical integrations, using the well-known Weddle's Rule formula (112). For a given integral the range of integration was divided into intervals of the type

$$\left[\frac{2^{n-1}-1}{2^{n-1}}\,y_{oi}\ ,\ \frac{2^{n}-1}{2^{n}}\,y_{oi}\right]\quad (n = 1,2,3,\ldots)\ .$$

Each of these intervals was then subdivided into six equal intervals to apply the mechanical quadrature formula. Due to the slow convergence in the neighborhood of the upper limit, values of the integrand had to be calculated at up to 420 points to reduce the error to less than 0.1%. This numerical procedure was tested by evaluating Beta functions, and its accuracy has been amply proved by checking certain intermediate values.

The heavy machine time requirement has somewhat limited the number of computations that could be carried out. Nevertheless, as shown in the Results and Discussion section, a sufficient volume of data was obtained to provide the information sought.

RESULTS AND DISCUSSION

It has been described in the previous section how the treatments of Saito (19) and Katsuura (21) were modified by introducing various corrections for branching. It has been found that, even at low doses, the calculated values of $[\eta]/[\eta]_o$ were strongly dependent on the $\psi(g)$ correction factors. Therefore the validity of several theories concerning the viscosity of branched polymers could be tested by comparing theoretical and experimental data.

Having decided on the numerical procedures to follow, it was a comparatively simple task to write the necessary computer programs. However, due to the heavy machine time requirements, very few calculations could be carried out to test the importance of possible or known uncertainties in the extent of degradation, or the value of the exponent in the Mark-Houwink equation, for a given polymer. Nevertheless, a number of interesting conclusions have been reached on the basis of the theoretical results tabulated in Appendix IV. Furthermore, it was possible to investigate the effect of initial molecular weight distribution, by comparing experimental results obtained for irradiated anionic polystyrene samples to theoretical and experimental data for polymers of initially random distribution.

Evaluation of Various Theories on the Effects of Branching on Viscosity

In Figs. II-1 to II-3 changes in the intrinsic viscosity as calculated on the basis of several theories are compared to the experimental data of Shultz and collaborators (3) and Kilb (30). As mentioned

previously, the computations described in the Theoretical section apply, in principle, only to samples of initially random distribution. It may be assumed (3,30) that the polystyrene samples used by Shultz, as well as Kilb's dimethylsilicone fluid, satisfied this criterion reasonably well.

The most extensive calculations were carried out using the experimental parameters of Shultz and collaborators. In their experiments, the extent of degradation was determined to be 0.7 main chain scission per crosslink, which corresponds to $\delta_c = 1.43$. The exponent a of the Mark-Houwink equation was taken to be 0.74, as quoted by Shultz et al. In Fig. II-1 the data of curves 2A, 4, and 5A were computed by means of Kataoka's formula for g (Eq. II-21), while curves 2B, 3, and 5B were obtained from the parallel expressions of Zimm and Stockmayer (Eqs. II-19 and II-20).

In the calculation of curve 1, the effect of branching on viscosity was neglected, while at the other extreme curves 5A and 5B correspond to Eq. II-6, i.e. to the Flory-Fox theory. It is obvious that branching lowers the viscosity considerably, but not nearly as much as predicted by Eq. II-6. The relationship

$$[\eta]_{br}/[\eta]_{lin} = g^{2-a} \quad , \qquad \text{(II-8)}$$

which is based on the Debye-Bueche treatment (97), and was employed in the original derivations of Katsuura (21), also appears to overestimate the effects of branching (curve 4). On the other hand, the

FIG. II-1

Comparison of experimental data for irradiated polystyrene in toluene, obtained by Shultz et al. (3), and theoretical curves, calculated from various equations proposed to describe the effects of branching on $[\eta]$. The theoretical curves were computed by assuming a = 0.74 and $\sigma_c = 1.43$. For curves 2A, 4, and 5A, g values were obtained from the formula of Kataoka (Eq. II-21), for curves 2B, 3, and 5B Zimm and Stockmayer's formulas (Eqs. II-19 and II-20) were employed. The following correction factors for branching were considered:

Curve 1	No correction $[\varphi(g)\equiv 1]$
Curves 2A and 2B	$\varphi(g) = g^{1/2}$
Curve 3	$\varphi(g) = h^3$
Curve 4	$\varphi(g) = g^{1.26}$
Curves 5A and 5B	$\varphi(g) = g^{3/2}$

The dashed curve represents the theoretical results of Shultz et al., whose calculations were based on the Stockmayer-Fixman treatment ($\varphi(g) = h^3$).

$$[\eta]_{br}/[\eta]_{lin} = g^{1/2} \qquad \text{(II-17)}$$

expression, which was used to calculate the values of curves 2A and 2B, has led to higher viscosities than those observed in the experiments. The best, and indeed excellent agreement between calculated and experimental data was found when Stockmayer and Fixman's approach (Eqs. II-18) was adopted. The results, shown in curve 3, are compared to the calculated values obtained by Shultz et al. (3), given as the dashed curve of Fig. II-1. The calculations of Shultz et al. were also based on Stockmayer and Fixman's treatment, but the mathematical approach was entirely different from that of the present work. From Fig. II-1, it is evident that the results of the method of computation adopted in the present investigation are in better agreement with the experiments. It is interesting to note, however, that common to both treatments is a decrease in $[\eta]$ predicted for high doses, which is at variance with experimental data. Such an expected decrease seems to be inherent in calculating intrinsic viscosities of irradiated polymers from the equations of Stockmayer and Fixman. This will become increasingly apparent in subsequent calculations. However, for solutions in 'good' solvents, and for doses not exceeding $R/R_g = 0.8$, the Stockmayer-Fixman treatment (27) appears to be at least as satisfactory as the more recent (28) $\varphi(g) = g^{1/2}$ formula.

There is a pronounced difference between curves 2A and 2B, and 5A and 5B, which indicates that application of the theories at high doses will be uncertain, unless it can be decided how to estimate radii of gyration of strongly branched molecules. It is beyond the scope of the

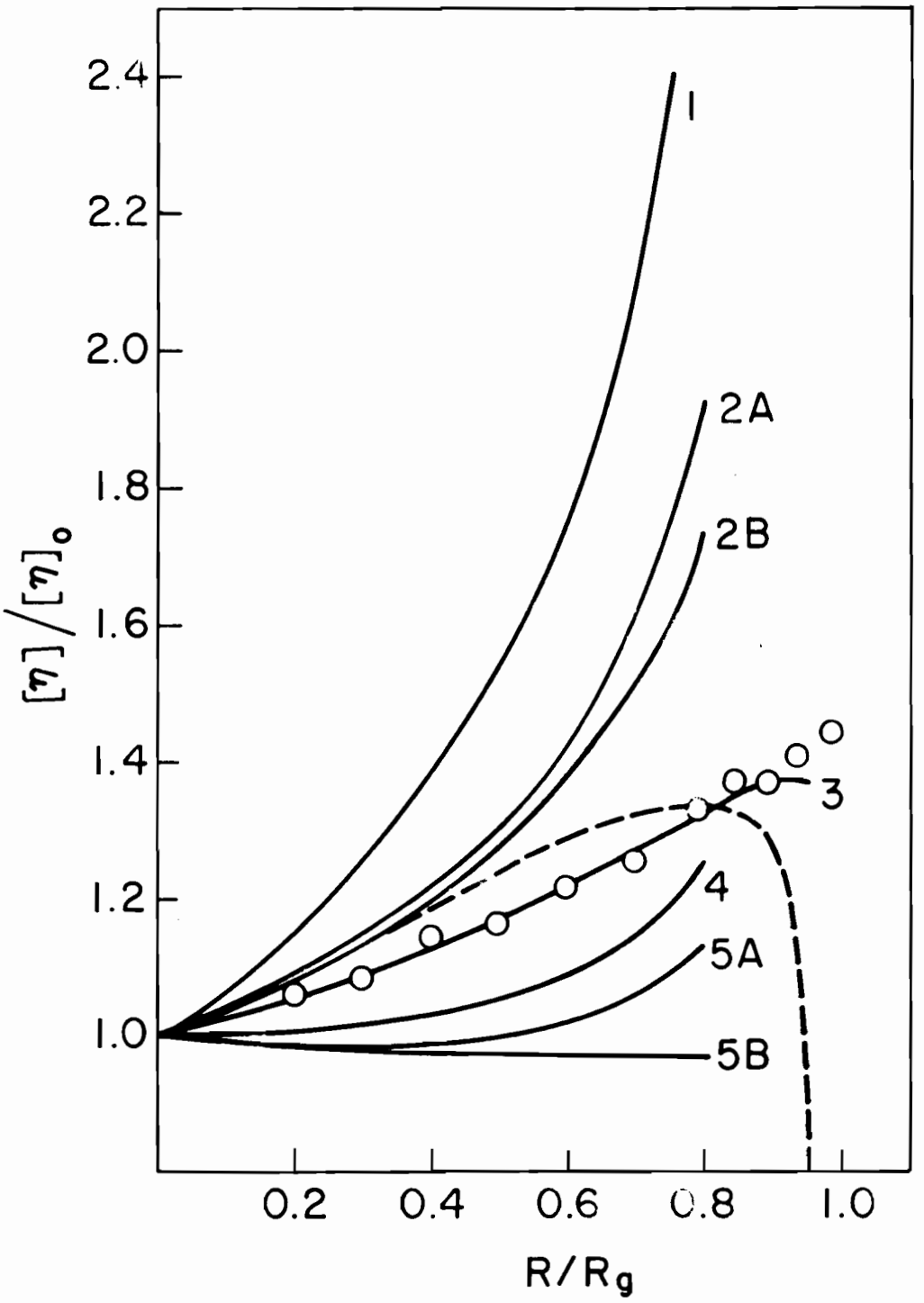
2.4
2.2
2.0
1.8
1.6
1.4
1.2
1.0
$[\eta]/[\eta]_o$
1
2A
2B
3
4
5A
5B
0.2
0.4
0.6
0.8
1.0
R/Rg

present work to comment on the relative merits of the treatments of Kataoka (109) and Zimm and Stockmayer (25). However, it will be noted that good agreement can be obtained with many of the experimental results given in Figs. II-2 to II-7 if the correction factor $\varphi(g) = g^{1/2}$ is used, with Zimm and Stockmayer's method of estimating g from q. Moreover, whenever the Zimm-Kilb correction fails (in 'good' solvents), it appears to underestimate the decreasing effect of branching on viscosity. Therefore its failure in these cases would be even more pronounced if Kataoka's formula for computing g were adopted. Thus it seems empirically justifiable to accept Zimm and Stockmayer's theoretical results, rather than those of Kataoka.

Evaluation of the experimental data of Kilb (30) has been more difficult, for the extent of degradation was not determined with accuracy in Kilb's experiments. The range of values suggested by Kilb corresponds to $0.66 \leq \sigma_c \leq \infty$, while according to the results of Miller (113) $\sigma_c = 10$. Also, the exponent a = 0.79 reported by Kilb for toluene solutions of dimethylsilicone is considerably higher than the previously obtained result of Barry (114). This has further contributed to the uncertainty.

Kilb's experimental data for irradiated dimethylsilicone in toluene solution, and the calculated values corresponding to these results, are given in Fig. II-2. Curves 1 and 2 were calculated from the $\varphi(g) = g^{1/2}$ formula, with g values obtained from the equations of Zimm and Stockmayer. Curve 1 was calculated by assuming a = 0.79 and $\sigma_c = 0.667$, curve 2 corresponds to a somewhat lower value of a, and less degradation. Both curves are in quite satisfactory agreement with the experimental data.

FIG. II-2

Comparison of experimental data for irradiated dimethylsilicone in toluene, obtained by Kilb (30), and theoretical curves, calculated from various equations proposed to describe the effects of branching on $[\eta]$. For the calculation of curves 1, 2, and 3, g values were obtained from the formulas of Zimm and Stockmayer (Eqs. II-19 and II-20), for curve 4 Kataoka's formula (Eq. II-21) was employed. The following parameters and correction factors for branching were used to compute the individual curves:

Curve 1	$a = 0.79$	$\sigma_c = 0.667$	$\varphi(g) = g^{1/2}$
Curve 2	$a = 0.74$	$\sigma_c = 1.43$	$\varphi(g) = g^{1/2}$
Curve 3	$a = 0.79$	$\sigma_c = \infty$	$\varphi(g) = h^3$
Curve 4	$a = 0.79$	$\sigma_c = \infty$	$\varphi(g) = g^{1.21}$

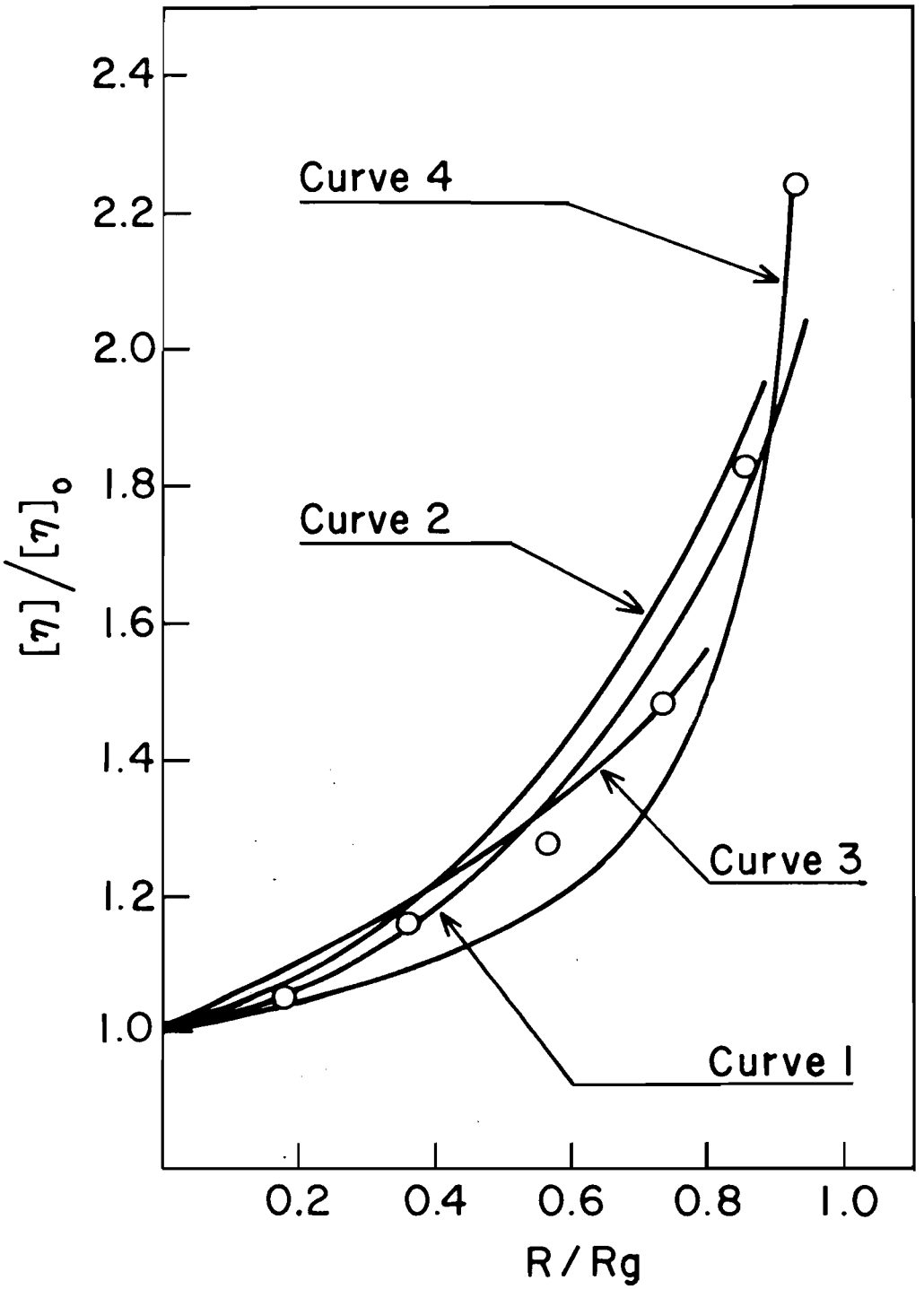
2.4
2.2
2.0
1.8
1.6
1.4
1.2
1.0
$[\eta]/[\eta]_o$
Curve 4
Curve 2
Curve 3
Curve 1
0.2
0.4
0.6
0.8
1.0
R/Rg

Curve 3, which was computed on the basis of the Stockmayer-Fixman treatment (27), with a = 0.79 and $\epsilon_c = \infty$, also agrees with the experiments.

It is then difficult to establish from the data of Fig. II-2 whether $\psi(g) = g^{1/2}$ or $\psi(g) = h^3$ describes the effects of branching more satisfactorily. It is, however, apparent from curve 4 of Fig. II-2 that the Debye-Bueche correction factor g^{2-a} overestimates the influence of branching in decreasing $[\eta]$. The latter curve was calculated from Eq. II-21 of Kataoka for g, with a = 0.79 and $\epsilon_c = \infty$, yet, except near the gel point, the predicted increase in $[\eta]$ is considerably lower than what was observed experimentally.

Kilb's results for irradiated dimethylsilicone in a toluene/diethylphthalate mixture, the θ solvent, are given in Fig. II-3, with the corresponding calculated values. For the calculation of the curves of Fig. II-3 the extent of degradation was considered negligible. Curves 1 and 2 were computed from Zimm and Kilb's $[\eta]_{br}/[\eta]_{lin} = g^{1/2}$ formula, using g values obtainable from the equations of Kataoka (109), and Zimm and Stockmayer (25), respectively. Curve 2 appears to be in good agreement with the experimental data even at high doses. It is interesting to note, however, that the Stockmayer-Fixman treatment this time definitely overestimated the effect of branching on $[\eta]$ (curve 3). For curve 4, g was calculated from the Kataoka formula (Eq. II-21). It is obvious that the g^{2-a} factor, which for θ solvents is identical to the $g^{3/2}$ formula derivable from the Flory-Fox theory, grossly exaggerates the influence of branching.

It is of interest to compare the theoretical results of the

FIG. II-3

Comparison of experimental data for irradiated dimethylsilicone in Θ solvent, obtained by Kilb (30), and theoretical curves, calculated from various equations proposed to describe the effects of branching on $[\eta]$. For the calculation of curves 1 and 4, g values were obtained from the formula of Kataoka (Eq. II-21), for curves 2 and 3 Zimm and Stockmayer's formulas (Eqs. II-19 and II-20) were employed. In all computations a = 0.50 and $\delta_c = \infty$ were assumed. The following correction factors for branching were used to compute the individual curves:

Curves 1 and 2 $\varphi(g) = g^{1/2}$

Curve 3 $\varphi(g) = h^3$

Curve 4 $\varphi(g) = g^{3/2}$

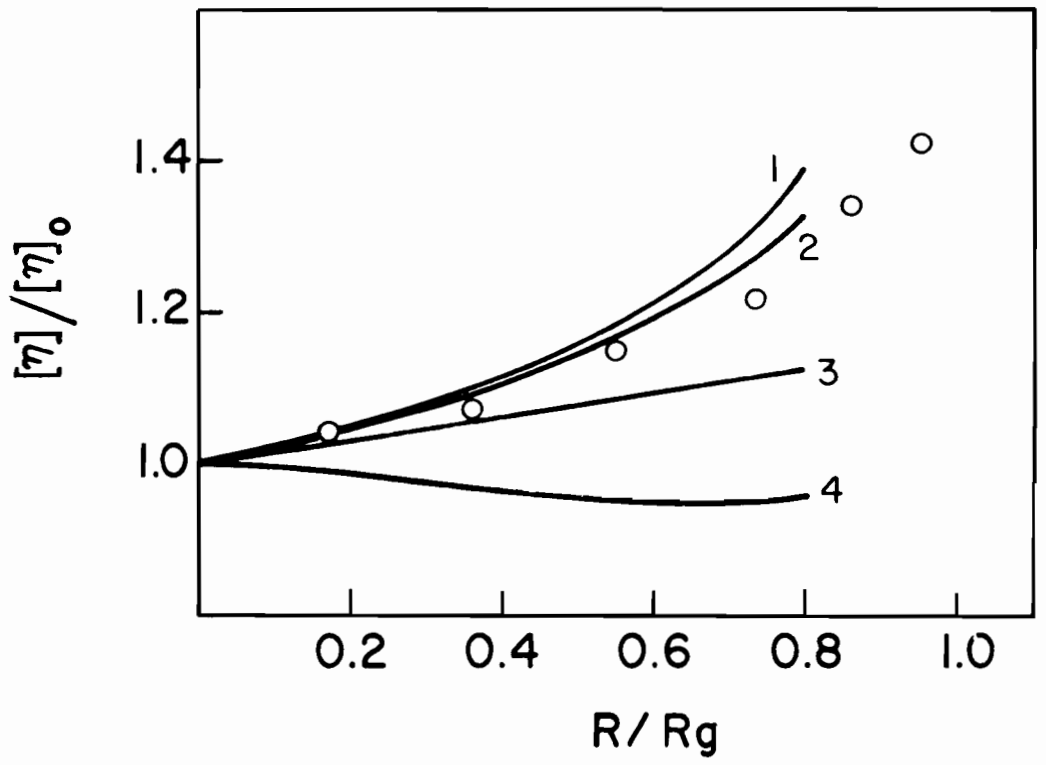
1.4
1.2
1.0
[η]/[η]o
1
2
3
4
0.2
0.4
0.6
0.8
1.0
R/ Rg

present work which were based on the $\varphi(g) = g^{1/2}$ relationship, g computed from the equations of Zimm and Stockmayer, to theoretical values obtained by Kilb (30). The calculations of this author were based on assumptions similar to those of the present work, with $[\eta]_{br}/[\eta]_{lin} = g^{1/2}$, but he used a mathematical approach which was entirely different from that of Saito (19) and Katsuura (21).

It can be seen from Table II-3 that the agreement between the two treatments is good, except near the gel point, at $R/R_g = 0.95$. At such high doses, however, both methods may be unreliable. As mentioned before, whenever the $\varphi(g) = g^{1/2}$ formula fails, it seems to predict a bigger increase in $[\eta]$ than is observed experimentally. Therefore, the somewhat lower $[\eta]/[\eta]_o$ values obtained in the present investigation may be easier to justify empirically than the results of Kilb.

It may be concluded that the theoretical and experimental data of Figs. II-1 to II-3 prove unequivocally that the correction factors $\varphi(g) = g^{3/2}$ and $\varphi(g) = g^{2-a}$ strongly overestimate the decrease in $[\eta]$ due to branching. It is more difficult to choose between the Zimm-Kilb and Stockmayer-Fixman treatments. However, it appears that the former is preferable for solutions in 'poor' solvents, while the latter may be superior when solutions in 'good' solvents are considered. It will be seen that results obtained for samples of non-random initial distribution support this conclusion.

TABLE II-3

Increase of the intrinsic viscosity in crosslinking without degradation, as computed from Eqs. II-17, II-19, II-20, and II-30. The results are compared to values calculated by Kilb (30).

a	R/R_g	$[\eta] / [\eta]_o$	
		Present work	Kilb
0.50	0.20	1.05	1.06
0.50	0.40	1.11	1.13
0.50	0.60	1.19	1.22
0.50	0.80	1.32	1.36
0.50	0.90	1.42	1.48
0.50	0.95	1.47	1.58
0.68	0.20	1.08	1.10
0.68	0.40	1.20	1.23
0.68	0.60	1.38	1.41
0.68	0.80	1.69	1.74
0.68	0.90	1.98	2.09
0.68	0.95	2.14	2.43
0.75	0.20	1.10	1.11
0.75	0.40	1.25	1.27
0.75	0.60	1.47	1.51
0.75	0.80	1.89	1.95
0.75	0.90	2.30	2.46
0.75	0.95	2.54	3.00

Effect of the Initial Distribution

Application of the statistical treatments of Saito (19) and Katsuura (21) to samples of non-random initial distribution poses considerable mathematical problems. As in the computation of various molecular weight averages, discussed in Part I, the Schulz function can be used advantageously when $[\eta]$ is calculated. However, even for this comparatively simple distribution function Katsuura's computations (21) were limited to the evaluation of the virial coefficient a_1 in the expansion

$$[\eta] / [\eta]_o = 1 + a_1(R/R_g) + a_2(R/R_g)^2 + \ldots \quad \text{II-32}$$

Katsuura has found that a_1 increases with increasing λ in the Schulz function (Eq. I-3 of Part I).

It will be recalled that the relative change in M_w with increasing R/R_g was found virtually independent of the initial distribution in crosslinking with degradation (Fig. I-6). The number average molecular weight, however, increases more quickly for narrow range polymers than for highly polydisperse samples. For Mark-Houwink exponents less than unity, M_v is intermediary between M_n and M_w. Therefore it may be expected that the increase of $[\eta]$ with dose will be somewhat more pronounced for narrow range polymers than for samples of initially random distribution. This would be in agreement with the results of Katsuura (21). However, it is difficult to estimate the magnitude of this effect, for in the calculation of $[\eta]$ the molecular weights of individual species are weighted with a correction factor for branching.

Kotliar and Podgor (33) have used an entirely different approach, based on Monte Carlo statistics. These authors were able to determine the molecular weight distribution of irradiated polymers for various λ values in the Schulz function. However, application of their technique to the computation of intrinsic viscosities involved the rough approximation of using a step function to describe the dependence of $[\eta]$ on branching. They assumed that for molecules containing one branch unit $\varphi(g) = 0.79$, and that for molecules with more than one branch unit $\varphi(g) = 0.72$, or, alternatively, 0.91. These values of $\varphi(g)$ were based on the calculations of Zimm and Kilb (28) and F. Bueche (31), carried out for simple star-shaped molecules. The computations of Kotliar and Podgor (33) showed that the relative change in $[\eta]$ of irradiated polymers as a function of R/R_g does not depend strongly on the initial distribution. However, the reliability of these calculations is doubtful, due to the rough approximations involved.

It is then difficult to predict theoretically how the initial distribution will affect changes in the intrinsic viscosity occurring upon irradiation. At the same time, experimental data which could be related to this problem are scarce, for the initial distribution of irradiated samples is usually not known. Therefore Charlesby's results on irradiated dimethylsilicone (105) are of particular interest.

In an effort to determine experimentally whether the initial molecular weight distribution influenced the change in $[\eta]$, Charlesby irradiated two kinds of silicone samples. One of them was a sample of $M_w = 28{,}000$, probably of a near-random initial distribution. The second

sample was a highly polydisperse mixture of silicone fluids: 80% by weight polymer of molecular weight 4,000, and 20% by weight polymer of molecular weight 100,000. Charlesby published the experimental data in the form of graphs of the ratio $M_{apparent}/M_{true}$ *versus* R/R_g, where values of $M_{apparent}$ were computed from intrinsic viscosities and the Mark-Houwink equation. Charlesby assumed that

$$M_{true} = \frac{(M_{true})_{R=0}}{1 - R/R_g} ,$$

in which $(M_{true})_{R=0}$ was the molecular weight of the unirradiated polymer calculated from the Mark-Houwink equation. The above equation is strictly valid only for weight average molecular weights.

In order to plot Charlesby's results as $[\eta] / [\eta]_o$ *versus* R/R_g, his data were recalculated, as follows. From Eq. II-1

$$M_{apparent} = \exp\left\{\frac{\ln[\eta] - \ln K}{a}\right\}$$

and

$$(M_{true})_{R=0} = \exp\left\{\frac{\ln[\eta]_o - \ln K}{a}\right\},$$

i.e.

$$\frac{M_{apparent}}{M_{true}} = \frac{M_{apparent}}{(M_{true})_{R=0}}(1-R/R_g) = (1-R/R_g)\left(\frac{[\eta]}{[\eta]_o}\right)^{1/a}.$$

Therefore

$$\frac{[\eta]}{[\eta]_o} = \left[\frac{M_{apparent}}{M_{true}} \cdot \frac{1}{1 - R/R_g}\right]^a .$$

On the basis of Barry's work (114) a = 0.68 was assumed by Charlesby, and accordingly also in the present calculations. The results are given in Fig. II-4. It appears that the relative increase in $[\eta]$ is the same for the two samples in question, notwithstanding the considerable difference in polydispersity. It is also shown in Fig. II-4 that the theoretical curve calculated for an initially random distribution, based on $\varphi(g) = g^{1/2}$ with g computed from the equations of Zimm and Stockmayer (Eqs. II-19 and II-20), is in good agreement with the data (curve 1). Curve 2, which was calculated from the Stockmayer-Fixman method (Eqs. II-18), seems to overestimate the influence of branching on $[\eta]$.

The experimental results of Charlesby (105), and the calculations of Kotliar and Podgor (33) have indicated that differences in initial distribution do not have a marked influence on the increase in $[\eta]$ during irradiation. Thus it seemed reasonable to assume that the theory developed for samples of initially random distribution would be a good approximation for narrow range polymers. As mentioned in the General Introduction, a number of irradiated anionic polystyrene samples became available in connection with investigations described in the first part of the thesis. It was therefore possible to test the above assumption, by a comparison of $[\eta]$ measured* in various solvents with the theoretically predicted behavior.

---

* The measurements discussed in the following paragraphs were carried out by Messrs. N.B. Glick and D.S.C. Lee.

FIG. II-4

Comparison of experimental data for irradiated dimethylsilicone in toluene, obtained by Charlesby (105), and theoretical curves, calculated from the theories of Zimm and Kilb (Curve 1, $\varphi(g) = g^{1/2}$) and Stockmayer and Fixman (Curve 2, $\varphi(g) = h^3$). The curves were computed by assuming $a = 0.68$ and $\sigma_c = \infty$. Values of g were obtained from the formulas of Zimm and Stockmayer (Eqs. II-19 and II-20).

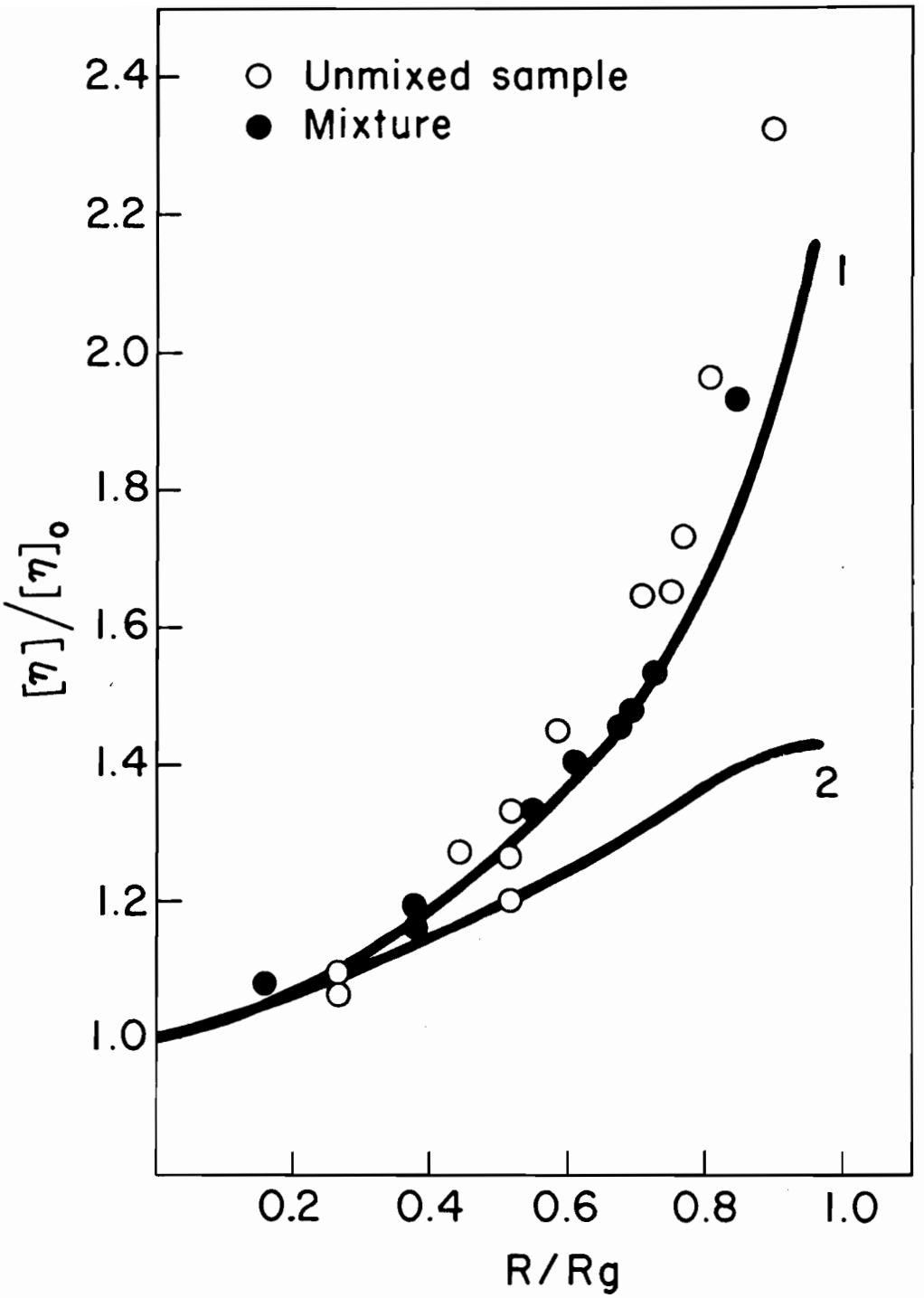
Unmixed sample
Mixture
2.4
2.2
2.0
1.8
1.6
1.4
1.2
1.0
[η]/[η]o
1
2
0.2
0.4
0.6
0.8
1.0
R/Rg

Results of the intrinsic viscosity determinations are shown in Figs. II-5 to II-7. Calculation of the theoretical curves given in these graphs was based on Zimm and Kilb's theory ($\varphi(g) = g^{1/2}$) and the Stockmayer-Fixman treatment ($\varphi(g) = h^3$). Values of g were computed from the formulas of Zimm and Stockmayer (Eqs. II-19 and II-20); $[\eta] / [\eta]_o$ as a function of dose was computed from Eq. II-30 of the Theoretical section, with $\sigma_c = 3.50$, as previously determined in Part I. The exponents of the Mark-Houwink equations for toluene and butanone solutions were taken to be 0.69 and 0.58, respectively, as given by Outer, Carr, and Zimm (115). The measurements in cyclohexane solutions were performed at 34°C, the Θ temperature (116). Determinations in toluene and cyclohexane solutions were carried out for samples of various initial molecular weights, ranging approximately from M = 80,000 to 260,000. Number and weight average molecular weights of the samples used are given in Table E-1 of the Experimental section. As expected from the nature of irradiation processes, and as was predictable from Eqs. II-30 and II-31, any dissimilarities between data obtained for samples of different molecular weights appear to be within experimental error.

In Fig. II-5 the increase of $[\eta]$ with dose is given for toluene solutions of anionic polystyrenes. Calculations based on the Stockmayer-Fixman treatment (curve 2) are in quite good agreement with the experimental data, except at the largest doses. The use of $\varphi(g) = g^{1/2}$ leads to somewhat too high values (curve 1). In this respect the results of Fig. II-5 resemble those given in Fig. II-1.

In Figs. II-6 and II-7 theoretical and experimental data for

FIG. II-5

Comparison of experimental data for irradiated anionic polystyrene in toluene, obtained in course of the present work, and theoretical curves, calculated from the theories of Zimm and Kilb (Curve 1, $\varphi(g) = g^{1/2}$) and Stockmayer and Fixman (Curve 2, $\varphi(g) = h^3$). Eq. II-30, with a = 0.69 and $\sigma_c = 3.50$, was used to compute the theoretical curves. Values of g were estimated from the formulas of Zimm and Stockmayer (Eqs. II-19 and II-20).

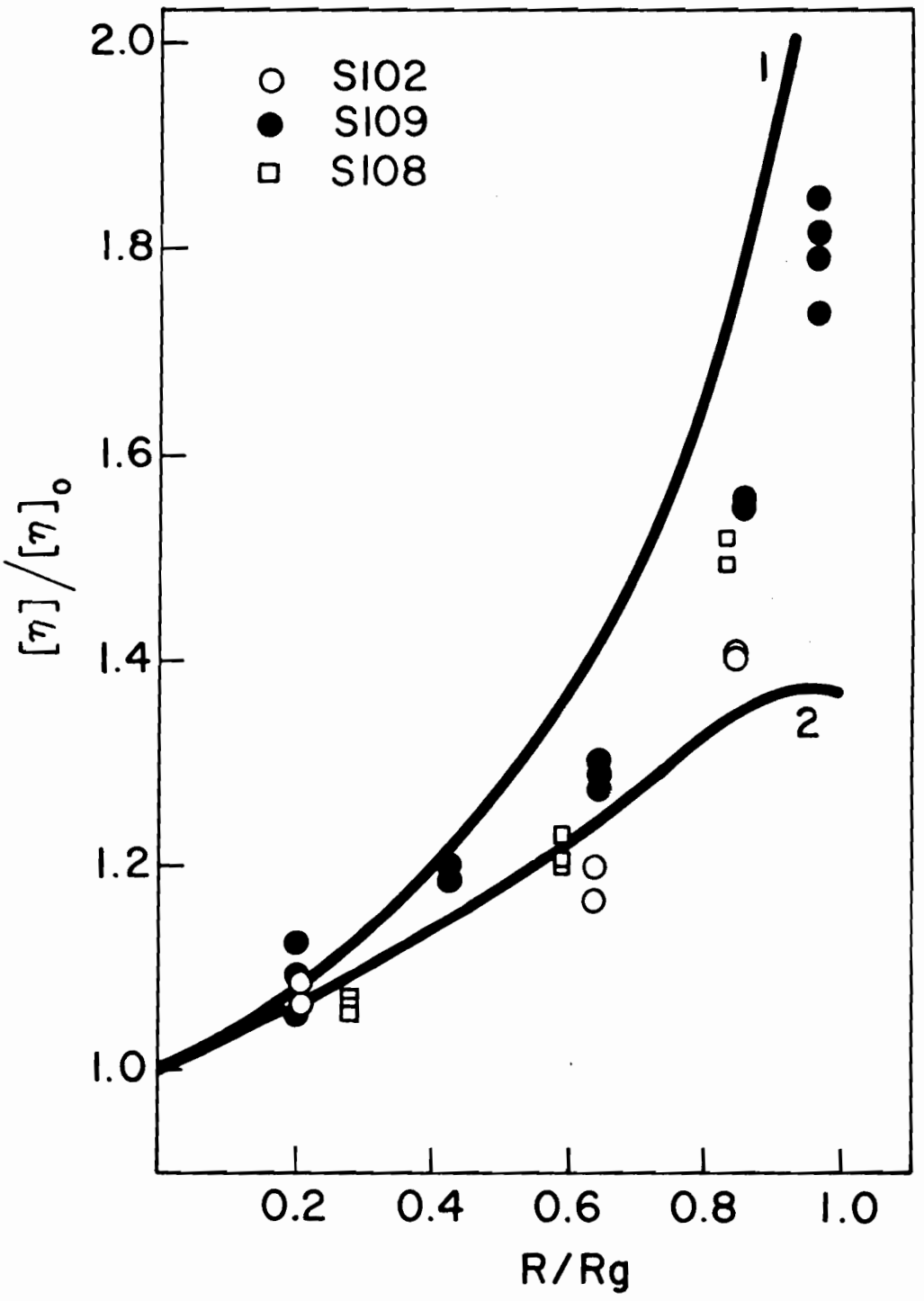
2.0
1.8
1.6
1.4
1.2
1.0
[η]/[η]₀
S102
S109
S108
1
2
0.2
0.4
0.6
0.8
1.0
R/Rg

FIG. II-6

Comparison of experimental data for irradiated anionic polystyrene (sample S109) in butanone, obtained in course of the present work, and theoretical curves, calculated from the theories of Zimm and Kilb (Curve 1, $\varphi(g) = g^{1/2}$) and Stockmayer and Fixman (Curve 2, $\varphi(g) = h^3$). Eq. II-30, with a = 0.58 and $\sigma_c = 3.50$, was used to compute the theoretical curves. Values of g were estimated from the formulas of Zimm and Stockmayer (Eqs. II-19 and II-20).

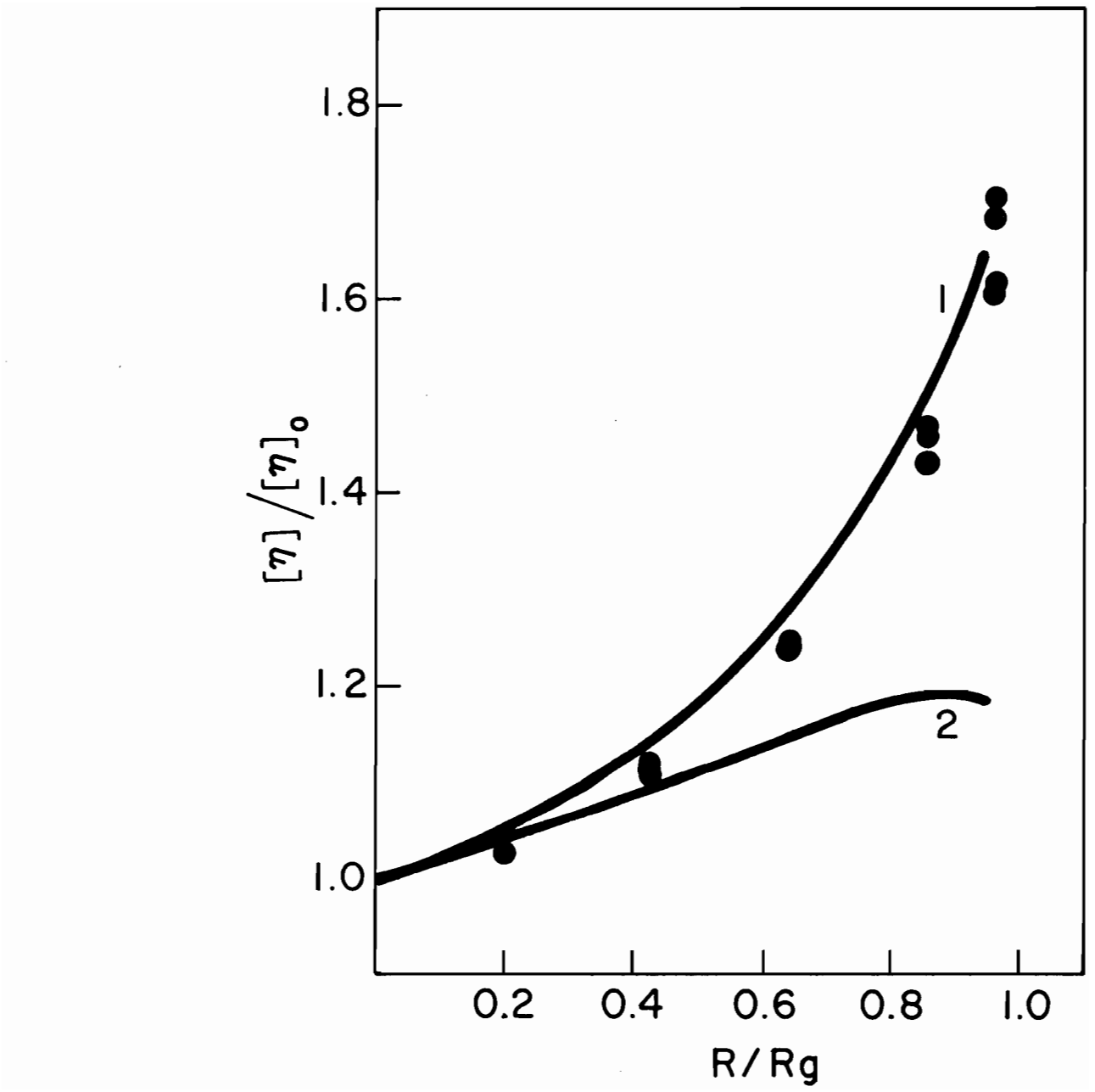
1.8
1.6
1.4
1.2
1.0
[η] / [η]o
1
2
0.2
0.4
0.6
0.8
1.0
R/Rg

FIG. II-7

Comparison of experimental data for irradiated anionic polystyrene in cyclohexane, obtained in course of the present work, and theoretical curves, calculated from the theories of Zimm and Kilb (Curve 1, $\varphi(g) = g^{1/2}$) and Stockmayer and Fixman (Curve 2, $\varphi(g) = h^3$). Eq. II-30, with a = 0.50 and $\sigma_c = 3.50$, was used to compute the theoretical curves. Values of g were estimated from the formulas of Zimm and Stockmayer (Eqs. II-19 and II-20).

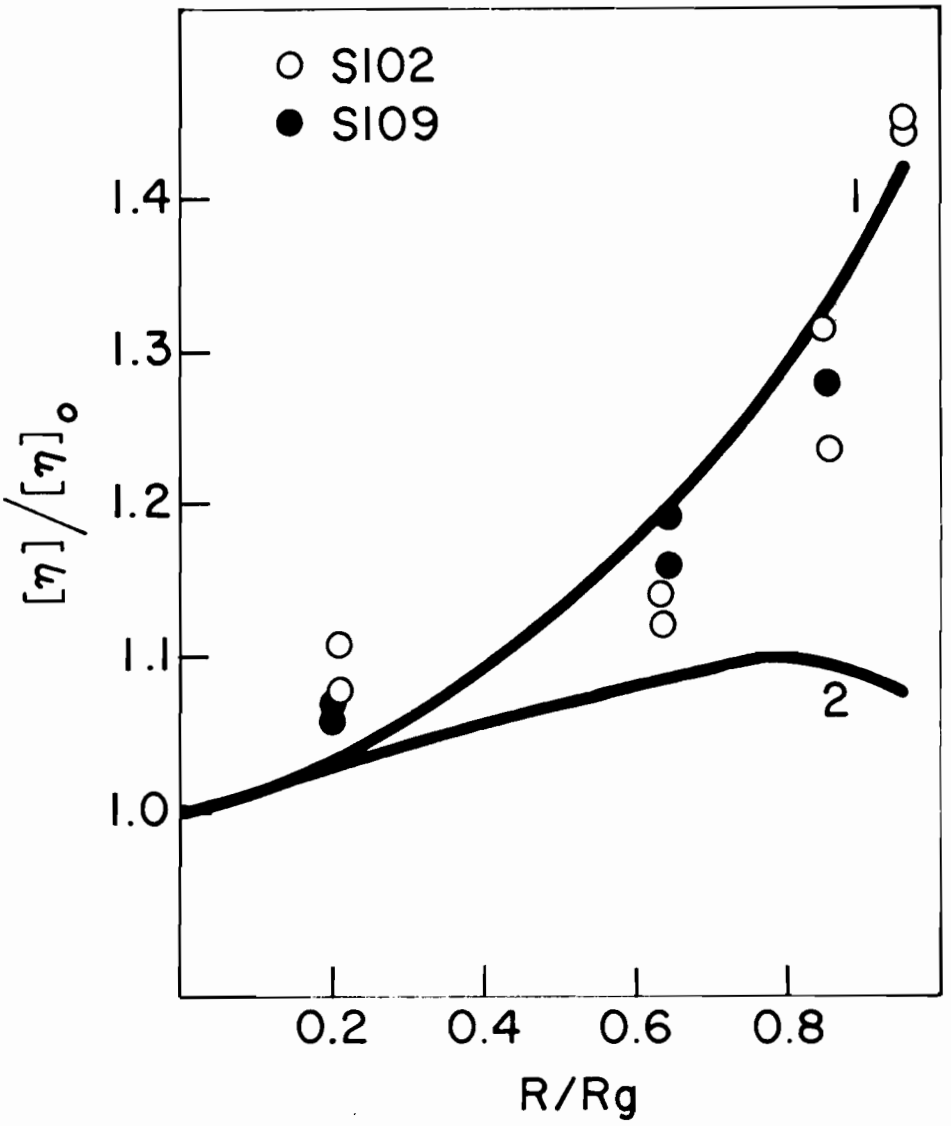
S102
S109
1.4
1.3
1.2
1.1
1.0
[η]/[η]o
1
2
0.2
0.4
0.6
0.8
R/Rg

butanone and cyclohexane solutions, respectively, are shown. Computations based on Zimm and Kilb's theory ($\psi(g) = g^{1/2}$) are in agreement with the experiments, while the $\psi(g) = h^3$ correction term leads to considerably lower values.

It can be seen that the relation of calculated and experimental results obtained for the narrow distribution samples is similar to that observed in Figs. II-1 to II-3 for samples of initially random distribution. It therefore appears that the initial molecular weight distribution has little effect on the relative change in $[\eta]$ caused by irradiation, and Eq. II-30 is applicable to polymers of arbitrary initial distribution, without serious loss of accuracy.

On the Relationship of R_e and $< S^2 >^{1/2}$

It has been seen that the Debye-Bueche and Flory-Fox theories, developed for linear polymers, cannot be directly applied to branched molecules. The semi-empirical formulas suggested by Stockmayer and Fixman, and Zimm and Kilb appear to be somewhat more reliable, however, neither of these formulas seems to fit the experimental results for solutions in both 'good' and 'poor' solvents. The discrepancies can perhaps be explained most logically on the basis of the complicated relationship between the hydrodynamic radius and radius of gyration of branched polymers.

Flory and Fox have assumed that these two quantities are always proportional to each other for linear polymers, but this assumption is not likely to hold for branched molecules. As Stockmayer and Fixman (27)

pointed out, a branched molecule of the same radius of gyration as a linear molecule has everywhere a greater mean segment density. This is likely to decrease the hydrodynamic permeability of branched molecules, and increase R_e. Therefore it is not surprising that the $\varphi(g) = g^{3/2}$ formula, which is based on the Flory-Fox theory, overestimates the influence of branching on decreasing $[\eta]$.

In order to set up reliable new correction factors for branching, it would be necessary to know the precise relation of R_e and $< S^2 >^{1/2}$. However, F. Bueche (31), who criticized the Zimm-Kilb treatment, claimed that the influence of segment density is so pronounced that it is meaningless to express R_e as a function of $< S^2 >$. The findings of the present work, which indicate that none of the existing theories on the effects of branching is generally applicable, seem to be in agreement with Bueche's conclusion. It appears that it may be necessary to introduce further parameters, characteristic to a particular polymer-solvent system. It should then be possible to test such modified treatments by the same method as that used in the present investigation.

SUMMARY AND CONCLUSIONS

Statistical calculations of the intrinsic viscosity of irradiated polymers were extended to include the effects of branching on $[\eta]$, as predicted by various theories. Thus it became possible to test these theories, by comparing calculated and experimental values of $[\eta]$ as a function of dose.

It was concluded that the $[\eta]_{br}/[\eta]_{lin} = g^{3/2}$ and $[\eta]_{br}/[\eta]_{lin} = g^{2-a}$ formulas, derivable from the Flory-Fox and Debye-Bueche treatments, respectively, considerably overestimate the influence of branching on the intrinsic viscosity. The $[\eta]_{br}/[\eta]_{lin} = g^{1/2}$ formula, suggested by Zimm and Kilb, was in good agreement with experimental data obtained for solutions of irradiated polymers in 'poor' solvents. For solutions in 'good' solvents, the Stockmayer-Fixman treatment, based on estimation of the hydrodynamic radius from the Kirkwood-Riseman theory, seems to be a better approximation. However, the latter method fails for solutions in 'poor' solvents.

Although the statistical treatment derived was limited to polymers of initially random distribution, experimental results obtained for irradiated samples of narrow distribution polystyrene indicate that the effect of molecular weight distribution is small. It therefore appears that the methods of calculation used in the present work will be generally applicable for the evaluation of radiation chemical experiments, at least when the mechanism is crosslinking.

The fact that none of the above mentioned theories can explain the hydrodynamic behavior of branched molecules in solvents of different types is attributed to the inadequacy of the radius of gyration as a measure of the hydrodynamic radius.

EXPERIMENTAL

EXPERIMENTAL

I. Materials

Anionic polystyrene. Most of the work was done with narrow molecular weight range polystyrene, prepared by anionic catalysis (62). These samples were generously donated by Dr. H.W. McCormick of the Dow Chemical Company. The number and weight average molecular weights of the samples were determined by Dr. McCormick from molecular weight distribution curves obtained by sedimentation velocity analysis and diffusion measurements (63). Molecular weights are given in Table E-1.

For measurements where the effect of molecular weight distribution was studied, in addition to narrow range polymers a mixture of samples S102 and S108 of Table E-1 was also used. This mixture was prepared by dissolving 14.39 g. of sample S102 and 11.32 g. of sample S108 in benzene, and recovering the polymer by freeze-drying. In these experiments the narrow distribution samples were also dissolved in benzene and freeze-dried. Otherwise, however, anionic polystyrenes were irradiated in the coarse granular form in which they had been received.

For preliminary studies on the possible effects of particle size two types of polystyrene were used.

a. Laboratory prepared polystyrene. High purity polystyrene samples

TABLE E-1

Number and weight average molecular weights of anionic polystyrene samples donated by Dr. McCormick

Sample	M_n	M_w
S102	78,500	82,500
S105	147,500	153,500
S 27	158,000	166,000
S104	175,000	186,000
S109	182,000	193,000
S108	247,000	267,000

were prepared by thermal polymerization of styrene. The monomer was of highest purity grade, and was obtained from the Fisher Scientific Company. It contained tert.-butylpyrocatechol as a polymerization inhibitor. The monomer was dried over Drierite, and then distilled at a reduced pressure of approximately 15 mm. of mercury, in an all glass apparatus of the Claisen type. The boiling point of styrene at this pressure was between 35 and 45°C, with a constant fluctuation due to pressure changes. To maintain the vacuum at 15 mm., dry nitrogen was bled into the system through a flutter valve, as described by McConnell (117). To avoid bumping, heat for the distillation was supplied by an infrared lamp. The first 10% of the distillate was discarded and only the next 60-70% was collected.

Immediately after the distillation, the main fraction was transferred into ampoules made of 9 mm. pyrex tubes, and was frozen in a dry ice-methanol mixture. After freezing, the ampoules were evacuated to a pressure of a few millimeters of mercury, flushed with dry nitrogen, then again evacuated, and sealed. Polymerization was carried out in the sealed tubes, by heating the samples in boiling water for 120 hours, and then in an oven at 125-130°C for three weeks. The polystyrene was obtained in the form of rods by breaking the tubes. One half of the polymer was dissolved in benzene, freeze-dried, dried in a vacuum oven at 70°C for 24 hours, and stored in a vacuum desiccator. The remaining polystyrene rods were cut up into pieces approximately 8 mm. long and 6.5 mm. in diameter, heated in vacuo at 70°C for 24 hours, and then stored with the freeze-dried samples.

b. Monsanto polystyrene. Two commercial polystyrene samples were obtained from the Monsanto Company. The materials were in bead form, with particle sizes as shown in Table E-2.

Molecular weights of both the thermally polymerized and Monsanto samples were obtained by viscometry. The intrinsic viscosities were determined in toluene solution at 25°C, and the viscosity average molecular weights (M_v) were calculated from the equation (115)

$$[\eta] = 1.7 \times 10^{-4} M_v^{0.69} , \qquad \text{E-1}$$

where $[\eta]$ is in dl.g.$^{-1}$ The results of these measurements are also given in Table E-2.

TABLE E-2

Polystyrene samples used in the study of surface effects

Sample	Average particle size	Approximate specific surface	Intrinsic viscosity in toluene solution at 25°C	M_v
	mm.	$cm.^{-1}$	$dl.g.^{-1}$	
M1 (Monsanto)	1.4	25	0.96	270,000
M2 (Monsanto)	0.34	100	0.83	220,000
Rods (Lab. made)	7	10	1.45	450,000
Freeze-dried (Lab. made)		large	1.45	450,000

Solvents. All solvents were reagent grade, and were distilled before use in an all glass apparatus, with a 20" Liebig condenser serving as an unpacked column. Toluene and cyclohexane were distilled from sodium, while butanone was dried with anhydrous potassium carbonate prior to distillation. In all cases the first 10% of the distillate was discarded and only the next 70 to 75% was collected. The densities of toluene and butanone were measured at 25°C and were found to be 0.861 and 0.797 $g.cm.^{-3}$, respectively. The density of cyclohexane was 0.766 $g.cm.^{-3}$ at 34°C. These values were in good agreement with data given in the literature, indicating purity of the solvents used.

II. Evacuation and Irradiation of the Samples

In all experiments Co^{60} gamma ray sources were used to irradiate the samples. Prior to irradiation the samples were evacuated to a pressure of approximately 10^{-4} cm. of mercury, as follows.

The samples were placed in 10 mm. diameter pyrex tubes, closed at one end, and these tubes were sealed onto a manifold that was capable of accommodating 17 ampoules. The vacuum system is shown in Fig. E-1. Preliminary work indicated that in order to pump out the last traces of air it was necessary to evacuate the apparatus repeatedly, for fairly long periods of time. Therefore, before the vials were sealed off, the apparatus was pumped down to a pressure of 10^{-4} cm. of mercury on five or six consecutive days, for six hours or more at a time. As an added precaution, during the first day of the evacuation the samples were flushed twice with dry nitrogen. The lower tips of the ampoules were immersed in water, to dampen the vibrations and avoid breakage of the capillaries through which the ampoules were connected to the vacuum system.

Samples were irradiated by Co^{60} gamma rays in GAMMACELL irradiation units, manufactured by the Atomic Energy of Canada Limited. Exposure dose-rates at any given time were calculated on the basis of the exponential decay law from the radiation flux at the time of calibration. By assuming that 1 g. of irradiated polystyrene absorbs 95 ergs per roentgen (118), the absorbed dose, R, was computed in megarads from the equation

FIG. E-1

Vacuum system for evacuation and opening of samples. When the apparatus was assembled for breaking the ampoules the part drawn in dashed lines was substituted for the cap.

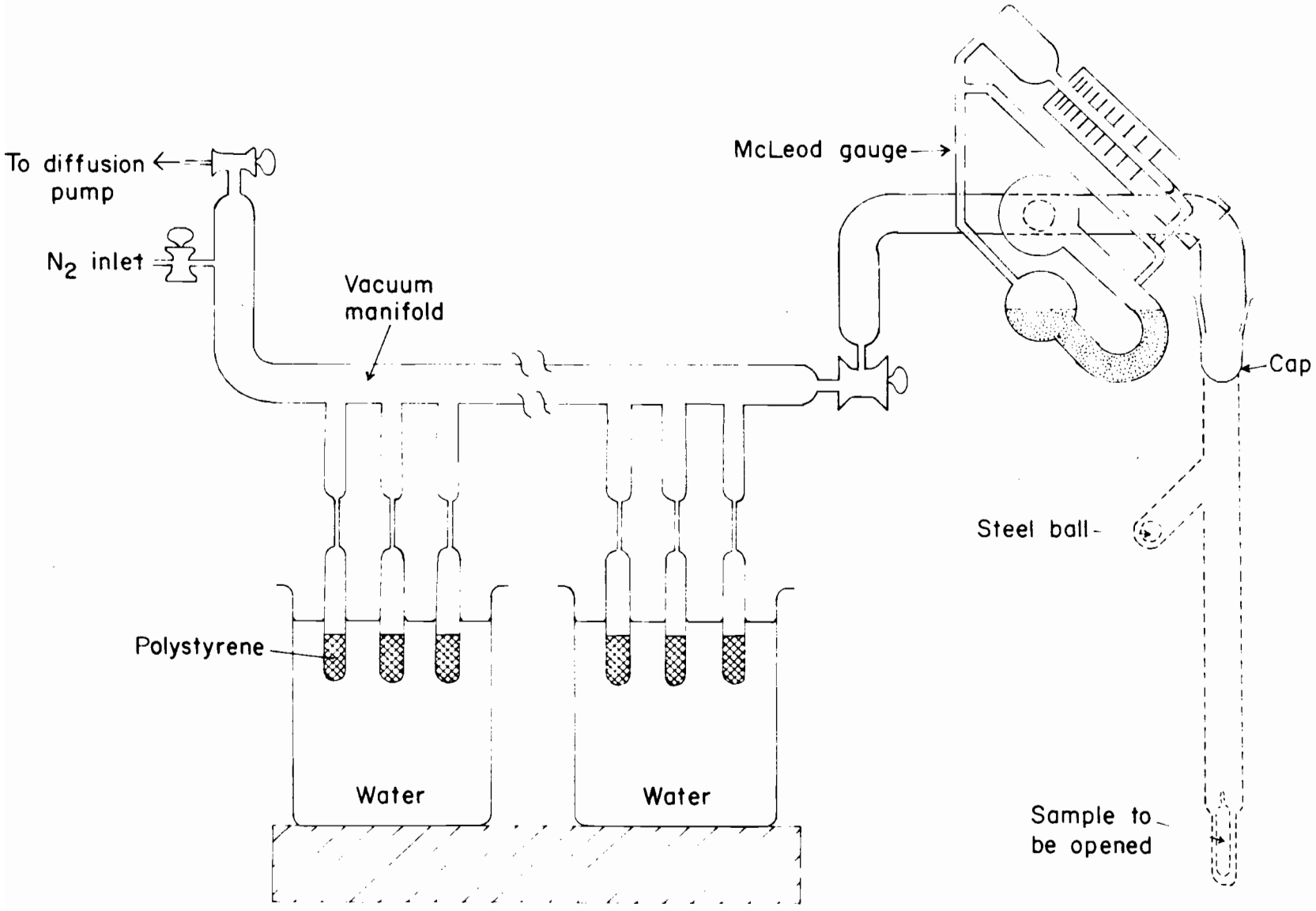
To diffusion pump
N_2 inlet
Vacuum manifold
McLeod gauge
Cap
Steel ball
Polystyrene
Water
Water
Sample to be opened

$$R = 0.95 \times 10^{-6} I_o \tau' \exp(-0.693\, t/t_{1/2}), \qquad E\text{-}2$$

in which I_o is the exposure dose-rate at the time of calibration in roentgens per hour, τ' is the exposure time in hours, $t_{1/2}$ is 5.3 years, the half-life of Co^{60}, and t is the time elapsed between calibration of the radiation source and the irradiation in question.

Due to anisotropy of the radiation fields of the gamma ray sources used, the absorbed dose-rate was not uniform in different regions of a single ampoule. In most cases the effect of anisotropy was considered negligible, and the dose was calculated from the intensity at the mid-point of the sample. For light-scattering samples, however, where the height of freeze-dried material in the vials often exceeded ten centimeters, corrections were applied for the anisotropy of the field. This was done by considering the effect of irradiation on 'layers' of the polymer. Using the experimentally obtained weight average molecular weights (Fig. E-2), the calculated mid-point dose values, and the known isodose curves of the irradiation chambers, an effective dose was estimated. The effective dose was defined as the dose that would have caused the observed increase in molecular weight if absorbed from an isotropic field. Graphs of $M_w''(R)/M_w(0)$ *vs.* R/R_g, corrected for anisotropy, are given in Fig. E-3.

After irradiation the samples were left unopened for at least 24 hours, to allow trapped radicals to react. The samples were usually opened up *in vacuo*, by breaking the seal with a steel ball. The apparatus used has been shown in Fig. E-1. The gas content was measured on a McLeod gauge, to verify that no air had leaked into the ampoules.

FIG. E-2

The effect of irradiation on the weight average molecular weight of samples S105 and S102/S108. $M''_w(R)/M_w(0)$ is plotted against the absorbed dose at the mid-point of the samples.

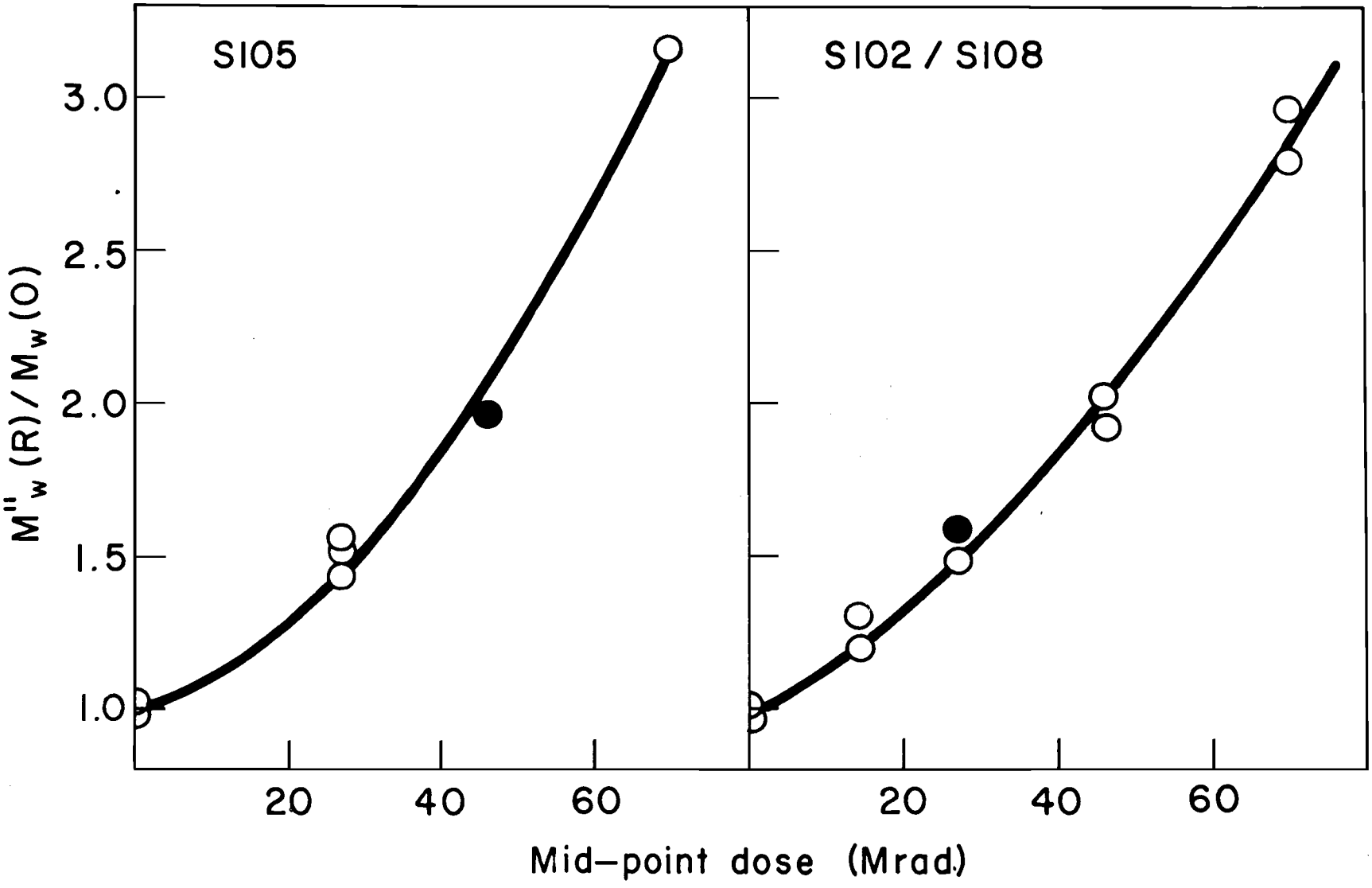
S105
S102 / S108
3.0
2.5
2.0
1.5
1.0
$M''_w(R)/M_w(0)$
20
40
60
20
40
60
Mid-point dose (Mrad)

FIG. E-3

The effect of irradiation on the weight average molecular weight of samples S105 and S102/S108. To plot these graphs, corrections have been applied for the anisotropy of the radiation field.

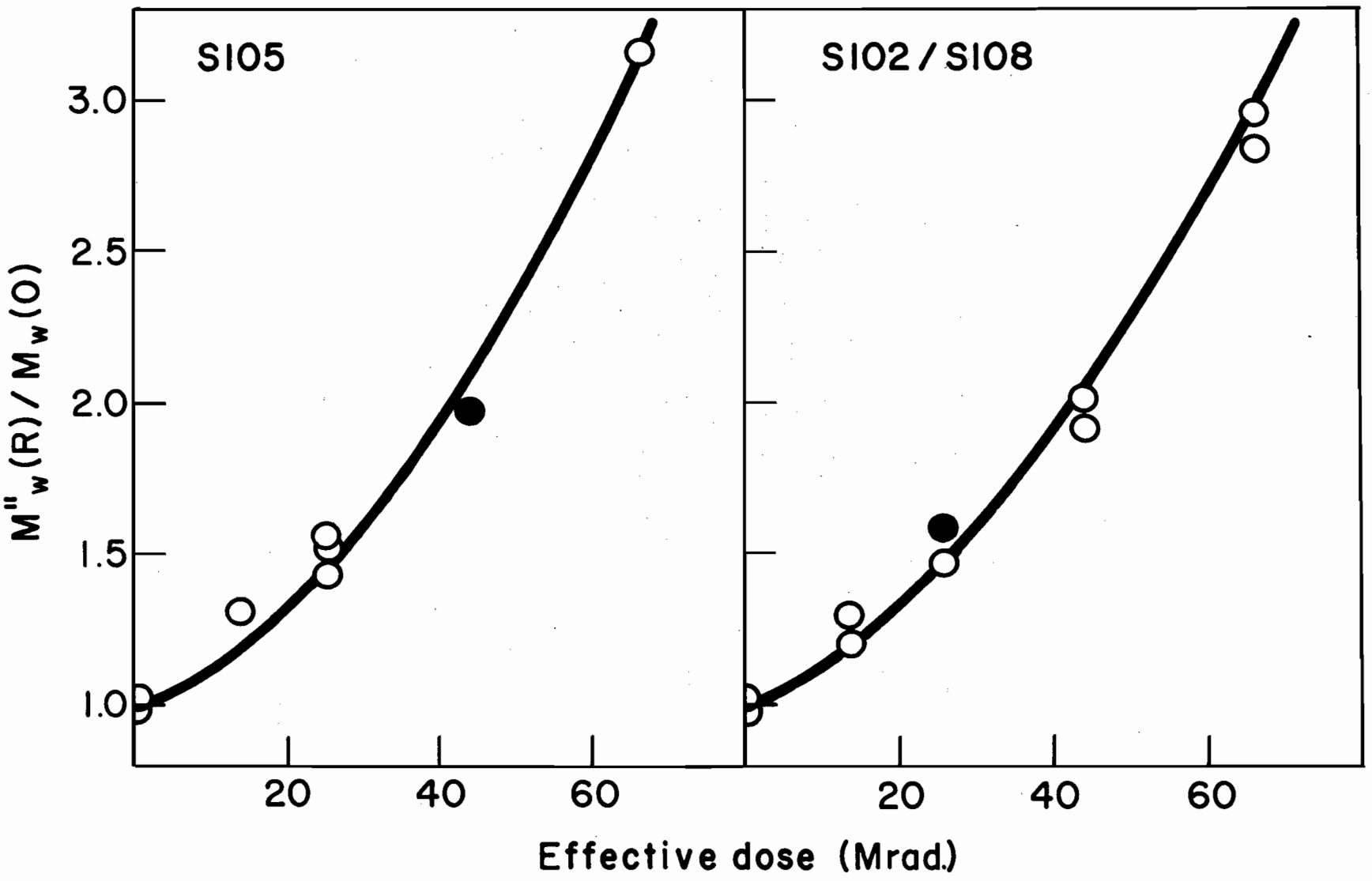
S105
S102 / S108
3.0
2.5
2.0
1.5
1.0
$M''_w(R) / M_w(0)$
20
40
60
20
40
60
Effective dose (Mrad.)

Whenever the amount of gas was higher than 2 $mm.^3$ per g. per Mrad. (at standard temperature and pressure) the samples were rejected. As more experience was gained in sealing the vials, such occasions for rejection very seldom arose.

III. Light-scattering

Technique. Light-scattering measurements were made at room temperature, in a Brice-Phoenix light-scattering photometer. The instrument had previously been modified (119), to accommodate cells amenable to ultracentrifugation. The light-scattering cells were an improved form (120) of the cells described by Dandliker and Kraut (121).

Polystyrene samples were dissolved in toluene and the solutions were filtered through sintered glass filters (B.S. 1752) before being made up to the final volume. Then five different concentrations of each sample were obtained by dilution. Prior to measurements the solutions were clarified by ultracentrifugation at 45,000 g for 30 minutes in the light-scattering cells. A Spinco Model L ultracentrifuge was used, and the cells were floated in carbon tetrachloride in the cups of the S.W. 25.1 swinging bucket rotor. Light-scattering determinations were made as soon as possible after ultracentrifugation.

Dibutyl phthalate was used as bath liquid and was also clarified by ultracentrifugation (two hours at 33,000 g). The refractive index of dibutyl phthalate was found to be 1.4918 at 23°C, which was near to the value of 1.4955 obtained for toluene at the same temperature. The scattering intensities were measured at five concentrations and for the pure solvent, at a wavelength of 546 mμ.

Concentrations were determined gravimetrically, by evaporating the solvent on a hot plate, and drying the polymer in aluminum foil dishes to constant weight in a vacuum oven at 70°C. It was found that overnight

drying was sufficient to reach constant weight.

Observations were made at angles of 0, 45, 90, and 135 degrees to the incident beam. The scattering intensity i_θ was expressed as the ratio of the galvanometer reading at the angle θ to the reading for the transmitted beam at 0°. This procedure eliminated the errors due to photocell fatigue and variations in lamp intensity.

The Rayleigh ratio at the angle θ, R_θ, was calculated from the equation

$$R_\theta = K_c C_n \left[\left(\frac{G_\theta}{G_o}\right)_{solution} - \left(\frac{G_\theta}{G_o}\right)_{solvent} \right], \qquad E\text{-}3$$

in which G_θ and G_o are the galvanometer readings at the angle θ and for the transmitted beam, respectively, C_n is the refractive index correction of Carr and Zimm (122), and K_c is the calibration constant. For the optical system used (119), the Carr-Zimm correction took the form

$$C_n = n\left[1 - \frac{1}{3}\left(\frac{n-1}{n}\right)\right], \qquad E\text{-}4$$

where n is the refractive index of the solution.

The data were plotted according to the equation

$$\frac{Kc}{R_{90}} P(90) = \frac{1}{M_w} + 2A_2^{\tau} P(90)c, \qquad E\text{-}5$$

where

$$K = \frac{2\pi^2 n_o^2 (dn/dc)^2}{N\lambda^4}. \qquad E\text{-}6$$

In the above equations n_o is the refractive index of the solvent, dn/dc is the refractive index increment, N is Avogadro's number, λ is the wavelength of the incident beam, c is the concentration in $g.cm.^{-3}$, M_w is the average molecular weight yielded by the dissymmetry method, and A_2 is the second virial coefficient. From measurements at 45 and 135 degrees R_{45} and R_{135} were computed by equation E-3, and the ratio R_{45}/R_{135} was extrapolated to zero concentration (Fig. E-4) to give the dissymmetry z. The particle scattering factor P(90) was then obtained from z and the tables of Doty and Steiner (123). Graphs of Kc/R_{90} versus c are shown in Fig. E-5. Molecular weights and virial coefficients were computed from the slope and intercept by means of equation E-5.

It should be noted that the molecular weight obtained from equation E-5 is not a pure weight average (124), since

$$\left(\frac{Kc}{R_{90}}\right)_{c=o} = \frac{\sum_i w_i}{\sum_i w_i M_i P(90)_i} \neq \frac{1}{P(90)} \cdot \frac{\sum_i w_i}{\sum_i w_i M_i}, \qquad \text{E-7}$$

where w_i, M_i and $P(90)_i$ are the weight fraction, molecular weight and particle scattering factor of the i^{th} species in the polymer. To obtain a true weight average it would be necessary to use Zimm's double extrapolation technique (125). However, due to the comparatively low molecular weights of the samples used in these experiments, the dissymmetries were, on the one hand, too low for constructing a Zimm plot, and, on the other hand, low enough for the difference between the true weight average and that calculated from Eq. E-5 to be well within experimental error.

FIG. E-4

Concentration dependence of R_{45}/R_{135} for unirradiated and irradiated samples of the S102/S108 mixture.

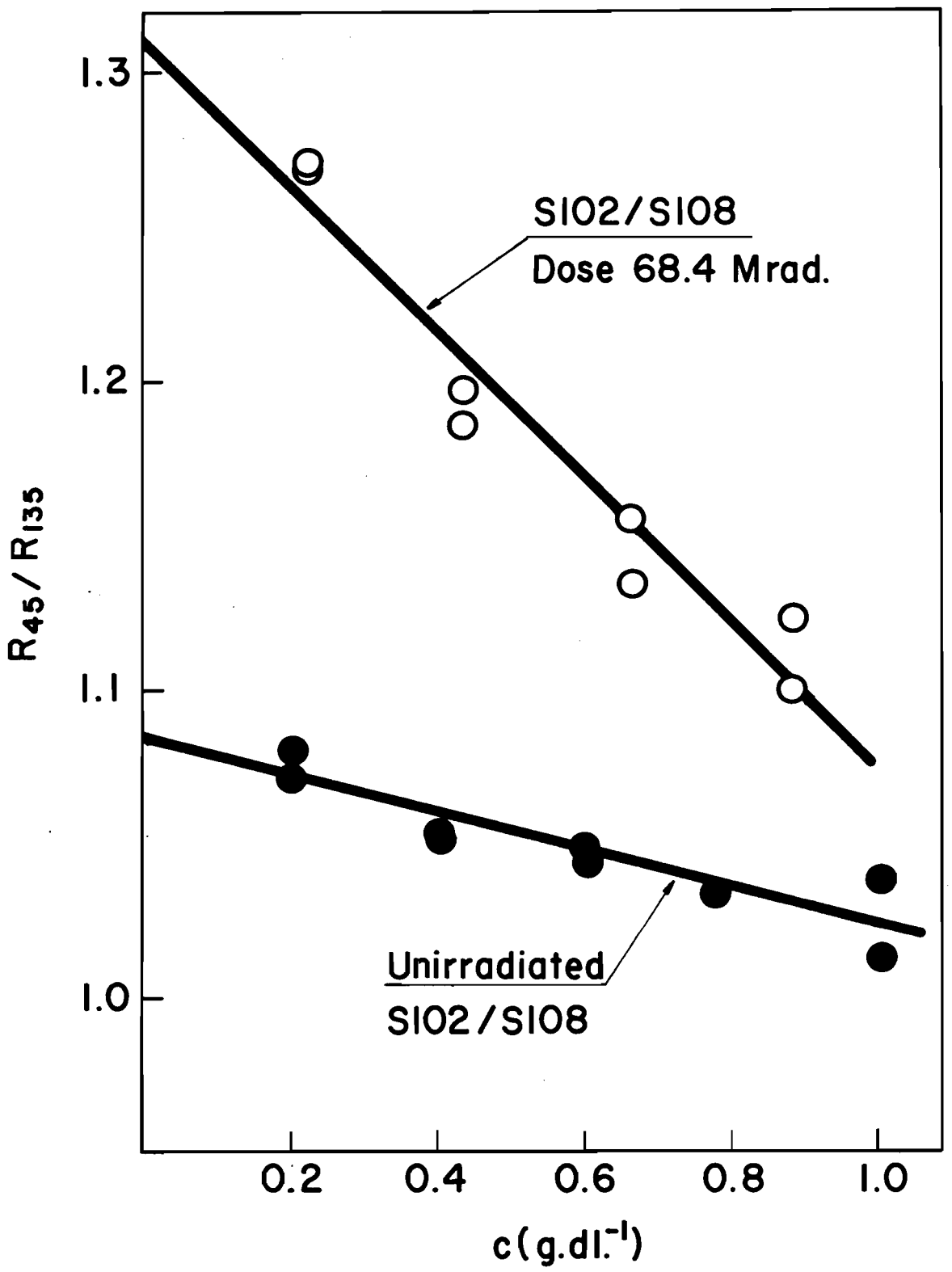
1.3
1.2
1.1
1.0
R_{45}/R_{135}
S102/S108
Dose 68.4 Mrad.
Unirradiated
S102/S108
0.2
0.4
0.6
0.8
1.0
c(g.dl.$^{-1}$)

FIG. E-5

Extrapolation of Kc/R_{90} values to zero concentration for several polystyrene samples.

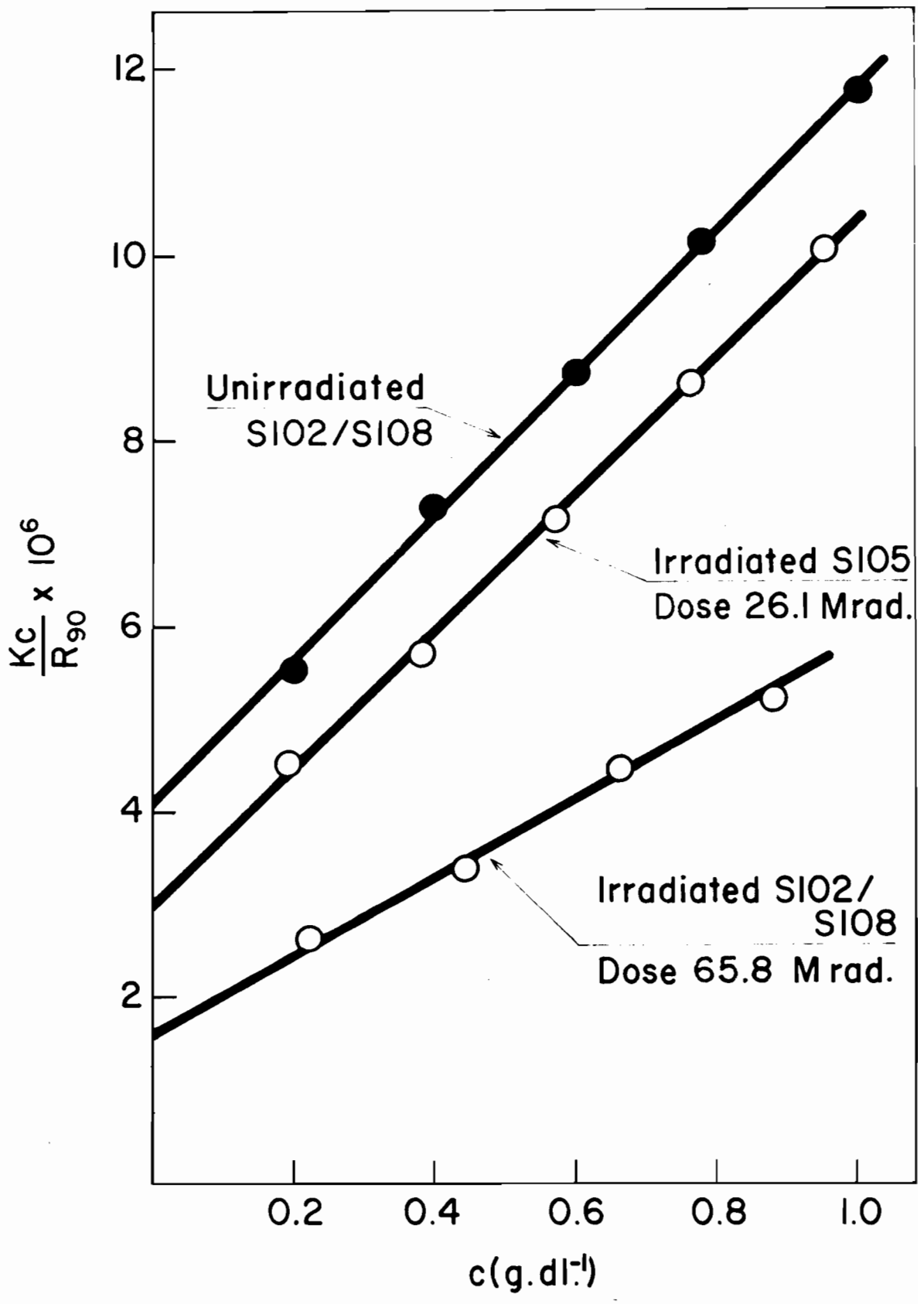
12
10
8
6
4
2
$\frac{Kc}{R_{90}} \times 10^6$
Unirradiated
S102/S108
Irradiated S105
Dose 26.1 Mrad.
Irradiated S102/
S108
Dose 65.8 M rad.
0.2
0.4
0.6
0.8
1.0
c(g.dl^{-1})

Light-scattering data were used mainly for determining the ratio of molecular weights of original and irradiated samples. For purposes of statistical calculations, the molecular weights given by Dr. McCormick and listed in Table E-1 were used.

While the molecular weights computed from equation E-5 are, for low dissymmetries, essentially pure weight average quantities, the dependence of the mean square radius of gyration on the shape and size distribution of molecules is pronounced. The value yielded by the dissymmetry method may vary from a weight or lower average up to a Z + 1 average (124). Therefore the evaluation of the mean square radius was not attempted.

Calibration. The constant K_c of equation E-3 was obtained from measurements made on a toluene solution of Cornell standard polystyrene, containing 0.5 g. of polymer per 100 ml. of solvent. In a critical discussion of light-scattering calibration techniques, Kratohvil and collaborators (126) have listed the excess turbidity of this polymer solution, as obtained by several methods. From Kratohvil's tabulation the average excess turbidity of the standard polystyrene solution was 3.485×10^{-3} cm.$^{-1}$ at 436 mμ and 1.335×10^{-3} cm.$^{-1}$ at 546 mμ. The excess turbidity is related to the Rayleigh ratio of Eqs. E-3 and E-5 by

$$\tau^\circ = \frac{16\pi R_{90}}{3} , \qquad \text{E-8}$$

where τ° is the excess turbidity.

The scattering of the standard polystyrene solution was measured at 436 and 546 mμ, and the calibration constant K_c was calculated from Eqs. E-3 and E-8. The calibration was tested by calculating R_{90} for toluene. At 436 mμ R_{90} was 59.5 x 10^{-6} $cm.^{-1}$ and at 546 mμ 21.0 x 10^{-6} $cm.^{-1}$, in good agreement with the average values of 56.3 x 10^{-6} $cm.^{-1}$ and 18.9 x 10^{-6} $cm.^{-1}$, respectively, computed from the tables of Kratohvil and collaborators (126).

Refractive index increment. The refractive index increment of S105 narrow range polystyrene (Table E-1) in toluene solution was measured in a Brice-Phoenix differential refractometer. The instrument had previously been calibrated (127) with sucrose solutions of different concentrations. The refractive index-concentration relationship was linear in the concentration range 0 to 1 $g.dl.^{-1}$, and dn/dc at 546 mμ was found to be 0.1076 $cm.^3g.^{-1}$, in excellent agreement with the value interpolated from the data of O'Mara and McIntyre (128).

Within experimental error, the refractive index increment of the above polymer sample was found the same after irradiation by a dose of 70 Mrads. Therefore it was assumed that the effect of irradiation on the refractive index could be neglected.

IV. Osmotic Measurements

Osmotic measurements were done as described by Goring and Timell (120). The instrument was the Stabin-Immergut (129) modification of the Zimm-Myerson osmometer (130). The temperature was 30 ± 0.01°C and the solvent was toluene. Very dense grade ultracella filters (131) were used as membranes. These membranes had been shipped in a dilute formalin solution, and were never allowed to dry. They were conditioned in a series of alcohol-water mixtures of successively increasing alcohol content, absolute alcohol, and toluene. Finally the membranes were conditioned overnight in the polystyrene solution to be examined. Syringes with long needles were employed to fill the osmometers. Before use the instruments were rinsed several times with the polymer solution. Mercury was used for sealing the osmometers during measurements.

The liquid levels in the capillaries were measured at various time intervals with a cathetometer. When the osmotic height became nearly constant, the height-time curves were extrapolated to obtain the equilibrium value, as shown in Fig. E-6. Six to nine hours were usually sufficient to establish the equilibrium osmotic height.

The osmotic height h was determined at four different concentrations, over a range of 0.17 to 1.11 $g.dl.^{-1}$ The data were plotted as h/c *versus* c (Fig. E-7) and the number average molecular weight M_n, and the osmotic second virial coefficient A_2^{π} were calculated from the equation

$$\frac{\rho gh}{c} = \frac{\pi}{c} = RT \left[\frac{1}{M_n} + A_2^{\pi} c \right] \qquad \text{E-9}$$

FIG. E-6

Decrease of osmotic height with time for three concentrations of unirradiated S105 sample dissolved in toluene.

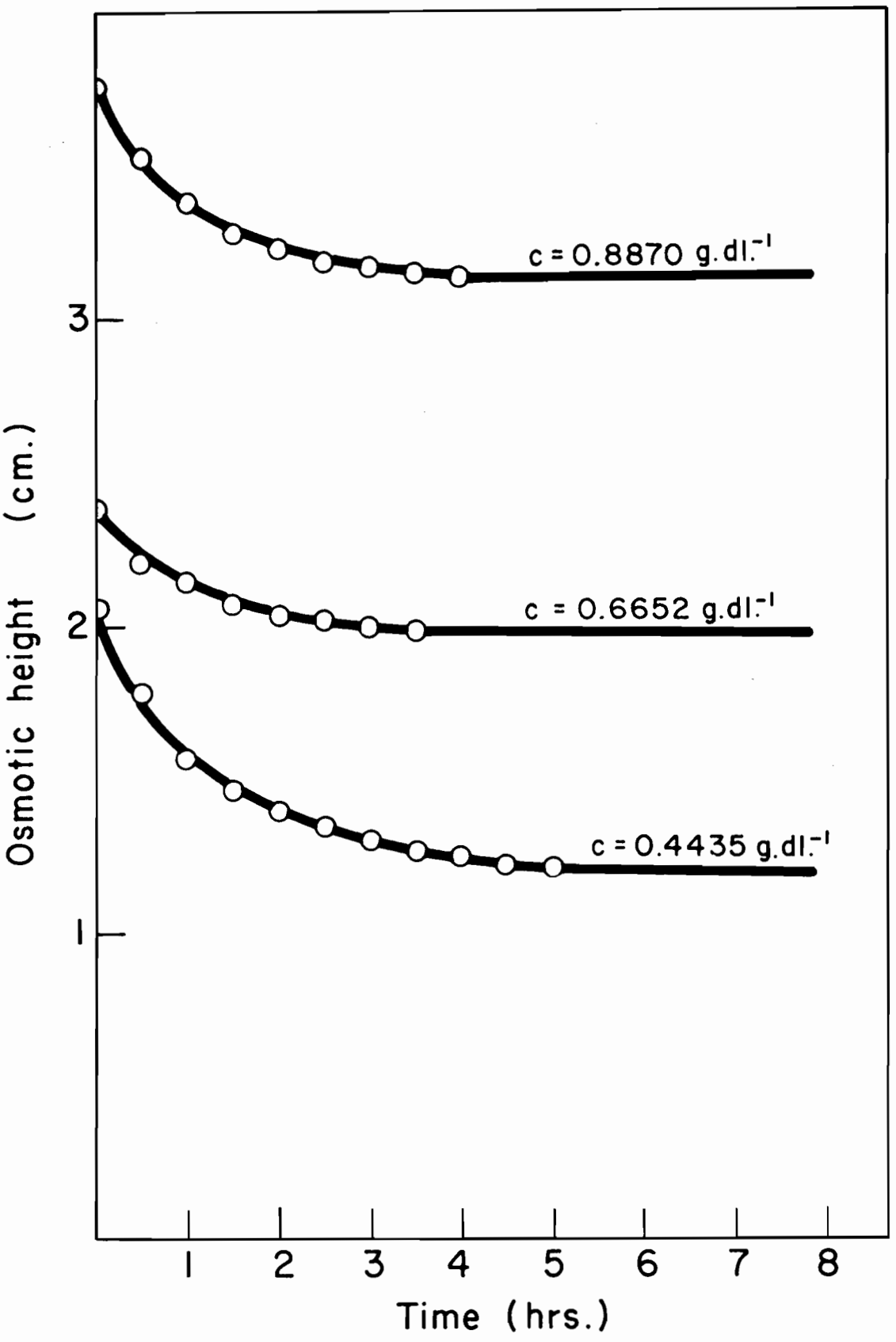
c = 0.8870 g.dl.⁻¹
c = 0.6652 g.dl.⁻¹
c = 0.4435 g.dl.⁻¹
Osmotic height (cm.)
1
2
3
1
2
3
4
5
6
7
8
Time (hrs.)

FIG. E-7

Graph of h/c *vs.* c for several samples of polystyrene.

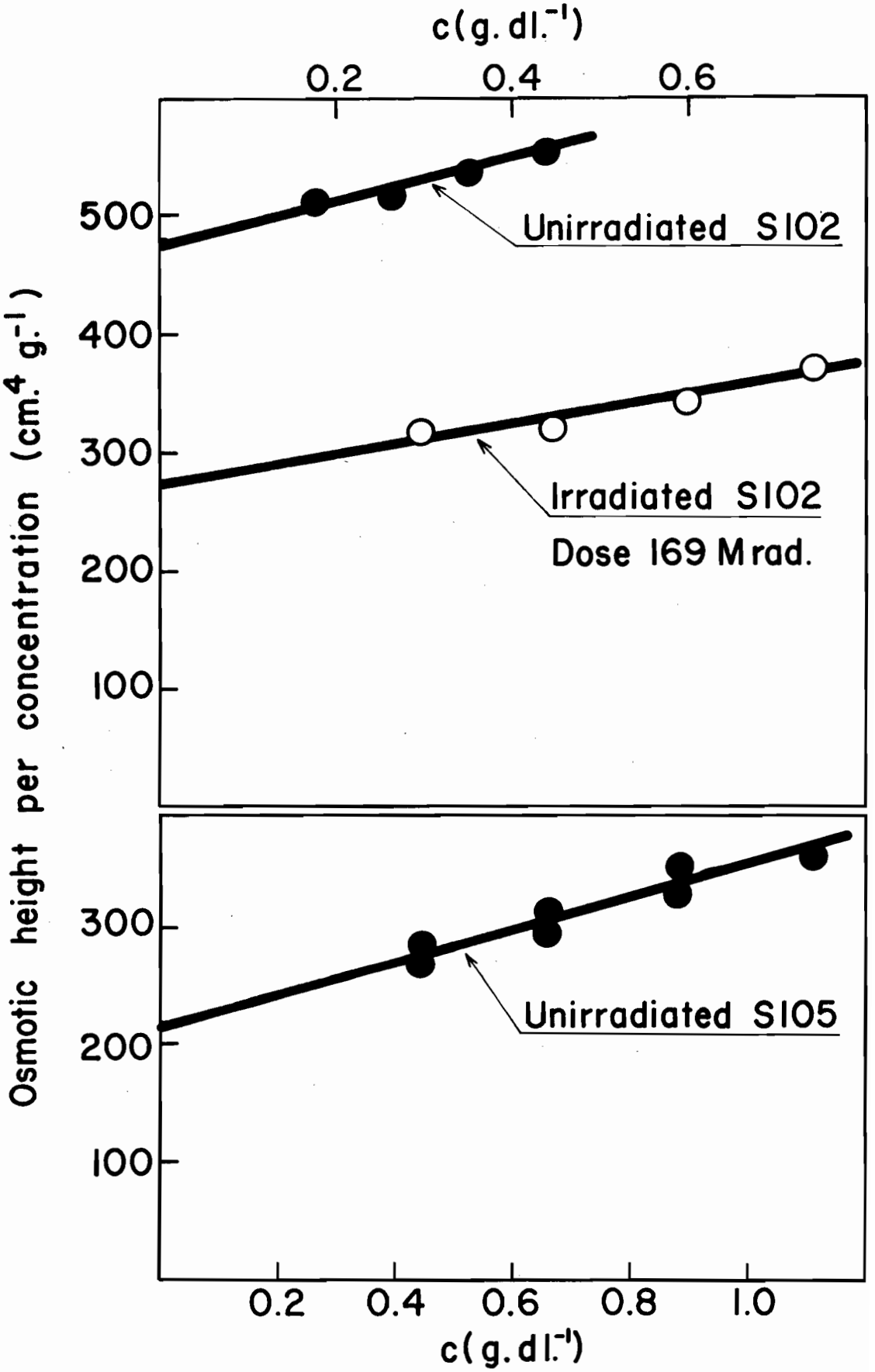
c(g. dl.$^{-1}$)
0.2
0.4
0.6
500
400
300
200
100
Unirradiated S102
Irradiated S102
Dose 169 Mrad.
Osmotic height per concentration (cm.^{4} g.$^{-1}$)
300
200
100
Unirradiated S105
0.2
0.4
0.6
0.8
1.0
c(g. dl.$^{-1}$)

where ρ is the density of the solution in $g.cm.^{-3}$, $\underline{g}$ is the acceleration due to gravity, c is the concentration in $g.cm.^{-3}$, π is the osmotic pressure in dyne $cm.^{-2}$, $\underline{R}$ is the gas constant, and T is the absolute temperature.

V. Viscometry

With the exception of some preliminary measurements, two Craig and Henderson suspended level viscometers (132) were used throughout the experiments. These viscometers (133) had been designed specifically to eliminate kinetic energy corrections, and such corrections therefore were not applied.

The solutions introduced into the viscometers were weighed by difference. Densities had been previously determined at 25°C for toluene and butanone solutions and at 34°C for cyclohexane solutions. The solvent used for subsequent dilutions was thermostatted in the viscosity bath, and was added using calibrated pipettes.

Efflux times were measured to 0.1 sec. at 25.00 $\pm$ 0.02°C for toluene and butanone solutions and at 34.00 $\pm$ 0.04°C for cyclohexane solutions. The efflux times were measured at five concentrations for each sample, and were frequently checked for pure solvents.

From data obtained in this way η_{sp}/c and $(\ln \eta_{rel})/c$ were computed. The intrinsic viscosity $[\eta]$ was determined by the usual extrapolation processes (Fig. E-8), using the equations

$$\frac{\eta_{sp}}{c} = [\eta] + k' [\eta]^2 c \qquad \text{E-10}$$

and

$$\frac{\ln \eta_{rel}}{c} = [\eta] - k'' [\eta]^2 c \, . \qquad \text{E-11}$$

In order to increase the accuracy, these extrapolations were done by a

FIG. E-8

Determination of the intrinsic viscosity by double extrapolation of η_{sp}/c vs. c and $\ln \eta_{rel}/c$ vs. c. Data in A are for a toluene solution of an S109 sample given a dose of 69 Mrad. Data in B are for a cyclohexane solution of an S102 sample given a dose of 112 Mrad.

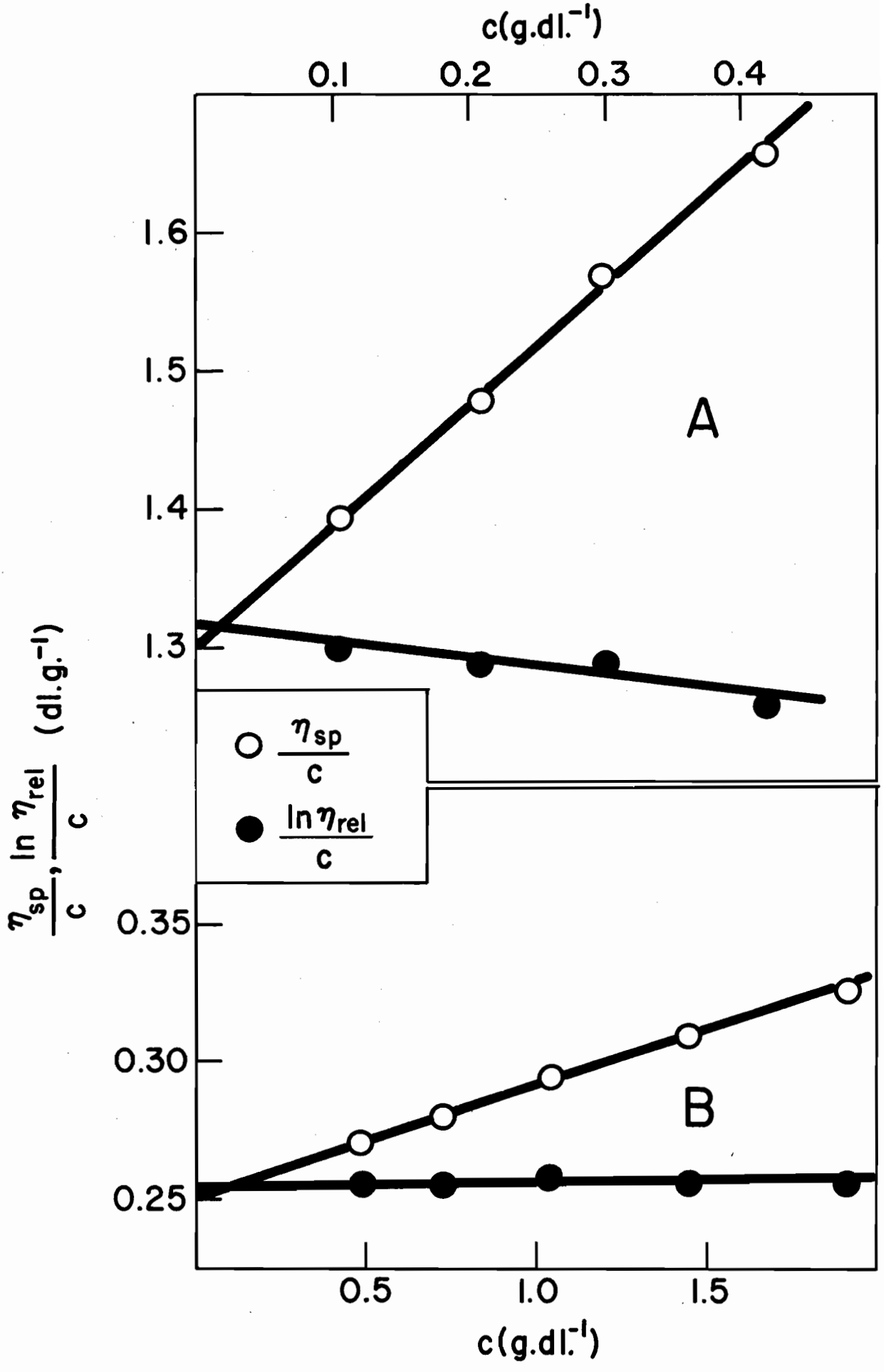
c(g.dl.⁻¹)
0.1
0.2
0.3
0.4
1.6
1.5
1.4
1.3
A
$\frac{\eta_{sp}}{c}$
$\frac{\ln \eta_{rel}}{c}$
$\frac{\eta_{sp}}{c}, \frac{\ln \eta_{rel}}{c}$ (dl.g.⁻¹)
0.35
0.30
0.25
B
0.5
1.0
1.5
c(g.dl.⁻¹)

least-squares technique (134), and due to the large volume of data calculations were performed on a digital computer. The agreement between viscosity numbers obtained by the two different extrapolation methods was in general very good, as illustrated by the data in Table E-3 for sample S109. The average of the two extrapolation results was accepted as the experimental value of the intrinsic viscosity.

Shear rates for the pure solvents were calculated from Kroepelin's equation (135)

$$\bar{G} = 8V/3\pi r^3 t_e \,, \qquad \text{E-12}$$

where $\bar{G}$ is the mean rate of shear, V is the efflux volume, t_e is the efflux time, and r is the radius of the viscometer capillary. The mean rates of shear were found to be 1250 and 1680 $sec.^{-1}$, respectively, for toluene and butanone at 25°C, and 780 $sec.^{-1}$ for cyclohexane at 34°C. To investigate whether shear dependence might affect the results of intrinsic viscosity measurements, the following preliminary experiment was carried out.

The highest molecular weight anionic polystyrene sample (sample S108 of Table E-1) was irradiated to 85% of the gelling dose. The irradiated polymer was dissolved in toluene, filtered through a sintered glass filter (B.S. 1752), and diluted to a concentration of 0.5 $g.dl.^{-1}$ Then viscosity measurements were made as described above, but using a modified form of the suspended level variable shear viscometer of Schurz and Immergut (136). It was found that within experimental error the intrinsic viscosity was independent of the shear rate.

TABLE E-3

Intrinsic viscosities of irradiated S109 samples in toluene and butanone solutions at 25°C

Dose	Solvent	$(\frac{\eta_{sp}}{c})_{c=o}$	$(\frac{\ln \eta_{rel}}{c})_{c=o}$
Mrad.		$dl.g.^{-1}$	$dl.g.^{-1}$
14.4	toluene	0.790	0.789
14.4	"	0.794	0.781
14.4	"	0.813	0.809
14.4	"	0.760	0.761
30.6	"	0.869	0.867
30.6	"	0.813	0.811
30.6	"	0.863	0.858
46.0	"	0.928	0.929
46.0	"	0.922	0.919
46.0	"	0.941	0.942
61.3	"	1.121	1.125
61.3	"	1.118	1.119
68.9	"	1.304	1.316
68.9	"	1.445	1.446
68.9	"	1.250	1.259
68.9	"	1.324	1.322
14.4	butanone	0.452	0.454
30.6	"	0.491	0.493
30.6	"	0.489	0.491
30.6	"	0.489	0.491

In view of the fact that other samples were of a lower molecular weight and usually lower degree of branching, it seemed justifiable to assume that shear dependence of the intrinsic viscosity was negligible throughout the experiments.

VI. Gelling Dose Determinations

In preliminary experiments it was found that the presence of small amounts of gel could be easily detected by the loss of filterability of solutions of the irradiated samples. Suction was required to filter solutions containing gel, and even with suction the filtration was usually difficult to perform after the gel point. Thus it was possible by a qualitative estimate of the filterability to obtain an approximate value of the dose required for incipient gel formation.

For more accurate work, relative viscosities at a given concentration, or intrinsic viscosities were plotted against the dose. The resulting curves were extrapolated to 'infinite' viscosity to find the gel point. The extrapolation techniques are shown in Figs. I-9 and I-10 of the Experimental Results and Discussion section of Part I.

As shown in Table I-8 of the above section, gelling doses obtained by different methods were in good agreement. The dependence on molecular weight was as expected on the basis of statistical theories.

APPENDICES

APPENDIX I

As discussed previously, gelling doses for anionic polystyrene samples and their mixtures were calculated from Eqs. I-34 and I-46 of the Theoretical section, by the method of inverse linear interpolation. Some of the results of these calculations have been given in Table I-2 of the Theoretical section. The following tables contain a complete list of values computed for samples used in the experimental work.

TABLE A-1

Values of τ_g in crosslinking with various extents of degradation for anionic polystyrene samples

σ_c	τ_g for crosslinking x 10^4				
	S102	S105	S108	S109	S102/S108
0.50	20.57	11.00	6.422	8.830	12.28
0.60	15.36	8.226	4.783	6.590	8.843
0.70	12.29	6.587	3.820	5.271	6.909
0.80	10.26	5.500	3.185	4.398	5.669
0.90	8.811	4.724	2.732	3.775	4.807
1.00	7.723	4.142	2.393	3.308	4.173
1.10	6.875	3.688	2.129	2.945	3.687
1.20	6.196	3.324	1.918	2.654	3.303
1.30	5.640	3.026	1.745	2.415	2.991
1.40	5.176	2.777	1.601	2.216	2.733
1.50	4.782	2.566	1.479	2.048	2.516
1.60	4.445	2.385	1.374	1.903	2.331
1.70	4.152	2.228	1.283	1.777	2.172
1.80	3.895	2.091	1.204	1.667	2.032
1.90	3.668	1.969	1.133	1.570	1.910
2.00	3.466	1.861	1.071	1.484	1.802
2.10	3.286	1.764	1.015	1.406	1.705
2.20	3.123	1.677	0.9645	1.337	1.618
2.30	2.976	1.598	0.9189	1.274	1.539
2.40	2.842	1.526	0.8774	1.216	1.468
2.50	2.719	1.460	0.8395	1.164	1.403
2.60	2.607	1.340	0.8047	1.116	1.344
2.70	2.503	1.344	0.7727	1.071	1.289
2.80	2.408	1.293	0.7432	1.030	1.239

continued

TABLE A-1 continued

σ_c	τ_g for crosslinking x 10^4				
	S102	S105	S108	S109	S102/S108
2.90	2.319	1.245	0.7158	0.9926	1.192
3.00	2.237	1.201	0.6904	0.9574	1.149
3.10	2.160	1.160	0.6667	0.9246	1.109
3.20	2.089	1.122	0.6446	0.8940	1.072
3.30	2.022	1.086	0.6239	0.8653	1.037
3.40	1.959	1.052	0.6045	0.8384	1.004
3.50	1.900	1.020	0.5863	0.8132	0.9731
3.60	1.845	0.9906	0.5692	0.7894	0.9441
3.70	1.792	0.9625	0.5530	0.7670	0.9169
3.80	1.743	0.9359	0.5377	0.7458	0.8911
3.90	1.696	0.9108	0.5232	0.7258	0.8668
4.00	1.652	0.8870	0.5095	0.7068	0.8438
4.10	1.610	0.8644	0.4965	0.6887	0.8219
4.20	1.570	0.8429	0.4841	0.6716	0.8012
4.30	1.531	0.8224	0.4724	0.6553	0.7815
4.40	1.495	0.8030	0.4612	0.6398	0.7627
4.50	1.461	0.7844	0.4505	0.6250	0.7448
4.60	1.428	0.7667	0.4403	0.6108	0.7277
4.70	1.396	0.7497	0.4306	0.5973	0.7114
4.80	1.366	0.7335	0.4212	0.5844	0.6958
4.90	1.337	0.7180	0.4123	0.5720	0.6809
5.00	1.309	0.7031	0.4038	0.5602	0.6666

TABLE A-2

Values of τ_g for anionic polystyrene samples in endlinking as a function of σ_e

σ_e	τ_g for endlinking x 10^4				
	S102	S105	S108	S109	S102/S108
0.30	69.89	37.20	22.19	30.14	48.61
0.32	50.79	27.04	16.11	21.89	35.07
0.34	40.05	21.33	12.69	17.26	27.44
0.36	33.12	17.64	10.48	14.27	22.54
0.38	28.26	15.06	8.943	12.17	19.12
0.40	24.66	13.14	7.799	10.62	16.59
0.42	21.87	11.66	6.916	9.423	14.66
0.44	19.66	10.48	6.213	8.467	13.12
0.46	17.85	9.517	5.641	7.688	11.88
0.48	16.34	8.716	5.165	7.040	10.85
0.50	15.07	8.039	4.763	6.493	9.991
0.52	13.99	7.460	4.419	6.025	9.253
0.54	13.05	6.958	4.121	5.620	8.617
0.56	12.22	6.520	3.861	5.265	8.062
0.58	11.50	6.133	3.632	4.953	7.574
0.60	10.85	5.790	3.428	4.675	7.142
0.62	10.28	5.483	3.246	4.427	6.757
0.64	9.764	5.206	3.082	4.204	6.411
0.66	9.295	4.956	2.934	4.002	6.098
0.68	8.869	4.729	2.800	3.818	5.815
0.70	8.481	4.522	2.677	3.651	5.557
0.72	8.124	4.332	2.564	3.498	5.320
0.74	7.797	4.157	2.461	3.357	5.103

continued

TABLE A-2 continued

σ_e	τ_g for endlinking x 10^4				
	S102	S105	S108	S109	S102/S108
0.76	7.495	3.996	2.365	3.227	4.903
0.78	7.215	3.847	2.277	3.106	4.718
0.80	6.955	3.709	2.195	2.994	4.547
0.82	6.713	3.580	2.119	2.890	4.388
0.84	6.488	3.459	2.048	2.793	4.239
0.86	6.277	3.347	1.981	2.702	4.100
0.88	6.079	3.242	1. 919	2.617	3.970
0.90	5.894	3.143	1.860	2.537	3.848
0.92	5.719	3.049	1.805	2.462	3.733
0.94	5.554	2.962	1.753	2.391	3.625
0.96	5.399	2.879	1.704	2.324	3.523
0.98	5.252	2.800	1.657	2.261	3.426
1.00	5.113	2.726	1.614	2.201	3.335

APPENDIX II

In the tables which follow, results of the finite Dirichlet series expansions of f(q) factors are given. Parameters of these expansions were computed by iterative least-squares analyses, as described in the Theoretical section of Part II. It can be seen that the agreement between calculated values of f(q) and those obtainable from the $\sum_i B_i e^{-c_i q}$ representations was always good.

Table A-3

Finite Dirichlet series expansion of the $[g(q)]^{3/2}$ correction factor, as computed from the formulas of Zimm and Stockmayer (Eqs. II-19 and II-20). The calculated values of $[g(q)]^{3/2}$ are compared to those obtainable from the $\sum_i B_i e^{-c_i q}$ representation with $B_1 = 0.1671$, $c_1 = 0.01117$, $B_2 = 0.4383$, $c_2 = 0.1224$, $B_3 = 0.9094$, and $c_3 = 0.7158$.

q	$[g(q)]^{3/2}$	$\sum_i B_i e^{-c_i q}$	q	$[g(q)]^{3/2}$	$\sum_i B_i e^{-c_i q}$
1	1.0000	0.9974	21	0.1725	0.1656
2	0.7155	0.7237	26	0.1484	0.1431
3	0.5737	0.5713	31	0.1310	0.1280
4	0.4860	0.4802	36	0.1178	0.1170
5	0.4254	0.4210	41	0.1074	0.1085
6	0.3805	0.3789	46	0.0990	0.1015
7	0.3456	0.3466	51	0.0920	0.0954
8	0.3177	0.3203	56	0.0860	0.0898
9	0.2946	0.2981	61	0.0809	0.0848
10	0.2753	0.2789	66	0.0765	0.0801
11	0.2588	0.2621	71	0.0725	0.0757
12	0.2444	0.2471	76	0.0691	0.0715
13	0.2319	0.2338	81	0.0660	0.0676
14	0.2208	0.2219	86	0.0632	0.0639
15	0.2109	0.2111	91	0.0607	0.0605
16	0.2020	0.2015	96	0.0584	0.0572
17	0.1940	0.1928	101	0.0563	0.0541
18	0.1866	0.1850	106	0.0543	0.0511
19	0.1800	0.1779	111	0.0525	0.0483
20	0.1738	0.1715	116	0.0509	0.0457

Table A-4

Finite Dirichlet series expansion of the $\left[g(q)\right]^{3/2}$ correction factor, as computed from the formula of Kataoka (Eq. II-21). The calculated values of $\left[g(q)\right]^{3/2}$ are compared to those obtainable from the $\sum_i B_i e^{-c_i q}$ representation with $B_1 = 0.2031$, $c_1 = 0$, $B_2 = 0.1116$, $c_2 = 0.04449$, $B_3 = 0.4579$, $c_3 = 0.2545$, $B_4 = 0.8144$, and $c_4 = 0.8893$.

q	$\left[g(q)\right]^{3/2}$	$\sum_i B_i e^{-c_i q}$	q	$\left[g(q)\right]^{3/2}$	$\sum_i B_i e^{-c_i q}$
1	1.0000	0.9995	21	0.2483	0.2491
2	0.7155	0.7179	26	0.2375	0.2388
3	0.5737	0.5706	31	0.2301	0.2314
4	0.4860	0.4851	36	0.2248	0.2256
5	0.4294	0.4302	41	0.2208	0.2211
6	0.3905	0.3919	46	0.2177	0.2175
7	0.3623	0.3635	51	0.2152	0.2146
8	0.3410	0.3417	56	0.2132	0.2123
9	0.3244	0.3245	61	0.2115	0.2105
10	0.3110	0.3106	66	0.2100	0.2090
11	0.3001	0.2994	71	0.2088	0.2078
12	0.2910	0.2901	76	0.2077	0.2069
13	0.2833	0.2824	81	0.2067	0.2061
14	0.2768	0.2759	86	0.2059	0.2055
15	0.2711	0.2704	91	0.2051	0.2050
16	0.2661	0.2656	96	0.2045	0.2047
17	0.2617	0.2615	101	0.2039	0.2043
18	0.2578	0.2579	106	0.2033	0.2041
19	0.2543	0.2546	111	0.2028	0.2039
20	0.2512	0.2517	116	0.2024	0.2037

Table A-5

Finite Dirichlet series expansion of the $\left[g(q)\right]^{1.26}$ correction factor, as computed from the formulas of Zimm and Stockmayer (Eqs. II-19 and II-20). The calculated values of $\left[g(q)\right]^{1.26}$ are compared to those obtainable from the $\sum_i B_i e^{-c_i q}$ representation with $B_1 = 0.2116$, $c_1 = 0.00875$, $B_2 = 0.4257$, $c_2 = 0.1064$, $B_3 = 0.7737$, and $c_3 = 0.6485$.

q	$\left[g(q)\right]^{1.26}$	$\sum_i B_i e^{-c_i q}$	q	$\left[g(q)\right]^{1.26}$	$\sum_i B_i e^{-c_i q}$
1	1.0000	0.9969	21	0.2285	0.2215
2	0.7549	0.7634	26	0.2014	0.1952
3	0.6270	0.6260	31	0.1814	0.1770
4	0.5455	0.5402	36	0.1659	0.1636
5	0.4877	0.4827	41	0.1535	0.1532
6	0.4441	0.4413	46	0.1433	0.1446
7	0.4097	0.4093	51	0.1347	0.1372
8	0.3816	0.3832	56	0.1273	0.1307
9	0.3583	0.3611	61	0.1209	0.1247
10	0.3384	0.3418	66	0.1153	0.1191
11	0.3212	0.3247	71	0.1103	0.1139
12	0.3062	0.3094	76	0.1059	0.1089
13	0.2930	0.2956	81	0.1019	0.1042
14	0.2812	0.2831	86	0.0983	0.0997
15	0.2705	0.2718	91	0.0950	0.0955
16	0.2609	0.2614	96	0.0920	0.0914
17	0.2522	0.2520	101	0.0892	0.0874
18	0.2441	0.2434	106	0.0866	0.0837
19	0.2368	0.2355	111	0.0842	0.0801
20	0.2300	0.2282	116	0.0820	0.0767

Table A-6

Finite Dirichlet series expansion of the $\left[g(q)\right]^{1.26}$ correction factor, as computed from the formula of Kataoka (Eq. II-21). The calculated values of $\left[g(q)\right]^{1.26}$ are compared to those obtainable from the $\sum_i B_i e^{-c_i q}$ representation with $B_1 = 0.2618$, $c_1 = 0$, $B_2 = 0.1123$, $c_2 = 0.04226$, $B_3 = 0.4194$, $c_3 = 0.2368$, $B_4 = 0.6818$, and $c_4 = 0.8241$.

q	$\left[g(q)\right]^{1.26}$	$\sum_i B_i e^{-c_i q}$	q	$\left[g(q)\right]^{1.26}$	$\sum_i B_i e^{-c_i q}$
1	1.0000	0.9994	21	0.3103	0.3109
2	0.7549	0.7573	26	0.2989	0.3001
3	0.6270	0.6243	31	0.2911	0.2923
4	0.5455	0.5445	36	0.2855	0.2864
5	0.4916	0.4921	41	0.2812	0.2816
6	0.4539	0.4550	46	0.2779	0.2778
7	0.4262	0.4273	51	0.2752	0.2748
8	0.4051	0.4058	56	0.2730	0.2723
9	0.3884	0.3887	61	0.2711	0.2703
10	0.3749	0.3748	66	0.2696	0.2687
11	0.3639	0.3634	71	0.2682	0.2674
12	0.3546	0.3539	76	0.2671	0.2663
13	0.3467	0.3459	81	0.2660	0.2654
14	0.3399	0.3391	86	0.2651	0.2647
15	0.3340	0.3333	91	0.2643	0.2642
16	0.3289	0.3283	96	0.2636	0.2637
17	0.3243	0.3240	101	0.2630	0.2633
18	0.3202	0.3201	106	0.2624	0.2630
19	0.3166	0.3167	111	0.2618	0.2628
20	0.3133	0.3137	116	0.2613	0.2626

Table A-7

Finite Dirichlet series expansion of the $\left[g(q)\right]^{1.21}$ correction factor, as computed from the formula of Kataoka (Eq. II-21). The calculated values of $\left[g(q)\right]^{1.21}$ are compared to those obtainable from the $\sum_i B_i e^{-c_i q}$ representation with $B_1 = 0.2760$, $c_1 = 0$, $B_2 = 0.1119$, $c_2 = 0.04181$, $B_3 = 0.4102$, $c_3 = 0.2332$, $B_4 = 0.6548$, and $c_4 = 0.8104$.

q	$\left[g(q)\right]^{1.21}$	$\sum_i B_i e^{-c_i q}$	q	$\left[g(q)\right]^{1.21}$	$\sum_i B_i e^{-c_i q}$
1	1.0000	0.9994	21	0.3251	0.3256
2	0.7633	0.7658	26	0.3135	0.3147
3	0.6388	0.6361	31	0.3057	0.3069
4	0.5587	0.5577	36	0.3000	0.3009
5	0.5057	0.5061	41	0.2957	0.2962
6	0.4684	0.4694	46	0.2924	0.2924
7	0.4409	0.4420	51	0.2896	0.2893
8	0.4198	0.4206	56	0.2874	0.2868
9	0.4032	0.4036	61	0.2856	0.2847
10	0.3898	0.3897	66	0.2840	0.2831
11	0.3788	0.3783	71	0.2826	0.2817
12	0.3695	0.3688	76	0.2814	0.2807
13	0.3616	0.3608	81	0.2804	0.2798
14	0.3548	0.3540	86	0.2795	0.2791
15	0.3489	0.3482	91	0.2787	0.2785
16	0.3437	0.3432	96	0.2779	0.2780
17	0.3391	0.3388	101	0.2773	0.2776
18	0.3350	0.3349	106	0.2767	0.2773
19	0.3314	0.3315	111	0.2761	0.2771
20	0.3281	0.3284	116	0.2756	0.2769

Table A-8

Finite Dirichlet series expansion of the $\left[g(q)\right]^{1/2}$ correction factor, as computed from the formulas of Zimm and Stockmayer (Eqs. II-19 and II-20). The calculated values of $\left[g(q)\right]^{1/2}$ are compared to those obtainable from the $\sum_i B_i e^{-c_i q}$ representation with $B_1 = 0.5087$, $c_1 = 0.00282$, $B_2 = 0.2951$, $c_2 = 0.06606$, $B_3 = 0.3335$, and $c_3 = 0.4482$.

q	$\left[g(q)\right]^{1/2}$	$\sum_i B_i e^{-c_i q}$	q	$\left[g(q)\right]^{1/2}$	$\sum_i B_i e^{-c_i q}$
1	1.0000	0.9965	21	0.5566	0.5532
2	0.8944	0.9004	26	0.5294	0.5257
3	0.8309	0.8333	31	0.5079	0.5042
4	0.7862	0.7850	36	0.4903	0.4870
5	0.7520	0.7491	41	0.4754	0.4728
6	0.7246	0.7213	46	0.4626	0.4610
7	0.7018	0.6990	51	0.4513	0.4508
8	0.6823	0.6805	56	0.4414	0.4417
9	0.6654	0.6646	61	0.4324	0.4336
10	0.6505	0.6507	66	0.4244	0.4261
11	0.6372	0.6382	71	0.4170	0.4192
12	0.6252	0.6268	76	0.4103	0.4126
13	0.6144	0.6164	81	0.4040	0.4063
14	0.6044	0.6066	86	0.3983	0.4003
15	0.5952	0.5976	91	0.3929	0.3944
16	0.5867	0.5890	96	0.3879	0.3887
17	0.5788	0.5810	101	0.3831	0.3831
18	0.5715	0.5735	106	0.3787	0.3776
19	0.5646	0.5663	111	0.3745	0.3723
20	0.5581	0.5596	116	0.3705	0.3670

Table A-9

Finite Dirichlet series expansion of the $[g(q)]^{1/2}$ correction factor, as computed from the formula of Kataoka (Eq. II-21). The calculated values of $[g(q)]^{1/2}$ are compared to those obtainable from the $\sum_i B_i e^{-c_i q}$ representation with $B_1 = 0.5865$, $c_1 = 0$, $B_2 = 0.7785$, $c_2 = 0.03528$, $B_3 = 0.2211$, $c_3 = 0.1814$, $B_4 = 0.2833$, and $c_4 = 0.6129$.

q	$[g(q)]^{1/2}$	$\sum_i B_i e^{-c_i q}$	q	$[g(q)]^{1/2}$	$\sum_i B_i e^{-c_i q}$
1	1.0000	0.9995	21	0.6285	0.6285
2	0.8944	0.8960	26	0.6192	0.6195
3	0.8309	0.8298	31	0.6128	0.6133
4	0.7862	0.7855	36	0.6081	0.6086
5	0.7544	0.7542	41	0.6044	0.6049
6	0.7309	0.7311	46	0.6016	0.6019
7	0.7129	0.7133	51	0.5993	0.5993
8	0.6986	0.6991	56	0.5974	0.5972
9	0.6871	0.6875	61	0.5958	0.5955
10	0.6775	0.6778	66	0.5944	0.5940
11	0.6695	0.6697	71	0.5932	0.5928
12	0.6627	0.6627	76	0.5922	0.5918
13	0.6568	0.6567	81	0.5913	0.5909
14	0.6517	0.6515	86	0.5905	0.5902
15	0.6472	0.6469	91	0.5898	0.5896
16	0.6432	0.6429	96	0.5891	0.5891
17	0.6396	0.6393	101	0.5886	0.5886
18	0.6364	0.6361	106	0.5880	0.5883
19	0.6335	0.6333	111	0.5876	0.5880
20	0.6309	0.6308	116	0.5871	0.5877

Table A-10

Finite Dirichlet series expansion of Stockmayer and Fixman's h^3 correction factor, as calculated from Eqs. II-18 and the formulas of Zimm and Stockmayer (Eqs. II-19 and II-20). The calculated values of h^3 are compared to those obtainable from the $\sum_i B_i e^{-c_i q}$ representation with $B_1 = 0.2760$, $c_1 = 0.00748$, $B_2 = 0.4212$, $c_2 = 0.06970$, $B_3 = 0.4667$, and $c_3 = 0.3464$.

q	h^3	$\sum_i B_i e^{-c_i q}$	q	h^3	$\sum_i B_i e^{-c_i q}$
1	1.0000	0.9967	21	0.3379	0.3336
2	0.8680	0.8716	26	0.2996	0.2960
3	0.7731	0.7766	31	0.2706	0.2674
4	0.7023	0.7032	36	0.2478	0.2451
5	0.6468	0.6456	41	0.2293	0.2273
6	0.6019	0.5994	46	0.2139	0.2127
7	0.5645	0.5617	51	0.2008	0.2005
8	0.5328	0.5303	56	0.1895	0.1900
9	0.5054	0.5036	61	0.1797	0.1809
10	0.4815	0.4804	66	0.1710	0.1727
11	0.4603	0.4601	71	0.1633	0.1653
12	0.4415	0.4420	76	0.1564	0.1584
13	0.4245	0.4257	81	0.1502	0.1521
14	0.4091	0.4109	86	0.1446	0.1461
15	0.3951	0.3973	91	0.1394	0.1405
16	0.3823	0.3847	96	0.1347	0.1351
17	0.3705	0.3731	101	0.1303	0.1300
18	0.3596	0.3622	106	0.1263	0.1252
19	0.3495	0.3521	111	0.1225	0.1205
20	0.3400	0.3426	116	0.1190	0.1160

APPENDIX III

On the following pages one of the derivations of Katsuura (21) is partially repeated, in order to uncover a misprint in reference 21. For the sake of simplicity, throughout this derivation the notation of Katsuura will be used, and Eqs. (17), (18), (20), and (22) are identical to the similarly numbered equations of reference 21.

Katsuura's Eq. (17) is

$$\exists(a) = \frac{1}{\Gamma(1-\alpha)} \int_{\rho=0}^{\rho=\infty} \frac{G''(\rho_o, a)}{\rho^{\alpha}} d\rho_o \quad , \tag{17}$$

where

$$\rho = \rho_o - 2\left\{1 + G'(\rho_o, a)\right\} t \quad , \tag{18}$$

and

$$G(\rho_o, a) = u^{-1} (1 + u\rho_o)^{-1} e^{-a} \quad . \tag{20}$$

In the above equations u is the initial number average degree of polymerization, α is the exponent of the Mark-Houwink equation for the unirradiated polymer, a corresponds to c_i in the notation of the present work, and t is the number of crosslinks per monomer unit. ρ_o is merely a dummy variable.

From Eq. (20)

$$G'(\rho_o, a) = \frac{\partial G}{\partial \rho_o} = - \frac{e^{-a}}{(1 + u\rho_o)^2} \qquad \text{A-1}$$

and

$$G''(\rho_o, a) = \frac{\partial^2 G}{\partial \rho_o^2} = \frac{2ue^{-a}}{(1 + u\rho_o)^3} . \qquad \text{A-2}$$

Putting

$$1 + u\rho_o = y^{-1} \qquad \text{A-3}$$

we obtain

$$G'(\rho_o, a) = - y^2 e^{-a} \qquad \text{A-4}$$

and

$$G''(\rho_o, a) = 2uy^3 e^{-a} . \qquad \text{A-5}$$

From Eq. A-3

$$\rho_o = \frac{1 - y}{uy} , \qquad \text{A-6}$$

i.e.

$$d\rho_o = - \frac{dy}{uy^2} , \qquad \text{A-7}$$

and from Eqs. (18), A-4, and A-6

$$\rho = \frac{1 - y}{uy} - 2 \left\{ 1 - y^2 e^{-a} \right\} t. \qquad \text{A-8}$$

Saito, to whom the basic mathematical approach is due, has shown (19) that the variables ρ and ρ_o are related in such a way that $\lim_{\rho \to \infty} \rho_o = \infty$. Therefore when Eqs. A-3, A-5, A-7, and A-8 are substituted into Eq. (17) we obtain

$$\Gamma(a) = \frac{1}{\Gamma(1-\alpha)} \int_{y_o}^{0} \left[2uy^3 e^{-a} \left\{ - \frac{dy}{uy^2 \left[\frac{1-y}{uy} - 2t(1-y^2 e^{-a}) \right]^{\alpha}} \right\} \right]$$

A-9

$$= \frac{2u^{\alpha} e^{-a}}{\Gamma(1-\alpha)} \int_{0}^{y_o} \frac{y^{\alpha+1} dy}{\left[1 - y - 2uty(1-y^2 e^{-a}) \right]^{\alpha}} ,$$

where y_o is a root of the equation

$$1 - y - 2uty\,(1 - y^2 e^{-a}) = 0 , \qquad (22)$$

such that $0 < y_o \leq 1$.

In Eq. (21) of Katsuura, which corresponds to the present Eq. A-9, the denominator of the integrand is given as

$$\left[1 - y - 2ut\,(1 - e^{-a} y^2) \right]^{\alpha} ,$$

an obvious misprint.

Eq. II-24 of the Theoretical section of Part II is identical to the above Eq. A-9, except for the notation.

APPENDIX IV

In the following table the final results of the viscosity calculations are given, as computed from various theories on the effects of branching. Most of these results have been presented in the form of graphs in the Results and Discussion section of Part II.

Table A-11

Final results of the viscosity calculations, as computed from various theories on the effects of branching

a	σ_c	$\varphi(g)$	Method used for calculation of g	R/R_g	$[\eta]/[\eta]_o$
0.79	0.667	$g^{1/2}$	Zimm and Stockmayer	0.20	1.071
"	"	"	"	0.50	1.256
"	"	"	"	0.65	1.419
"	"	"	"	0.80	1.694
"	"	"	"	0.95	2.034
"	∞	$g^{1.21}$	Kataoka	0.15	1.031
"	"	"	"	0.30	1.073
"	"	"	"	0.45	1.129
"	"	"	"	0.60	1.216
"	"	"	"	0.75	1.386
"	"	"	"	0.90	1.933
"	"	"	"	0.95	2.639
"	"	h^3	Zimm and Stockmayer	0.20	1.091
"	"	"	"	0.50	1.277
"	"	"	"	0.80	1.561
0.75	"	$g^{1/2}$	"	0.20	1.101

continued

Table A-11 (continued)

a	σ_c	$\varphi(g)$	Method used for calculation of g	R/R_g	$[\eta]/[\eta]_o$
0.75	∞	$g^{1/2}$	Zimm and Stockmayer	0.40	1.245
"	"	"	"	0.60	1.466
"	"	"	"	0.80	1.886
"	"	"	"	0.90	2.298
"	"	"	"	0.95	2.544
0.74	1.43	"	"	0.20	1.085
"	"	"	"	0.50	1.287
"	"	"	"	0.65	1.454
"	"	"	"	0.80	1.737
"	"	"	Kataoka	0.20	1.086
"	"	"	"	0.50	1.301
"	"	"	"	0.65	1.506
"	"	"	"	0.80	1.925
"	"	$g^{1.26}$	Zimm and Stockmayer	0.20	1.008
"	"	"	"	0.50	1.033
"	"	"	"	0.65	1.054
"	"	"	"	0.80	1.083
"	"	"	Kataoka	0.20	1.009
"	"	"	"	0.50	1.051
"	"	"	"	0.65	1.111
"	"	"	"	0.80	1.263
"	"	$g^{3/2}$	Zimm and Stockmayer	0.20	0.987
"	"	"	"	0.50	0.975
"	"	"	"	0.65	0.971
"	"	"	"	0.80	0.967

continued

Table A-11 (continued)

a	σ_c	$\varphi(g)$	Method used for calculation of g	R/R_g	$[\eta]/[\eta]_o$
0.74	1.43	$g^{3/2}$	Kataoka	0.20	0.988
"	"	"	"	0.50	0.992
"	"	"	"	0.65	1.023
"	"	"	"	0.80	1.125
"	"	h^3	Zimm and Stockmayer	0.10	1.029
"	"	"	"	0.20	1.063
"	"	"	"	0.30	1.099
"	"	"	"	0.40	1.138
"	"	"	"	0.50	1.179
"	"	"	"	0.60	1.224
"	"	"	"	0.70	1.275
"	"	"	"	0.75	1.302
"	"	"	"	0.80	1.330
"	"	"	"	0.85	1.356
"	"	"	"	0.90	1.372
"	"	"	"	0.95	1.366
0.69	3.50	$g^{1/2}$	"	0.20	1.082
"	"	"	"	0.50	1.271
"	"	"	"	0.65	1.423
"	"	"	"	0.80	1.673
"	"	"	"	0.95	2.093
"	"	h^3	"	0.15	1.046
"	"	"	"	0.30	1.100
"	"	"	"	0.45	1.160
"	"	"	"	0.60	1.227
"	"	"	"	0.70	1.277
"	"	"	"	0.80	1.332
"	"	"	"	0.95	1.375

continued

Table A-11 (continued)

a	δ_c	$\varphi(g)$	Method used for calculation of g	R/R_g	$[\eta]/[\eta]_o$
0.68	∞	$g^{1/2}$	Zimm and Stockmayer	0.20	1.085
"	"	"	"	0.40	1.202
"	"	"	"	0.50	1.279
"	"	"	"	0.60	1.376
"	"	"	"	0.65	1.434
"	"	"	"	0.80	1.689
"	"	"	"	0.90	1.976
"	"	"	"	0.95	2.136
"	0.667	"	"	0.20	1.046
"	"	"	"	0.50	1.165
"	"	"	"	0.65	1.266
"	"	"	"	0.80	1.425
"	∞	h^3	"	0.20	1.068
"	"	"	"	0.50	1.196
"	"	"	"	0.65	1.274
"	"	"	"	0.80	1.364
"	"	"	"	0.95	1.422
0.58	3.50	$g^{1/2}$	"	0.20	1.058
"	"	"	"	0.50	1.185
"	"	"	"	0.65	1.282
"	"	"	"	0.80	1.430
"	"	"	"	0.95	1.647
"	"	h^3	"	0.15	1.030
"	"	"	"	0.30	1.065
"	"	"	"	0.45	1.101
"	"	"	"	0.60	1.137

continued

Table A-11 (continued)

a	σ_c	$\varphi(g)$	Method used for calculation of g	R/R_g	$[\eta]/[\eta]_o$
0.58	3.50	h^3	Zimm and Stockmayer	0.70	1.161
"	"	"	"	0.80	1.184
"	"	"	"	0.95	1.182
0.50	∞	$g^{1/2}$	"	0.20	1.046
"	"	"	"	0.40	1.108
"	"	"	"	0.50	1.146
"	"	"	"	0.60	1.192
"	"	"	"	0.80	1.323
"	"	"	"	0.90	1.424
"	"	"	"	0.95	1.469
"	3.50	"	"	0.20	1.042
"	"	"	"	0.50	1.132
"	"	"	"	0.65	1.198
"	"	"	"	0.80	1.294
"	"	"	"	0.95	1.419
"	0.667	"	"	0.20	1.012
"	"	"	"	0.50	1.052
"	"	"	"	0.65	1.087
"	"	"	"	0.80	1.139
"	∞	"	Kataoka	0.20	1.048
"	"	"	"	0.50	1.152
"	"	"	"	0.80	1.387
"	"	$g^{3/2}$	"	0.20	0.983
"	"	"	"	0.50	0.957

continued

Table A-11 (continued)

a	σ_c	$\varphi(g)$	Method used for calculation of g	R/R_g	$[\eta]/[\eta]_0$
0.50	∞	$g^{3/2}$	Kataoka	0.80	0.960
"	"	h^3	Zimm and Stockmayer	0.20	1.033
"	"	"	"	0.50	1.087
"	"	"	"	0.80	1.131
"	3.50	"	"	0.15	1.020
"	"	"	"	0.30	1.042
"	"	"	"	0.45	1.063
"	"	"	"	0.60	1.082
"	"	"	"	0.70	1.092
"	"	"	"	0.80	1.099
"	"	"	"	0.95	1.076

CLAIMS TO ORIGINAL RESEARCH AND CONTRIBUTIONS TO KNOWLEDGE

1. It is believed that the investigation described in the first part of the thesis is the first thorough study of the effect of initial molecular weight distribution on the properties of irradiated polymers.

2. A number of mathematical equations have been developed for calculating various parameters of irradiated narrow distribution polymers.

3. A new, simple method has been introduced for distinguishing between crosslinking and endlinking as basic mechanisms of radiation-induced network formation in polymers.

4. Some radiation chemical parameters have been determined for irradiated anionic polystyrene.

5. Statistical calculations of the intrinsic viscosity of irradiated polymers have been extended, in such a manner that various theories on the viscosity of branched molecules could be tested.

6. The applicability and inadequacies, respectively, of some of the existing theories on hydrodynamic properties of branched polymers have been demonstrated.

7. The study of irradiated anionic polystyrene samples has indicated that initial molecular weight distribution has little effect on the increase in intrinsic viscosity produced by irradiation in polymers.

LIST OF THE PRINCIPAL SYMBOLS

An attempt has been made to achieve a compromise between self-consistency and retention of those symbols which are widely accepted in the literature. Where a symbol is used for more than one quantity, the context should prevent confusion.

A few trivial symbols, as well as obvious subscripted modifications of others, have not been listed.

A_o	Total number of molecules in a system
A_2	Second virial coefficient (osmotic or light-scattering)
A_2^{π} , A_2^{τ}	Osmotic and light-scattering virial coefficients, respectively
a	Exponent in the Mark-Houwink equation (Eq. II-1)
B_n , B_w	Number and weight average branching indices, respectively
c	Concentration
$\dot{c}$	Number of crosslinks per monomer per unit dose
f(q)	Correction factor for branching (see Eq. II-13)
G	Number of radiation chemical events per 100 eV of absorbed energy
g , g(q)	Ratio of the mean-square radius of gyration of a branched molecule to that of the corresponding linear molecule of equal molecular weight
h	Ratio of the hydrodynamic radius of a branched molecule to that of the corresponding linear molecule of equal molecular weight, as predicted by the theory of Stockmayer and Fixman (see Eqs. II-18)
K	Coefficient in the Mark-Houwink equation (Eq. II-1)
$\langle L^2 \rangle$	Mean-square end-to-end distance

LIST OF THE PRINCIPAL SYMBOLS (continued)

M	Molecular weight
M_n , M_w , M_v	Number, weight, and viscosity average molecular weights, respectively
$M_n(0)$, $M_w(0)$	Number and weight average molecular weights, respectively, of unirradiated systems
$M_n'(\tau)$, $M_w'(R)$	Number and weight average molecular weights, respectively, of degraded polymer
$M_n''(R)$, $M_n''(t)$, $M_n''(\tau)$	Number average molecular weight of polymer after crosslinking or endlinking
$M_w''(R)$, $M_w''(t)$, $M_w''(\tau)$	Weight average molecular weight of polymer after crosslinking or endlinking
N	Total number of monomer units in a system
$\underline{N}$	Avogadro's number
$n(u)$, $n(u,R)$, $n(u,t)$, $n(u,\tau)$	Number of molecules of degree of polymerization u
p	Radiation dose expressed as a function of gelling dose ($= R/R_g$)
q	Half the number of ends of a given molecule
R	Radiation dose, Mrad.
R_g	Gelling dose, Mrad.
R_θ	Rayleigh ratio at the angle θ
$\underline{R}$	Gas constant
$\dot{r}$	Number of fractures per monomer per unit dose
$\langle S^2 \rangle_{br}$, $\langle S^2 \rangle_{lin}$	Mean-square radii of gyration of branched and corresponding linear molecules of equal molecular weight
T	Absolute temperature
t	Number of crosslinks per monomer

LIST OF THE PRINCIPAL SYMBOLS (continued)

u	Degree of polymerization
u_1 , u_2	Number and weight average degrees of polymerization, respectively, of unirradiated systems
$u_1'(\tau)$, $u_2'(\tau)$	Number and weight average degrees of polymerization, respectively, of degraded polymer
$u_2''(R)$, $u_2''(\tau)$	Weight average degree of polymerization after cross-linking or endlinking
w_o	Monomer molecular weight
z	Dissymmetry in light-scattering
α	Expansion factor of the Flory-Fox theory
Γ	Designates a mathematical gamma function
γ	Number of main chain fractures per number average primary molecule
γ_g	γ at the gel point
η_{rel}	Relative viscosity
η_{sp}	Specific viscosity
$[\eta]$	Intrinsic viscosity
$[\eta]_o$	Intrinsic viscosity of unirradiated system
$[\eta]_{br}$, $[\eta]_{lin}$	Intrinsic viscosities of branched and corresponding linear molecules of equal molecular weight
θ	Angle
θ	Flory temperature
λ	Parameter giving the sharpness of a Schulz distribution
π	Osmotic pressure
ρ	Density
$\dot{\rho}$	Number of main chain fractures per monomer per unit dose, in endlinking

LIST OF THE PRINCIPAL SYMBOLS (continued)

Σ	Summation sign
σ_c	Number of crosslinks per number of main chain fractures
σ_e	Probability that an end produced by scission will link with another molecule
τ	Number of main chain fractures per monomer
τ^o	Excess turbidity in light-scattering
Φ , Φ^1	Universal constants of the Flory-Fox theory
$\varphi(g)$	Correction factor for branching (= f(q))

REFERENCES

1. E.J. Lawton, A.M. Bueche, and J.S. Balwit, Nature 172, 76 (1953).
2. A. Charlesby, J. Polym. Sci. 11, 513 (1953).
3. A.R. Shultz, P.I. Roth, and G.B. Rathmann, J. Polym. Sci. 22, 495 (1956).
4. W. Burlant, J. Neerman, and V. Serment, J. Polym. Sci. 58, 491 (1962).
5. L. Wall and M. Magat, J. Chim. Phys. 50, 308 (1953).
6. A. Chapiro et al., Simposio internazionale di chimica macromoleculare. Supplement to La Ricerca Scientifica 25, 207 (1955).
7. J. Durup, J. Chim. Phys. 54, 739 (1957).
8. J. Durup, Ibid. 54, 746 (1957).
9. J. Durup, J. Polym. Sci. 30, 533 (1958).
10. J. Durup, J. Chim. Phys. 56, 873 (1959).
11. A. Henglein and Ch. Schneider, Z. Phys. Chem. Neue Folge (Frankfurt) 18, 56 (1958).
12. I.G. Soboleva, N.V. Makletsova, and S.S. Medvedev, Kolloid Zh. 21, 625 (1959).
13. A. Charlesby, Proc. Roy. Soc. A224, 120 (1954).
14. P.J. Flory, J. Am. Chem. Soc. 63, 3096 (1941).
15. A. Charlesby, Proc. Roy. Soc. A222, 542 (1954).
16. A. Charlesby, Proc. Roy. Soc. A231, 521 (1955).
17. O. Saito, J. Phys. Soc. Japan 13, 198 (1958).
18. O. Saito, Ibid. 13, 1451 (1958).
19. O. Saito, Ibid. 13, 1465 (1958).
20. A.M. Kotliar and A.D. Anderson, J. Polym. Sci. 45, 541 (1960).
21. K. Katsuura, J. Phys. Soc. Japan 15, 2310 (1960).
22. P.Y. Feng and J.W. Kennedy, J. Am. Chem. Soc. 77, 847 (1955).

23. M. Inokuti, J. Phys. Soc. Japan 14, 79 (1959).

24. M. Inokuti and K. Katsuura, Ibid. 14, 1379 (1959).

25. B.H. Zimm and W.H. Stockmayer, J. Chem. Phys. 17, 1301 (1949).

26. C.D. Thurmond and B.H. Zimm, J. Polym. Sci. 8, 477 (1952).

27. W.H. Stockmayer and M. Fixman, Ann. N.Y. Acad. Sci. 57, 334 (1953).

28. B.H. Zimm and R.W. Kilb, J. Polym. Sci. 37, 19 (1959).

29. R.W. Kilb, J. Polym. Sci. 38, 403 (1959).

30. R.W. Kilb, J. Phys. Chem. 63, 1838 (1959).

31. F. Bueche, J. Polym. Sci. 41, 549 (1959).

32. M. Dole, J. Phys. Chem. 65, 700 (1961).

33. A.M. Kotliar and S. Podgor, J. Polym. Sci. 55, 423 (1961); Ibid. 62, S177 (1962).

34. A. Chapiro, Radiation Chemistry of Polymeric Systems. Vol. XV of High Polymers. Interscience, 1962. Page 13 et seq.

35. A.J. Swallow, Radiation Chemistry of Organic Compounds. Vol. II of International Series of Monographs on Radiation Effects in Materials. Pergamon Press, 1960. Page 11.

36. H. Eyring, J.O. Hirschfelder and H.S. Taylor, J. Chem. Phys. 4, 570 (1936).

37. R.H. Schuler, J. Phys. Chem. 62, 37 (1958).

38. E.E. Schneider, Disc. Faraday Soc. 19, 158 (1955).

39. J. Weiss, J. Polym. Sci. 29, 425 (1958).

40. B.G. Collyns, J.F. Fowler and J. Weiss, Chemistry and Industry, 1957, p. 74.

41. C. Smith and H. Essex, J. Chem. Phys. 6, 188 (1938);
A.D. Kolumban and H. Essex, Ibid. 8, 450 (1940);
N.T. Williams and H. Essex, Ibid. 16, 1153 (1948);
N.T. Williams and H. Essex, Ibid. 17, 995 (1949).

42. J.M. Caffrey, Jr. and A.O. Allen, J. Phys. Chem. 62, 33 (1958).

43. A.N. Pravednikov and In Shen-Kan, J. Polym. Sci. 53, 61 (1961).

44. L.A. Wall and D.W. Brown, J. Phys. Chem. 61, 129 (1957).

45. R.E. Florin, L.A. Wall and D.W. Brown, Trans. Faraday Soc. 56, 1304 (1960).

46. In Shen-Kan, A.N. Pravednikov and S.S. Medvedev, Doklady Akademii Nauk 122, 254 (1958).

47. W. Burlant and J. Neerman, J. Org. Chem. 26, 3602 (1961).

48. N.A. Slovokhotova, Z.F. Ilyicheva, and V.A. Kargin, Vysokomol. Soedineniya 3, 191, No. 2 (1961).

49. C.D. Bopp and O. Sisman, Nucleonics 13 (7), 28 (1955); Ibid. 14 (3), 52 (1956).

50. F.T. Farmer, Nature 150, 521 (1942).

51. A. Charlesby, J. Polym. Sci. 11, 521 (1953).

52. P.J. Flory and J. Rehner, J. Chem. Phys. 11, 521 (1943).

53. W. Kuhn, Ber. 63, 1503 (1930).

54. H. Mark and R. Simha, Trans. Faraday Soc. 36, 611 (1940).

55. E.W. Montroll and R. Simha, J. Chem. Phys. 8, 721 (1940).

56. I. Sakurada and S. Okamura, Z. Physik. Chem. A187, 289 (1940).

57. W.F. Watson, Trans. Faraday Soc. 49, 1369 (1953).

58. N. Grassie and W.W. Kerr, Trans. Faraday Soc. 53, 234 (1957); Ibid. 55, 1050 (1959).

59. G.V. Schulz, Z. Physik. Chem. B52, 50 (1942).

60. H. Okamoto and A. Isihara, J. Polym. Sci. 20, 115 (1956).

61. R. Simha and L.A. Wall, J. Phys. Chem. 61, 425 (1957).

62. M. Szwarc, M. Levy and R. Milkovich, J. Am. Chem. Soc. 78, 2656 (1956).

63. H.W. McCormick, J. Polym. Sci. 36, 341 (1959).

64. J.F. Rudd, J. Polym. Sci. 44, 459 (1960).

65. A. Charlesby, Atomic Radiation and Polymers. Vol. I of International Series of Monographs on Radiation Effects in Materials. Pergamon Press, 1960. Page 132.

66. Same as reference 65, page 135.

67. Same as reference 65, page 138.

68. Same as reference 65, page 177.

69. A. Charlesby, Proc. Roy. Soc. A215, 187 (1952).

70. P. Alexander and D. Toms, J. Polym. Sci. 22, 343 (1956).

71. H.W. Melville and J.C. Robb, Proc. Roy. Soc. A196, 494 (1949).

72. O. Saito, J. Phys. Soc. Japan 14, 792 (1959).

73. Same as reference 65, page 287 et seq.

74. H.P. Frank and H. Mark, J. Polym. Sci. 6, 243 (1951).

75. W.R. Krigbaum and P.J. Flory, J. Am. Chem. Soc. 75, 1775 (1953).

76. J.M.G. Cowie, D.J. Worsfold, and S. Bywater, Trans. Faraday Soc. 57, 705 (1961).

77. W. Cooper et al., J. Polym. Sci. 50, 159 (1961).

78. P.J. Flory and W.R. Krigbaum, J. Chem. Phys. 18, 1086 (1950).

79. T.B. Grimley, Proc. Roy. Soc. A212, 339 (1952).

80. H. Yamakawa and M. Kurata, J. Chem. Phys. 32, 1852 (1960).

81. W. Cooper, D.E. Eaves and G. Vaughan, J. Polym. Sci. 59, 241 (1962).

82. E.F. Casassa, Polymer 1, 169 (1960).

83. W.R. Krigbaum and Q.A. Trementozzi, J. Polym. Sci. 28, 295 (1958).

84. R.L. Cleland, J. Polym. Sci. 27, 349 (1958).

85. K.A. Granath, J. Colloid Sci. 13, 308 (1958).

86. A. Peterlin, Ricerca Sci. 254, 553 (1955).
Quoted in reference 77.

87. M. Morton et al., J. Polym. Sci. 57, 471 (1962).

88. B.H. Zimm, W.H. Stockmayer, and M. Fixman, J. Chem. Phys. 21, 1716 (1953).

89. H. Tompa, Polymer Solutions. Butterworths Scientific Publications, London, 1956. Page 270.

90. S. Chandrasekhar, Rev. Mod. Phys. 15, 1 (1943).

91. H. Eyring, Phys. Rev. 39, 746 (1932).

92. H. Benoit, J. Polym. Sci. 3, 376 (1948).

93. M. Kurata, H. Yamakawa, and E. Teramoto, J. Chem. Phys. 28, 785 (1958);
M. Kurata and H. Yamakawa, Ibid. 29, 311 (1958);
H. Yamakawa and M. Kurata, Ibid. 32, 1852 (1960).

94. Same as reference 89, p. 271 et seq.

95. P. Debye, J. Chem. Phys. 14, 636 (1946).

96. J.G. Kirkwood and J. Riseman, J. Chem. Phys. 16, 565 (1948).

97. P. Debye and A.M. Bueche, J. Chem. Phys. 16, 573 (1948).

98. H. Mark, Der Feste Körper, Leipzig, 1938; R. Houwink, J. prakt. Chem. 157, 15 (1940). (Quoted in Techniques of Polymer Characterization, Edited by P.W. Allen, Butterworths Scientific Publications, London, 1959. P. 177.)

99. G. Sitaramaiah and D.A.I. Goring, J. Polym. Sci. 58, 1107 (1962).

100. P.J. Flory, J. Chem. Phys. 17, 303 (1949).

101. T.G. Fox, Jr. and P.J. Flory, J. Phys. Chem. 53, 197 (1949).

102. P.J. Flory and T.G. Fox, Jr., J. Am. Chem. Soc. 73, 1904 (1951).

103. W.R. Krigbaum and D.K. Carpenter, J. Phys. Chem. 59, 1166 (1955).

104. J.R. Schaefgen and P.J. Flory, J. Am. Chem. Soc. 70, 2709 (1948).

105. A. Charlesby, J. Polym. Sci. 17, 379 (1955).

106. B.H. Zimm, Ann. N.Y. Acad. Sci. 57, 332 (1953).

107. P.J. Flory, J. Am. Chem. Soc. 65, 372 (1943).

108. Same as reference 89, pp. 267-268.

109. S. Kataoka, Mimeographic circular on chemical physics in Japanese, Busseironkenkyu 66, 102 (1953). Quoted in reference 21.

110. P.C. Rogers, FRANTIC Program for Analysis of Exponential Growth and Decay Curves. Technical Report No. 76, Massachusetts Institute of Technology, Laboratory for Nuclear Science, June 1962.

111. D.R. Hartree, Numerical Analysis. Second Edition, Clarendon Press, Oxford, 1958. Page 110 et seq.

112. K.L. Nielsen, Methods in Numerical Analysis. Macmillan Company, New York, 1960. Page 120.

113. A.A. Miller, unpublished work, quoted in reference 30.

114. A.J. Barry, J. Appl. Phys. 17, 1020 (1946).

115. P. Outer, C.I. Carr, and B.H. Zimm, J. Chem. Phys. 18, 830 (1950).

116. W.R. Krigbaum and P.J. Flory, J. Polym. Sci. 11, 37 (1953).

117. C.W. McConnell, Ind. Eng. Chem. Anal. Ed. 7, 4 (1935).

118. Same as reference 34, page 22.

119. M.M. Huque, J. Jaworzyn, and D.A.I. Goring, J. Polym. Sci. 39, 9 (1959).

120. D.A.I. Goring and T.E. Timell, J. Phys. Chem. 64, 1426 (1960).

121. W.B. Dandliker and J. Kraut, J. Am. Chem. Soc. 78, 2380 (1956).

122. C.I. Carr, Jr. and B.H. Zimm, J. Chem. Phys. 18, 1616 (1950).

123. P. Doty and R.F. Steiner, J. Chem. Phys. 18, 1211 (1950).

124. W.H. Beattie and J.T. Bailey, Paper presented at the 10th Canadian High Polymer Forum, St. Marguerite, P.Q., 1960.

125. B.H. Zimm, J. Chem. Phys. 16, 1093, 1099 (1948).

126. J.P. Kratohvil et al., J. Polym. Sci. 57, 59 (1962).

127. M.M. Huque, D.A.I. Goring, and S.G. Mason, Can. J. Chem. 36, 952 (1958).

128. J.H. O'Mara and D. McIntyre, J. Phys. Chem. 63, 1435 (1959).

129. J.V. Stabin and E.H. Immergut, J. Polym. Sci. 14, 209 (1954).

130. B.H. Zimm and I. Myerson, J. Am. Chem. Soc. 68, 911 (1946).

131. Manufactured by the Schleicher and Schuell Company, Keene, N.H.

132. A.W. Craig and D.A. Henderson, J. Polym. Sci. 19, 215 (1956).

133. Made by Canadian Laboratory Supplies Ltd., Montreal, P.Q.

134. J.B. Scarborough, Numerical Mathematical Analysis. Oxford University Press, 1930. Page 365.

135. H. Kroepelin, Kollid-Z. 47, 294 (1929).

136. J. Schurz and E.H. Immergut, J. Polym. Sci. 9, 279 (1952).